ИЗМЕРИТЕЛЬНАЯ ТЕХНИКА

Number 11, November 1961

Translation Published May, 1962

SOVIET INSTRUMENTATION AND CONTROL TRANSLATION SERIES

Measurement Techniques

(The Soviet Journal *Izmeritel'naya Tekhnika* in English Translation)

■ This translation of a Soviet journal on instrumentation is published as a service to American science and industry. It is sponsored by the Instrument Society of America under a grant in aid from the National Science Foundation with additional assistance from the National Bureau of Standards.

SOVIET INSTRUMENTATION AND CONTROL TRANSLATION SERIES

This translation of the Soviet Journal *Izmeritel'naya Tekhnika* is published and distributed at nominal subscription rates under a grant in aid to the Instrument Society of America from the National Science Foundation. This translated journal, and others in the Series (see back cover), will enable American scientists and engineers to be informed of work in the fields of instrumentation, measurement techniques, and automatic control reported in the Soviet Union.

The original Russian articles are translated by competent technical personnel. The translations are on a cover-to-cover basis and the Instrument Society of America and its translators propose to translate faithfully all of the scientific material in *Izmeritel'naya Tekhnika*, permitting readers to appraise for themselves the scope status, and importance of the Soviet work. All views expressed in the translated material are intended to be those of the original authors and not those of the translators nor the Instrument Society of America.

Publication of *Izmeritel'naya Tekhnika* in English translation started under the present auspices in August, 1959, with Russian issue No. 1 of Jan.-Feb. 1958. The program has been continued with the translation and printing of the 1959-1961 issues, which are monthlies.

Transliteration of the names of Russian authors follows the system known as the British Standard. This system has recently achieved wide adoption in the United Kingdom, and is currently being adopted by a large number of scientific journals in the United States.

Readers are invited to submit to the Instrument Society of America comments on the quality of the translations and the content of the articles. Pertinent correspondence will be published in the Society's monthly publication, the ISA JOURNAL. Space will also be made available in the ISA JOURNAL for such replies as may be received from Russian authors to comments or questions by the readers.

1961 Volume Subscription Prices:

Per year (12 issues), starting with 1961, No. 1

General:	*United States and Canada*	$25.00
	Elsewhere	28.00
Libraries of nonprofit academic institutions:		
	United States and Canada	$12.50
	Elsewhere	15.50
Single issues to everyone, each		$ 6.00

1958, 1959, and 1960 issues also available. Prices upon request.

See back cover for combined subscription to entire Series.

Subscriptions and requests for information on back issues should be addressed to the:

Instrument Society of America
530 William Penn Place, Pittsburgh 19, Penna.

Translated and printed by Consultants Bureau Enterprises, Inc.

Measurement Techniques

A translation of Izmeritel'naya Tekhnika, a publication of the Academy of Sciences of the USSR

(Russian Original Dated November, 1961)

1961, No. 11, pp. 857-934 May, 1962

CONTENTS

CONTENTS (continued)

METHODS FOR CONTINUOUS AUTOMATIC CHECKING OF CYLINDRICAL COMPONENTS WITH CURVILINEAR CROSS SECTIONS

N. M. Karelin and V. I. Kiparenko

Translated from Izmeritel'naya Tekhnika, No. 11,
pp. 7-12, November, 1961

In engineering and instrument-making a large number of cylindrical components is used with cross sections described by epi- and hypocycloids and their equidistantials. These components consist of cams with outlines described by Pascal's limacon or a cardioid which are used in automatic dosage machines, sewing machines, etc.; two- and three-blade Rutt-type rotors used in rotating gas-meters, air-blowers, and in internal combustion engine pumps; pump rotors of different outlines, such a sabre-shaped, crescent-shaped, etc.; wheels of planetary driving-pin reduction-gears; elliptical wheels, etc. It should be noted that at present there is intensive development of machines (motors and compressors) whose casings or rotors are described by epi- or hypotrochoids [1].

Since these components, as a rule, work coupled to each other, the accuracy of their profile manufacture must be very high at all points. The following technological processes in manufacturing components with curvilinear cross sections do not, in the majority of cases, provide a theoretically accurate profile, since the designing, manufacture and inspection of the shaped cutting tools, guide blocks, etc. are made according to given values of the radius vector at a limited number of points, or by means of approximations of a given curve to arcs of circumferences.

The manufacture of component profiles without the use of guide blocks is discussed in [2], but continuous and highly efficient checking of such profiles has not been provided up to the present and this problem still has to be solved.

A common method of checking components with noncircular cross sections consists in measuring the radius vector at given values of the component's rotation angle. In many instances this method (for an economically feasible expenditure) does not provide the required accuracy of the profile in the intervals between the points at which the checking is made. Moreover, this method is inefficient owing to the large amount of labor consumed in manual checking operations. The method involving the use of a reference component is also unsuitable for checking components whose profiles must be made with great accuracy. As a rule, it is impossible to make according to requirements the reference component at least three times as accurate as the component being checked [3]. In cases when this method is used, the expensive reference component has to be changed often, since in use its profile varies rapidly with wear.

At present a small number of kinematic inspection devices has been developed and is used for checking curvilinear profiles of components at all the points. An evolventometer may serve as an example of such a device used for measuring the involute of a circle.

Below we describe and provide a theoretical basis for the method developed by us of arranging the monitoring devices for a continuous automatic and visual determination of the error at all the points of the profile described by epi- and hypocycloids and their equidistantials as well as curves which are approximated by them.

A continuous automatic checking of components with curvilinear cross sections can be accomplished by means of various arrangements. One of the simplest schematics of such a device, which provides the inspection of components with any profiles, is shown in Fig. 1. The signals from the transducer of linear displacements which are proportional to the instantaneous actual value of the tested profile L radius vector are recorded either in the form of a graph which expresses the tested profile radius vector as a function of the rotation angle (either in rectilinear or polar coordinates), or in the form of a table of the radius vector numerical values for a sufficiently large number of the component's rotation angle values. The main drawback of the above arrangement consists in the need to compare the recorded results with the nominal values of the tested profile. Another essential drawback of this arrangement

consists in the large range of the linear displacements transducer (or the position transducer), which either leads to a considerable decrease in accuracy of measurements, or makes the development of complicated and expensive transducers necessary.

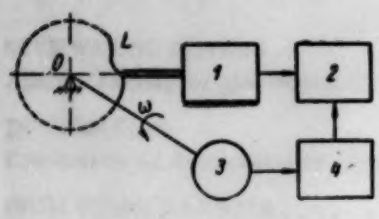

Fig. 1. 1) Linear displacements transducer; 2) recording instrument; 3) rotation angle transducer; 4) synchronizing unit.

The design of accurate and relatively simple monitoring devices intended for measuring profiles formed by epi- and hypocycloids and their equidistantials can be based on a three-link kinematic chain which reproduces these curves [2] and is shown in Fig. 2. In this chain a_0 is the stationary link, a_1 and a_2 are the links rotating with constant angular velocities w_1 and w_2 respectively, and M is the point which describes the epi- or hypocycloid q-q. The parametric equation of this curve has the form

$$\left.\begin{aligned} x &= \sum_{j=0}^{2} a_j \cos(\varphi_j + \alpha_j) \\ y &= \sum_{j=0}^{2} a_j \sin(\varphi_j + \alpha_j) \end{aligned}\right\}. \qquad (1)$$

where $\varphi_j = \omega_j t$ is the rotation angle of the j-th link; α_j is the initial phase of the j-th link (α_0 is the angle between the stationary link a_0 and axis OX).

In the case when the profiles of the components are closed cycloidal curves we have $\varphi_2/\varphi_1 = k$, where [k]= 1,2. . . .

In certain components the profile (or part thereof) may be formed by an open cycloidal curve, then k will not be an integer.

For k> 0 point M will describe an epicycloid and for k< 0 it will describe a hypocycloid.

The number of branches of curve N is determined by the relation

$$N = |k-1|. \qquad (2)$$

If the epi- and hypocycloid equations are written in a parametric form (1) it can easily be shown that the number of known mathematical curves such as an ellipse, a straight line produced by a point being displaced sinusoidally, a cardioid, Pascal's limacon, a nephroid, an astroid, Steiner's curve, multipetal roses, etc., are in fact cycloidal [4].

If point M is made to coincide with the center of a circle of radius R (Fig.2), the periphery of the circle will describe equidistant curves (p-p and p'-p') whose parametric equations will have the following form:

$$\left.\begin{aligned} X &= x \mp R \frac{\frac{dy}{dx}}{\sqrt{1+\left(\frac{dy}{dx}\right)^2}} \\ Y &= y \pm R \frac{1}{\sqrt{1+\left(\frac{dy}{dx}\right)^2}} \end{aligned}\right\} \qquad (3)$$

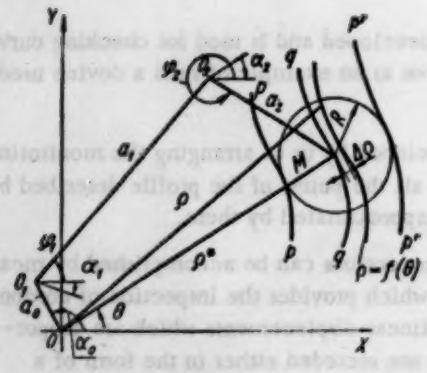

Fig. 2

The top signs refer to curves p-p and the lower signs to curves p'-p'.

A curve which is represented by equation $\rho = f(\Theta)$ or by discrete values of $\rho_1, \Theta_1, \rho_2, \Theta_2, \ldots, \rho_n, \Theta_n$ over a period Ω, but does not belong to the class of epi- or hypocycloids, can be represented with a certain approximation by one of the cycloidal curves. Moreover, k is determined by means of(z), and then by methods of function approximations parameters a_j and α_j are determined.

It is possible to study approximations and evaluate errors (both for non-cycloidal curves and for those of the

epi- or hypocycloid class) in the direction of a normal to a given curve, of the radius vector, of link a_2 of the kinematic chain (Fig.2), of one of the coordinate axes, etc.

If an approximation is studied in the direction of radius vector ρ of a given curve which describes the profile of a component, we have

$$\Delta\rho=\rho-\rho^*, \tag{4}$$

where ρ^* is the radius vector which describes an epi- or hypocycloid.

By projecting the sections of the broken line O, O_1, O_2, M on to the radius vector and a direction perpendicular to it we obtain

$$\rho^*=a_0\cos(\alpha_0-\theta)+a_1\cos(\varphi_1+\alpha_1-\theta)+ \\ +a_2\cos(k\varphi_1+\alpha_2-\theta), \tag{5}$$

$$0=a_0+a_1\sin(\varphi_1+\alpha_1-\theta)+a_2\sin(k\varphi_1+\alpha_2-\theta). \tag{6}$$

By using, for instance, the method of quadratic approximations of functions we obtain from (4) and (5) the following equation:

$$(\Delta\rho)^2=\int_0^{\Omega}[\rho-[a_0\cos(\alpha_0-\theta)+a_1\cos(\varphi_1+\alpha_1-\theta)+a_2\cos(k\varphi_1+\alpha_2-\theta)]]^2\,d\theta. \tag{7}$$

Angle φ_1 is determined from (6) as an explicit function of Θ

$$\varphi_1=F(a_0,\ a_1,\ a_2,\ \alpha_1,\ \alpha_2,\ \theta). \tag{7a}$$

By solving the system of equations

$$\frac{\partial(\Delta\rho)^2}{\partial a_j}=0 \qquad \frac{\partial(\Delta\rho)^2}{\partial \alpha_j}=0, \tag{7b}$$

where $j=0, 1, 2$, we find the values of a_j, α_j.

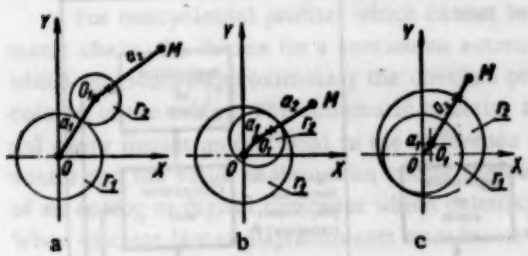

Fig. 3

Thus, by using the criterion of the accuracy of approximation it is easy to find the parameters of the approximating curve. Two of these, namely a_0 and α_0 will determine the center of the component when the latter is being checked. By analogy with a term of "technological center of the component" accepted in engineering we shall call the above point the checking center of the component. The checking center of the component must be made in its manufacture in the form of holes, centers, etc. In order to reduce measurement errors the checking center of the component should coincide with its technological center.

In designing control devices we used diagrams derived from the original one (Fig.2); moreover, both in the original diagram and its transformations link a_0 remains coupled to the component, and link a_2 to the instrument. In order to obtain the transformed diagrams let us rotate all the links of the diagram with a velocity ω_j. As a result of the transformation link j becomes stationary and the remaining links obtain angular velocities shown in the table. The diagrams derived from the original one are denoted by 3' and 3", and the original diagram by 3 (see table).

In order to obtain a direct reading it is possible to use, for instance, a clock-type indicator, and for automatic registration of the tested profile a linear displacements transducer.

The planetary motion of the article, the measuring instrument or the transducer (original diagram 3 and derived diagram 3") can be obtained from a planetary, a differential crankshaft-planetary mechanism, a hinged parallelogram, etc.

The same direction of rotation for the links of a functional diagram is provided by epicyclic (Fig.3a) and pericyclic (Fig.3c) mechanisms and different directions of rotation by a hypocyclic mechanism (Fig.3b). In these mechanisms gear r_2 rolls over a stationary gear r_1.

The gear ratios of r_1 and r_2 are determined from the relation

$$\frac{r_1}{r_2}=\left|\frac{\omega'-\omega''}{\omega''}\right|. \tag{8}$$

where ω'' is the angular velocity of the link connected to a stationary support, ω' is the angular velocity of the second link.

The dimensions of r_1 and r_2 can be determined from the equations: $r_1 + r_2 = a$, for an epicyclic mechanism; $r_1 - r_2 = a$, for a hypocyclic mechanism; $r_2 - r_1 = a$, for a pericyclic mechanism, where a is the link connected to a stationary support.

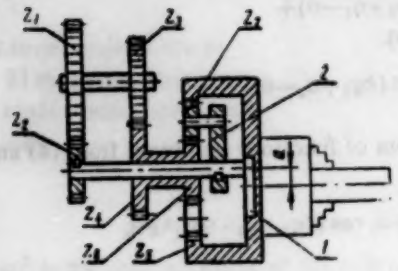

Fig. 4

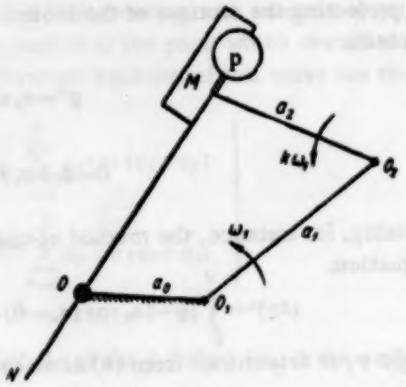

Fig. 5

Functional diagram designation	Angular velocities of links a_0	a_1	a_2	Functional diagram	Error recording diagram: Checked profile reproduction which does not require corrections	Error recording diagram: Approximate checked profile reproduction which requires corrections
Original 3	0	ω_1	$k\omega_1$	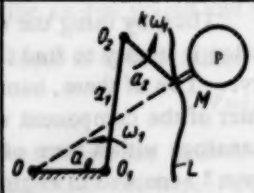	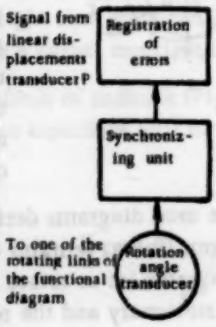	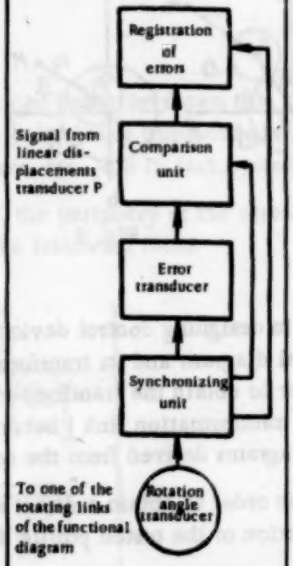
Derived 3'	$-\omega_1$	0	$(k-1)\omega_1$	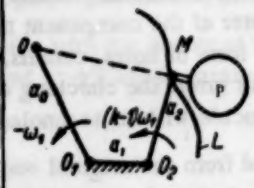		
Derived 3''	$-k\omega_1$	$(1-k)\omega_1$	0	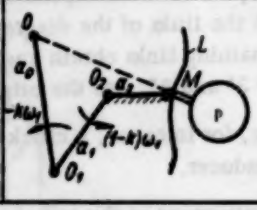		

Sometimes in designing the devices it is difficult to obtain the required relations of the link dimensions to the angular velocities of the mechanism, especially in cases when a is small. These difficulties can be overcome by introducing into the kinematic chains of the above mechanisms idler gears. Thus, differential planetary mechanisms are obtained. One is shown in Fig.4. In this the component is fixed to face plate Z_5 which is fitted on an eccentric 1 rotated by gears Z_1 and Z_2. The face plate is coupled to gear Z_7 which is freely mounted on the pin of carriage 2 and is coupled to gear Z_6 which is driven from gears Z_3 and Z_4.

Thus, the axis of the component rotates over a circumference of radius a, and the component itself rotates about its axis.

The gear ratio of these gears is

$$\frac{Z_3}{Z_4}\omega = \left(1+\frac{Z_5}{Z_6}\right)\omega'' - \omega'; \quad \frac{Z_1}{Z_2}\omega = \omega'' \tag{9}$$

and their ratio is

$$\frac{Z_2 Z_3}{Z_1 Z_4} = 1 + \frac{Z_5}{Z_6} - \frac{Z_2\omega'}{Z_6\omega''} \tag{10}$$

In view of the fact that the measuring instrument or transducer in the application of these diagrams is connected to link a_2, it is necessary, in order to determine the error in a given direction, to use auxiliary mechanisms which fix the instrument probe or transducer in that direction. If the axis of the probe is not fixed in the right direction in which the error has to be determined, the instrument readings will be distorted and it will be necessary in deciphering them to take into consideration the actual parameters of the functional diagram.

For instance, in order to obtain the profile errors in the direction of the radius vector, the casing of the measuring instrument or the transducer should be fixed to link MN (Fig.5). This link rotates about the axis passing through point M and is displaced along a guide which rotates about axis O. If it is necessary to determine the error in the direction normal to the checked profile, it is possible to use a link motion described in [2].

For an automatic registration of the checked profile error it is possible to use one of the diagrams shown in the table.

The first diagram is intended for cases in which the checked profile is cycloidal and the functional diagram point M at which the end of the probe of the linear displacements transducer (or position transducer) P is located describes accurately the given profile, or in which the checked profile is not a cycloidal curve, but its approximation by a cycloidal curve is satisfactory and does not require corrections for approximations. In this case the transducer probe will only be displaced due to errors in the profile, the signal at the transducer output will be proportional to the error, and the controlling instrument will record this value as a function of the component's angle of rotation.

For noncycloidal profiles which cannot be reproduced with sufficient precision by means of a three-link kinematic chain, the device for a continuous automatic monitoring should consist of a functional diagram (see table) which reproduces approximately the checked profile, and of an error registering schematic shown in the right-hand column of the table. This schematic contains a device which is called an error transducer and which produces a signal every instant proportional to the difference between the instantaneous nominal value of the checked profile radius vector and the value of the radius vector reproduced by the functional diagram. Such an error transducer can consist of an analog or digital computer which calculates the corrections for the instantaneous values of the radius vector. When discrete linear displacements transducers are used the error transducer can consist of a device similar to a digital computer memory which is stored in advance with the values of the corrections for the radius vector which is being reproduced.

The correction transducer is controlled by a signal which synchronizes the issuing of corrections with a given rotation angle of the component.

The signal corresponding to the error is subtracted algebraically in the comparator unit from the signal obtained from the linear displacements transducer. The difference signal which is proportional to the absolute error of the radius vector is fed to the device which registers the error as a function of the component's angle of rotation.

Any of the three functional diagrams shown in the table can, in theory, be used for designing monitoring devices and installations for checking automatically curvilinear profiles. However, one instance when the original diagram 3 is advantageous as compared with its derivatives 3' and 3" entails the checking of very large and heavy components whose rotation requires cumbersome and expensive devices. However, derivatives 3' and 3" are of the greatest practical interest, since the initial diagram 3 provides considerable difficulties, as compared with the other two, in registering the measuring instrument reading or obtaining electrical signals from the linear displacements transducer P.

The derived diagram 3' is most convenient for cases when the checking devices or installations for automatic registration of errors are intended for checking components with different profiles, and hence the functional diagram requires to be readjusted. Moreover, such a readjustment (changes in parameters a_j, ω_j, and α_j) can be achieved with sufficient simplicity

and speed. In the case of monitoring devices in which an indicating measuring instrument is used for reading the error, it is convenient and easy to employ a device with a roof-shaped Dove prism [5] in order to obtain a stationary image of the measuring instrument scale. When the casing of the measuring instrument P is fixed to link a_2, the diagram of the Dove prism device will appear in the form shown in Fig.6. Link a_2 carries two mirrors 1 and 2 which direct the light of illuminators 7 which is reflected from the scale of measuring instrument P to prism 3. From the prism the light passes through objective 4, and is reflected from mirror 5 on to the frosted glass screen 6 and forms on it an image of the measuring instrument scale, which is observed from the side indicated by an arrow. Providing the prism rotates at a speed which is half that of link a_2 ($Z_1Z_3/Z_2Z_4=1/2$), the image of the scale on screen 6 will remain stationary.

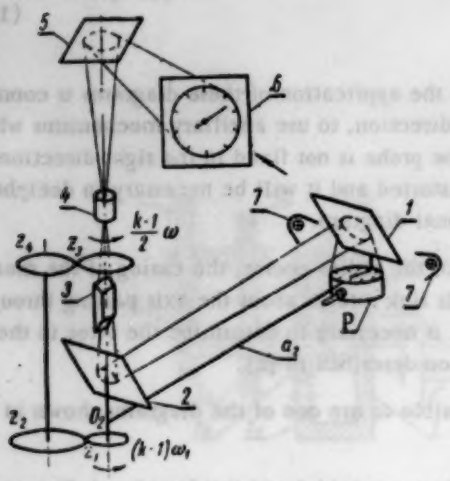

Fig. 6

The derived diagram 3" is the most suitable for recording errors, since in this case the transducer does not rotate, but is only deflected through a certain angle ($< \pi/2$) in the direction of the tested profile radius vector, and hence, there is no difficulty in obtaining an electrical signal from the transducer. However, this diagram is less convenient for checking components with wide variations in types of profiles, since its readjustment for different parameters is more complicated than that of diagram 3'.

The error of the monitoring devices and installations made according to the diagrams shown in the table consists of two basic components.

The first component represents the error in reproducing a precise or approximate profile of the tested functional diagram. This error is examined in [6].

The second basic error component is provided by the measuring instruments or linear displacements transducers (position transducers), as well as by the error transducers and recording devices.

It should be noted that the relative values of these errors may be considerably larger than the tolerance of the device as a whole, since they enter into the final result error as quantities of the second order of magnitude if the first method of recording errors is used, and if the second method is used the effect of these errors on the total error is decreased by a factor which is several times larger than the minimum ratio of the tested component's radius vector to the error of approximation $\Delta\rho$.

Conclusions. The above methods can be used for producing devices for an automatic or visual continuous checking of curvilinear detail profiles represented by epi- or hypocycloids and their equidistantials, or by curves which are approximated by the former.

LITERATURE CITED

1. Bauart und gegenwärtiger Entwicklungsstand einer Trochoiden Rotationskolbenmaschine. Techniche Rundschau, 1960, No. 7.
2. N. M. Karelin, Vestnik mashinostroeniya, 1958, No. 1.
3. M. F. Malikov, Basic Metrology [in Russian] (Moscow, 1949).
4. N. M. Karelin, Method for Making Curvilinear Cross Section Components without the use of Cams [in Russian] (Works of the Moscow Aviation Technological Institute, No. 5, 1949).
5. R. V. Dybskii, Instrument for Efficient Checking of Clock-Type Indicators with a Multiplying Factor of 0.01 mm [in Russian] (Informational Materials for Rationalizing the Equipment and Methods in Checking Measures and Measuring Instruments, 1952).
6. N. M. Karelin, Izmeritel'naya Tekhnika, 1959, No. 8.

INDUCTION TRANSDUCER WITH COMPUTER

M. I. Kochenov and V. S. Chaman

Translated from Izmeritel'naya Tekhnika, No. 11,
pp. 12-17, November, 1961

The Institute of Engineering of the USSR Academy of Sciences has developed a circuit and tested models of electrical computers which automatically process the information received from special linear-measuring instruments. By their means it is possible, among other things, to compute automatically the arithmetic mean of a number of measurements (from 2 to 40). The dimensions for which the arithmetic mean value is calculated may refer to one or several articles, depending on the task in hand. The measurement and computation results can be presented by the computer in the form of a point recording on a chart or converted into command pulses for trimming lathes and other equipment. The command pulses can also be fed to a perforator in order to record the results on a perforated card.

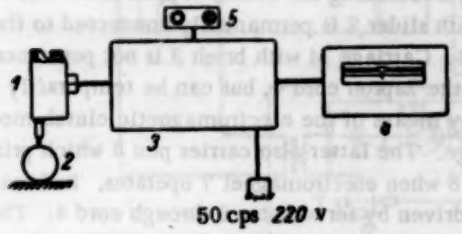

Fig. 1

The block schematic of such a measuring device is shown in Fig.1. The measuring rod of a differential inductive transducer 1 rests on the measured component 2. An electric signal proportional to the dimension of the component is fed to the electronic unit 3, is amplified and then fed to a computer and a printing device 4, which automatically (on receiving appropriate commands from the electronic unit 3) sums up algebraically the selected figures of consecutively measured dimensions, and at the end of summation prints a point on the diagram. The electronic unit 3 also controls the lighting of two indicator lamps on signalling device 5. The first lamp lights when the measurements of a given component have been completed, and the second when the summing and measuring cycle has been completed and the point printed on the chart. The signalling device is only required for manual operation of the measuring equipment.

The above measuring equipment is based on a self-balancing bridge which consists of an inductive transducer and a purely resistive slidewire used for balancing the bridge.

The inductive transducer is shown in Fig.2. Its casing 1 is made of massive annealed steel (for the purpose of screening the internal parts of the transducer from external magnetic fields), it carries inside it on two flat springs 2 the magnetic core 3, which can be displaced by means of micro-screw 4 with respect to casing 1 during setting operations. A pair of plane-parallel springs 5 attached to core 3 carry armature 6 whose lower end is attached to measuring rod 7, which passes through guide bush 8. The transducer is fixed in its measuring position either by bush 8 or by means of its casing. Core 3 carries two coils 9 whose impedances vary when armature 6 is displaced from its middle position. The two impedances vary in opposite directions. For convenience of the initial adjustment of the air gap in the differential magnetic system consisting of the core and the armature, the operating surfaces of the poles in core 3 and armature 6 are made at an angle of 45° to the displacement axis of armature 6. The upper part of the inductive transducer is provided with a special terminal 10 which has an 8 mm through hole intended either for fixing a spring stopper, which provides the required measuring effort, or for a measuring head with a scale. Springs 5 which carry armature 6 have at their fixing places narrow transverse slots occupying practically the whole width of the spring. Thus, a relatively small stiffness is obtained in the suspension of the armature (the bending effort of the suspension springs does not exceed 50 g-wt), preserving at the same time high accuracy in its displacement. When springs 5 are deformed by the movement of armature 6, they assume an S-shape,

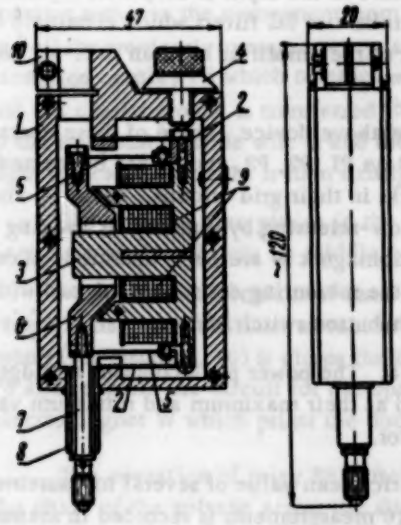

Fig. 2

owing to the slots cut in them. This arrangement also eliminates to a considerable extent mechanical hysteresis which is peculiar to flat springs of a normal type.

The magnetic circuit of each inductance includes two air gaps, namely, an operating and an auxiliary air gap which do not vary with vertical displacements of the armature. The second air gap is provided by a projection in core 3 which enters with a small clearance (0.2-0.5 mm) into a rectangular window in armature 6. This air gap extends to both branches of the differential magnetic circuit. The above design of the magnetic circuit slightly lowers its total sensitivity as compared with transducers which have normal cores; however, it greatly improves the possibility of obtaining a linear relationship between the displacement of the rod and the voltage in the measuring diagonal of the bridge. Since the bridge diagonal is connected to a high-impedance amplifier input and the bridge is fed with a 50 cps voltage, the transducer windings are made of many turns of thin wire.

Tests of the new inductive transducer have shown that its maximum error amounts to 0.2 μ.

It has already been pointed out that this instrument is based on a self-balancing bridge. A balancing element (slidewire) is used in the summing and registering parts of the instrument, and the summing of the measured dimensions is accomplished by means of an automatic control of the order of connecting two sliders which balance the bridge and are driven by a servomotor fed by the amplified bridge unbalance voltage.

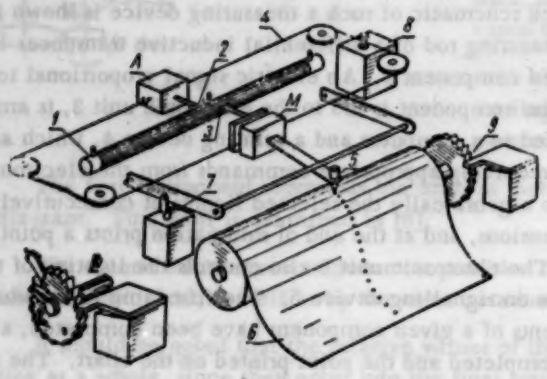

Fig. 3

The schematic of the summing and printing parts of the instrument is shown in Fig.3. Two balancing sliders 2 and 3 are displaced along the center-tapped slide wire 1. Carriage A with slider 2 is permanently connected to the driving cord 4. Carriage M with brush 3 is not permanently connected to the kapron cord 4, but can be temporarily connected to it by means of the electromagnetic clutch mounted on the carriage. The latter also carries pen 5 which prints dots on chart 6 when electromagnet 7 operates. Both carriages A and M are driven by servomotor 8 through cord 4. The paper is displaced by the periodic switching-in of the electromagnetic ratchet 9. Another similar ratchet mechanism is used in contact device 10 for counting the number of measurements whose mean value is to be obtained.

The schematic of the instrument is shown in Fig.4 (the functionally separated parts of the instrument are enclosed in dotted lines). Inductive bridge 1 consists of the inductive transducer IT and a purely resistive slide wire R. The bridge-balancing servomotor SM drives the two slide wire sliders, one of which on carriage A is permanently coupled to the cord, and the other on carriage M is coupled to it by means of an electromagnetic clutch.

The bridge unbalance voltage is fed either from the first or second slider to the input of amplifier 2 which feeds the controlling winding of servomotor SM. The amplifier circuit contains two RC filters which eliminate harmonic components from the bridge unbalance voltage. The two last stages of the amplifier have an over-all negative feedback, which is proportional to the speed of servomotor SM.

Relay circuit 3 controls the operation sequence of the elements of the above device. Some of these operations have to be carried out with a given time delay, therefore, the actuating relays P1, P2, P3, and P4 are connected to the anode circuits of tubes T1-T4 whose operation is delayed by RC networks in their grid circuits. Relay P5 and the electromagnetic clutch C operate without time delay. Relay P6 is made slow-releasing by shunting its winding with a capacitor. Both ratchet electromagnets X1 and X2 and the printing electromagnet W are pulse operated, since they are actuated by a short capacitor discharge current. For manual operation the measuring desk 4 is equipped with a signalling device consisting of two lamps SL1 and SL2 and of a starting push-button switch BS.

The device is supplied from 50 cps, 220 v mains through power pack 5. The power pack contains a bridge supply stabilizer which uses tube T11 whose anode current pulses are limited at their maximum and minimum values by feeding its grid circuit from the 220 v ac mains through a limiting resistor.

The operation of the device in calculating and recording the arithmetic mean value of several measurements consist of the following. Let us assume that the arithmetic mean value of 10 measurements is recorded in manual operation.

In its initial position the starting button switch BS (Fig.4) is closed and both carriages A and M are placed against the center tap of slide wire R. The operator places a tested component in the measuring position and presses starting button BS, disconnecting its contacts. Relay P1 operates with a delay, which provides a reliable positioning of the component, and switches in through its contacts the electromagnetic clutch of carriage M, computer X_1, relay P6 and the electronic relay P2.

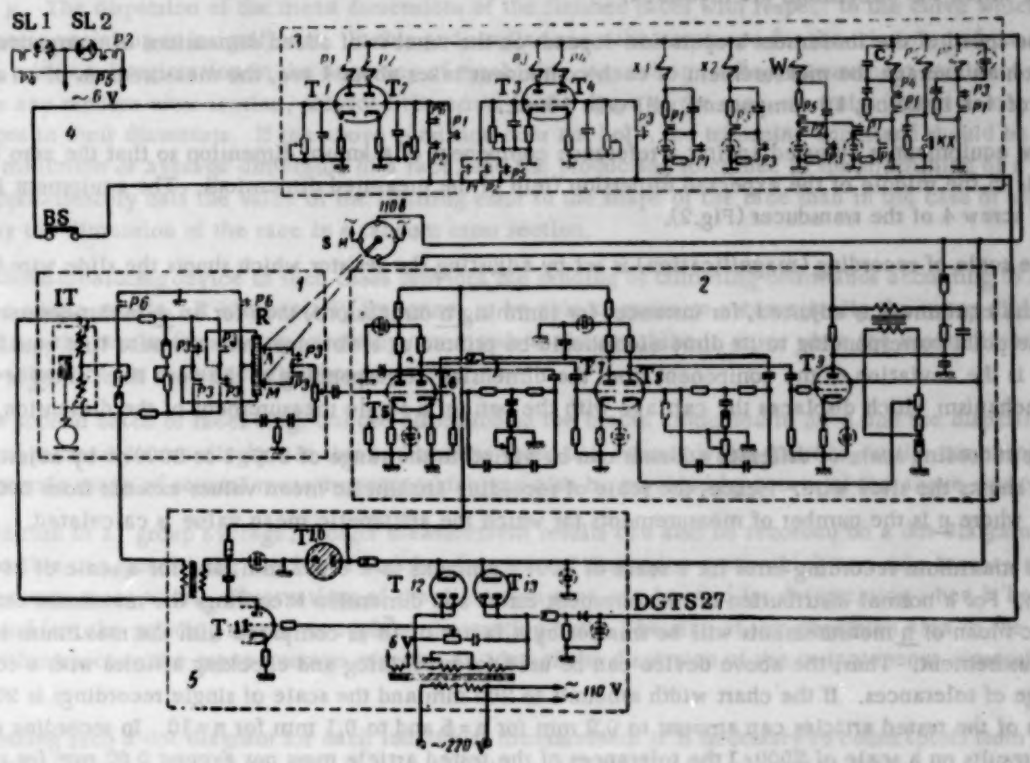

Fig.4

These devices operate in the sequence given above. When relay P6 operates the chassis potential (ground) is transferred from the midpoint of rheostat R to the midpoint of transducer IT. This produces a displacement of carriages A and M. Hence, pen 5 (Fig.3) is also displaced from the middle of the chart over a distance proportional to the dimensions of the component placed under the inductive transducer. When the carriages stop, relay P2 operates and lights through its contacts lamp Sl_2 of the signalling device, thus indicating: "Measurement completed." The operator removes the component from the measuring position, the contacts of the starting button switch then closes and all the previously operated relays and the electromagnetic clutch of carriage M release instantaneously (with the exception of relay P6 which releases with a slight delay). At this instant carriage M is disconnected from the cord and the chassis ground is transferred (by means of relay P6 contacts) from the midpoint of the inductive transducer IT to the midpoint of slide wire R and the bridge balance is reestablished by placing slider A in the middle position. Light indicator lamp Sl_2 is then extinguished.

The operator then places in the measuring position the next component and, according to its dimensions, carriage A is displaced from its middle position and carriage M from its previous position.

After the measurement of each component single electrical pulses are fed to the electromagnetic counting device X1; its contact ratchet advances by one step for each measurement and finally, after a given number of measurements (for instance, 10) it closes the contact of counter KX, thus operating relay P5 which in turn switches-in relay P3 and prepares the circuit for the operation of the printing electromagnet W. The operation of relay P2 switches in electromagnet W which prints the dots on the chart.

The operation of relay P3 switches the amplifier input from slider A to slider M, and at the same time changes the phase of the voltage across the slidewire by 180°. Relay P3 also disconnects the supply of relay P6 which de-energizes and switches over the chassis potential (ground) from the midpoint of transducer IT to the midpoint of slide

wire R. As the result of the mentioned switching slider M is placed in the middle position of slide wire R, and slider A is moved to any random position.

As soon as the last of the 10 components is removed from the measuring position all the relays and the electromagnetic clutch are released, thus, placing carriage A in the middle position of slide wire R, i.e., the instrument returns to its initial condition. When the instrument returns to the initial position another dot is printed on the zero line from which the dimensions are measured.

The speed of the instrument's operation depends on the number of added dimensions of components. Considering that on an average the measurement of each component takes about 1 sec, the measurement of an average dimension of, for instance, 10 components will take 10 sec.

The equipment is adjusted against a reference component of a known dimension so that the zero line of the chart falls in the middle of the expected dispersion field of the measured dimensions. The equipment is adjusted by means of screw 4 of the transducer (Fig.2).

The scale of recording (magnification) is set by adjusting the resistor which shunts the slide wire (Fig.4).

If the equipment is adjusted, for instance, for summing n dimensions, then for an n-fold measurement of a component the point corresponding to its dimension should be printed at a distance from the zero line equal to $\Delta l n i$, where Δl is the deviation of the component from the dimension corresponding to the zero line, and i is the gear ratio of the mechanism which displaces the carriage with the pen for a single measurement of the dimension.

The recording scale of different addends can be varied in the range of 200:1 to 2000:1 by adjusting the resistor which shunts the slide wire. Hence, the scale of recording arithmetic mean values extends from 200n:1 to 2000n:1, where n is the number of measurements for which the arithmetic mean value is calculated.

The maximum recording error for a scale of 200:1 amounts to ± 0.002 mm, and for a scale of 2000:1 to ± 0.001 mm. For a normal distribution of measurement errors and dimension recordings the maximum error in an arithmetic mean of n measurements will be smaller by a factor of $\sqrt{n}$ as compared with the maximum error of any single measurement. Thus, the above device can be used for machining and checking articles with a comparatively large range of tolerances. If the chart width amounts to 200 mm and the scale of single recordings is 200:1 the tolerances of the tested articles can amount to 0.2 mm for n=5 and to 0.1 mm for n=10. In recording single measurement results on a scale of 2000:1 the tolerances of the tested article must not exceed 0.02 mm for n=5 and 0.01 mm for n=10.

If necessary the recording scale can be changed by virtually any extent by small variations in the inductive transducer parameters.

The effect of the instability of the supply voltage has been reduced to a minimum, since the instrument operates on the basis of a self-balancing inductive bridge, in which the position of the zero balance, in theory, does not depend on the supply voltage. In practice deviations of the supply voltage by ±15% from the nominal did not produce any perceptible effects on the instrument readings.

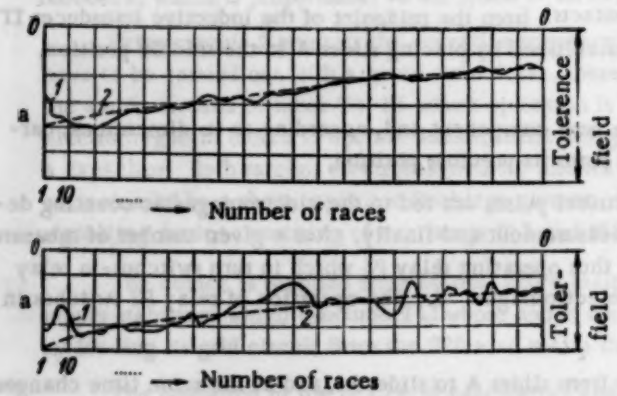

Fig. 5

Point diagrams are used for statistical analysis of production processes and are employed in systems of nonautomatic control (statistical) monitoring both of automatic and nonautomatic measurement operations. The measurement results recorded on perforated cards are used for calculating, by means of tabulators, various production process parameters which are not normally used for operative control of the production process, but are only determined for research purposes (dispersion of mean values, correlation coefficients, etc.). The computation of such parameters directly during the production process is not expedient, since it involves complicated computers.

The sending of commands for automatic trimming of the machine to the mean value of a given parameter, in many cases is more advantageous than sending a command

corresponding to the limiting dimension of one or several consecutively machined articles (as is normally done at the persent time).

Curves 1 in Fig. 5 show dimensions of bearing races machined one after another on a centerless automatic grinding machine. Dotted lines 2 represent the systematic variation of the race dimensions.

Curves in Fig. 5a represent a batch of races whose blanks were selected with a dispersion of dimensions not exceeding 10 μ. The dispersion of the mean dimensions of the finished races with respect to the curve which represents their systematic variation is insignificant. In this and similar cases the command for the trimming of the machine can be sent, without deterioration in the accuracy of machining, according to the measurement results of a single race taken across any random cross section, provided the errors in the shape of the race are insignificant as compared with the tolerances in their diameters. If the above condition does not hold, the trimming command should be set by the maximum, minimum or average dimension of a race, and the production tolerance in the machining of a race can be larger by approximately half the value of the limiting error in the shape of the race than in the case of setting the command by the dimension of the race in a random cross section.

The above measuring device in such cases provides the sending of trimming commands according to a mean dimension of a single article. It is especially important to be able to measure automatically the mean dimension of articles and use the results for sending trimming commands to the machine in cases when the mean dimension is normalized (for instance, in manufacturing bearing races).

In the second batch of races (Fig. 5b) the dispersion in the blanks amounted to 30 μ and the dispersion of the finished races increased accordingly. In this and similar cases it is more advantageous to set the trimming command by the arithmetic mean of several measurements which can also be provided by means of the above equipment.

In addition to a "group average," single measurement results can also be recorded on a dot diagram. Thus, it becomes possible to supervise the machined articles, dimensions' dispersion area, which as a rule increases as the cutting tool becomes more blunt. Observations of the dipsersion area can be used for determining when it becomes necessary to regrind (set the grinding wheel) or replace the cutting tool. The size of the dispersion area in the article dimensions with respect to the group average provides an idea of the dispersion of the instantaneous dimensions distribution.

In plotting such a dot diagram for each individual measurement it is necessary to count (plot) from a common zero line. The arithmetic mean of $\underline{n}$ measurements in this instance should be plotted to the same scale as separate measurement results.

In order to obtain such a diagram the printing part of the instrument is fitted with a second pen which is mounted on carriage A (Fig.3). The second pen prints dots for each individual measurement.

The first pen, which is mounted on carriage M (Fig.3) and prints the arithmetic mean value, is not actuated in this case directly from the common cord 4, but through a reduction gear which is equal to the number $\underline{n}$ of the added dimensions.

The changing of the transfer ratio for recording results by means of the first and second pen can be achieved without changing the mechanical reduction gear, but by a purely circuit method involving the variation of the transfer ratio by a factor of $\underline{n}$ through shunting the bridge slide wire with various fixed resistors by means of appropriate relay switching. In this case the recording of each dimension will, obviously, consist of three cycles, namely: a) recording of the dimension and the printing of the dot by the pen on carriage A; b) return of carriage A to the middle position; c) switching of the bridge circuit to a transfer ratio reduced by a factor of $\underline{n}$ and a corresponding displacement of carriage M.

Investigation of technological processes involves a wide use of dot diagrams which carry points corresponding to the maximum and minimum values of the checked articles parameters. Such a diagram can also be plotted automatically by means of the above device. For this purpose the dimensions of an article are measured at several cross sections and the results entered automatically in the form of dots on a single vertical line. The number of cross sections and directions, in which the articles are measured, is chosen according to the accuracy required in determining the extreme values of the dimensions.

The above device can also be used for automatically calculating and recording on a chart the difference of two dimensions, which may be required, for instance, in investigating deviations from a given shape of an article. In such

a case, when the second (subtracted) dimension is measured, the pen fixed to carriage M changes the phase of the voltage across the slide wire by 180° by switching appropriate relay groups. The servomotor is reversed at the same time by reversing the ends of one of its windings.

The measuring and computing devices can be supplemented by an attachment for plotting automatically a polygon or hystogram of the measured article dimensions' distribution.

BASIC METHOD FOR CHECKING LONG, GRADE 1 STRAIGHTEDGES

L. L. Medyantseva and V. V. Gorbacheva

Translated from Izmeritel'naya Tekhnika, No. 11,
pp. 17-18, November, 1961

High accuracy in manufacturing and checking plane surfaces of components is now required in machine-tool production and engineering. In the majority of plants the linearity of guiding frames is checked by means of straightedges. The basic manner of checking straightedges consists of comparing three of them to each other by means of the "painted surface" method. This method does not provide reliable results for straightedges longer than 2 mm owing to their insufficient rigidity [1]. It is known [1,2] that more accurate results are obtained by the micro-levelling and autocollimation methods. In order to select one of these methods as basic for checking Grade 1 reference straightedges we determined experimentally the maximum errors in measuring straightedges by the autocollimation and the micro-levelling methods.

The error in estimating surface linearity by either method was determined as a result of repeated measurements (20 measurements).

The measuring equipment we used for the autocollimation method consisted of autocollimator PKG-3, a plane glass placed on a support with a displacement of 400 mm, and for the micro-levelling method of a level 1 meter long calibrated in 0.02 mm and placed on a support with a displacement of 400 mm.

Both these methods are based on step by step measurements of the slope angle α_i (Fig.1) of consecutive sections placed in one direction which is provided by the beam of light (in the autocollimation method) or the horizontal plane (in the micro-levelling method). The profile of the surface is plotted by evaluating from the formula given below [1] the deviations h of the points along the profile from a straight line joining its ends.

$$h_i = y_i - \frac{i}{n} y_n, \qquad (1)$$

where

$$y_i = d \sum_{\kappa=1}^{i} \alpha_\kappa; \qquad y_n = d \sum_{\kappa=1}^{n} \alpha_\kappa;$$

d is the measuring pitch determined by the distance between the support bearings.

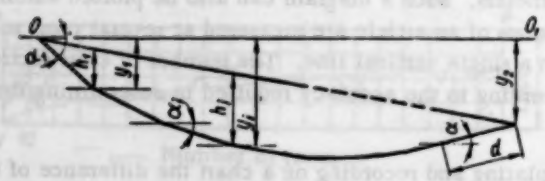

Fig. 1

The profile thus obtained indicates the deviation from linearity of the tested surface.

Despite the fact that GOST (All-Union State Standard) 8-53 provides a rigorous definition of nonlinearity, certain authors use different criteria for determining its quantitative characteristic.

They consider deviations from linearity to be: maximum distances from the crests of profile microirregularities

of the actual surface to a contiguous straight line [3]; maximum deviation from a straight line drawn through the extreme points of a profile [1]; half the maximum linear characteristic of the profile [2,4]. This impedes comparative analysis of test results obtained by various authors. In our work the value of nonlinearity is determined according to GOST 8-53 and GOST 8026-56 as the maximum deviation from a straight line drawn through the two most projecting points of the profile.

Fig.2 shows the curves of the surface profile we obtained by means of the autocollimation and micro-levelling methods.

By comparing the deviations from linearity for each interval obtained by both methods we see that the maximum discrepancy between them does not exceed 3 μ, i.e., it is within the limits of accuracy of the methods, which is contrary to the results given in [2], where the deviations obtained in measuring a plate by the autocollimation and micro-levelling methods differed by more than 20 μ.

In order to become convinced of the reliability of our measurements we compared the linear excesses established by means of block gauges with the measurements obtained by the autocollimation and micro-levelling methods.

We carried out 10 independent measurements of linear excesses established by block gauges of 1, 1.01, 1.02, and 1.04 mm. The actual size of the block gauges was measured on a telescope caliper. Since the maximum error involved in this measurement does not exceed 0.5 μ, i.e., it is a small fraction of the maximum error of the methods under investigation, we considered the linear excesses established by block gauges to be equal to the actual dimensions.

Fig. 2. 1) Profile curve of a 4-meter straightedge obtained by the autocollimation method (maximum error ± 5.4 μ); 2) profile curve of the same straightedge obtained by the micro-levelling method (maximum error ± 7.5 μ).

The differences between the actual linear excesses and the arithmetic mean of their values measured by the autocollimation method did not exceed 0.4 μ and when measured by the micro-levelling method did not exceed 0.8 μ.

These data confirm the reliability of the deviation measurements obtained by either method. The large discrepancies obtained in [2] can probably be explained by systematic errors in the measuring equipment and unfavorable effects of the external conditions.

Conclusions. Either method can be used for checking Grade 1 reference straightedges. However, the autocollimation method has several advantages as compared with the micro-levelling method, since it is more accurate (see caption to Fig.2), it is more efficient since measurements with a micro-level require considerable time for setting the air bubble in the correct position, neither does the method require the placing of the tested object in the horizontal position, which extends the field of its application; the processing of measurement results in the autocollimation method is simpler and more speedy.

Hence, in choosing the basic method for testing Grade 1 straightedges the autocollimation method should be preferred, providing an autocollimator calibrated in seconds is used.

LITERATURE CITED

1. Ya. S. Soloveichik, Collection of works of ÉNIMS [in Russian] (Vol. III, Moscow, 1942).
2. K. I. Abadzhi, Vestnik mashinostroeniya, No. 9, 1958.
3. G. L. Levin, Standartizatsiya, No. 11, 1959.
4. K. I. Abadzhi, Izmeritel'naya tekhnika, No. 2, 1961.

GRADE 0.02 REFERENCE MANOMETER WITH A RANGE OF 0 TO 2.5 kg-wt/cm²

V. N. Gramenitskii, Yu. A. Frolov, and K. I. Khansuvarov

Translated from Izmeritel,naya Tekhnika, No. 11, pp. 19-20, November, 1961

The All-Union Scientific Research Institute of the Committee of Standards, Measures, and Measuring Instruments (VNIIK) has developed a reference manometer type MP-2.5 Grade 0.02 (1st class) with a balanced piston and a range of 0-2.5 kg-wt/cm², intended for checking reference weighted-piston manometers type MP-2.5 and MPGr-4 Grade 0.05 (2nd class), vacuum gauges MVP-2.5 Grade 0.05 (2nd class), liquid portable instruments of A. I. Petrov's system for testing differential manometer flowmeters, weighted-piston manometers for measuring absolute pressure, and other manometric instruments which have a tolerance not exceeding 0.05%, as well as for precision measurements of excess pressure in the range of 0 to 2.5 kg-wt/cm².

The manometer (see figure) consists of piston 1 which is ground-in to cylinder 2, tank 7 with a level gauge 8, air-pump 9, liquid (bellows) pump 10 and funnel 11. The manometer cylinder, tank, liquid pump, and the pipes connecting them are filled with a transformer oil. Pulley 3 is fitted on to the manometer cylinder and driven from a motor. The pulley carries a retainer with a roller which presses against the pin of weight-holder 5, thus rotating the piston. The position of the piston is observed through device 4 which is placed near the cylinder and consists of a measuring microscope calibrated in 0.1 mm and a mirror which determine the position of the piston with great accuracy. The location of this device (at the side of the cylinder) makes it possible to observe the position of the piston directly (without the microscope), since the microscope is only used for measuring small pressures (below 0.1 kg-wt/cm²). The measuring part of the manometer is protected by a plexiglas jacket which serves as a thermal insulator. The temperature of the manometer is measured on a thermometer calibrated in 0.5°C.

The principle of operation of a manometer with a balanced piston consists of the following. When there is no excess pressure in the tank (i.e., when valves d and e are open) and in the absence of weights 6 on the piston weight-holder, the pressure due to the weight of the piston and the weight-holder is balanced by the liquid column in the tank. The piston is then set to its zero position which is indicated by the coincidence of the marks on the piston and the hinged frame.

The position of the piston is adjusted by pumping oil from the funnel to the tank by means of the liquid pump.

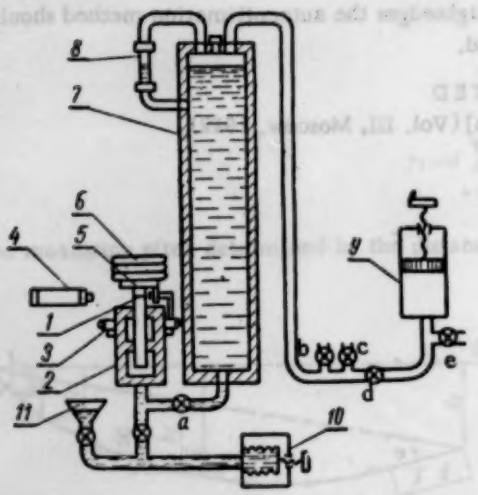

If, after setting the piston to its zero position, the upper part of the tank is connected to the medium whose excess pressure it is required to measure, the piston can be returned to its original position by placing appropriate weights on the holder.

The balance of the system will then be determined by the condition:

$$P = \frac{G}{F} = \frac{mg\left(1 - \frac{\rho_a}{\rho_s}\right)}{980.66F}, \qquad (1)$$

where P is the measured excess pressure, kg-wt/cm²; G is the weight (in air) of the loads, kg-wt; F is the effective area of the piston, cm²; m is the mass of the load, kg; g is the acceleration of a freely falling body, cm/sec²; ρ_a and ρ_s are the densities of air and steel respectively, g/cm³; 980.66 is a dimensionless coefficient.

It will be seen from (1) that the value of the measured pressure does not depend on the weight of the piston and the weight-holder.

The rotation of the piston during measurements prevents any nonliquid friction between the piston and the cylinder, thus providing the manometer with high sensitivity.

The following design peculiarities of manometer MP-2.5 Grade 0.02 as compared with manometer MP-2.5 Grade 0.05, which was also developed by the VNIIK [1,2] provide the former with higher accuracy.

1. In order to eliminate the effect of temperature variations of the liquid in the instrument on its readings, the manometer tank is made in the form of a vertical tube with a constant cross section and a height determined by that of the column of liquid which balances a nonloaded piston. The tank manometer MP-2.5 Grade 0.5 has a small height, is mounted at the top end of the stand and connected to the cylinder by a pipe of a small cross section.

2. The new manometer has a device for a forced rotation of the piston, thus making it more convenient in use and eliminating any handling of the weight holder, and ensuring a more constant temperature of the piston and cylinder during operation. In Grade 0.5 manometer the piston is rotated by hand.

3. The manometer is provided with a device for estimating accurately the position of the piston, which is required in measuring small pressures, with a thermometer socket and a plexiglas protective jacket.

The metrological characteristics of the new manometer are: the range for measuring excess pressure is 0-2.5 kg-wt/cm^2; the measurement error in the range of 0.1-2.5 kg-wt/cm^2 does not exceed ± 0.02% of the measured value, and in the range of 0-0.1 kg-wt/cm^2 does not exceed ± 0.00002 kg-wt/cm^2 (± 0.2 mm Hg).

Pressure measurements in the range of 0-0.1 kg-wt/cm^2 with the above accuracy are obtained by observing the position of the piston through the microscope (with a reading error not exceeding 0.1 mm), and by using reference weights of a Grade 2 gram set.

The nominal effective area of the piston is 1 cm^2; the tolerated deviation of the actual area from the nominal amounts to ± 0.2%; the maximum error in determining the effective area of the piston is ± 0.01%.

The maximum error in determining the mass of the weights is ± 0.01%. The radial gap between the piston and the cylinder amounts to 1.5-3 μ.

The manometer is mounted and fixed to a solid table or brackets.

There exist two types of pressure measurements, namely when a given pressure is measured (for instance, in checking another instrument), or when an unknown pressure is measured of a certain medium which is connected to the instrument.

In the first instance the tested instrument is connected to one of the two manometer nipples, valves a, d, and e are open, and the zero position of the unloaded piston checked. Weights are then placed on the holder, which correspond to a given pressure. Valve e is closed and either valve b or c opened and the required excess pressure is established in both instruments by means of the air pump. The instant the required pressure is obtained is judged by the location of the piston which must be in the same position as it was when the tank was connected to the atmosphere.

When excess pressure is measured directly the instrument is also balanced twice, namely, when the tank is connected to the atmosphere and when it is connected to the measured medium. The value of the measured pressure is determined from (1).

The piston is loaded by weights of a set in which their masses are adjusted to nominal values of 0.5, 0.1, and 0.05 kg with an error not exceeding ± 0.01%, as well as by Grade 2 weights of a mass of 20 g and smaller.

If temperature t of a piston and cylinder differs from 20°C, the value of the pressure obtained from (1) should be corrected by adding

$$\Delta P = 3 \cdot 10^{-5} P (20 - t), \qquad (2)$$

where ΔP and P are expressed in the same units.

If the level of the working liquid in the tested instrument or the level at which the measurement has to be made

falls below the level gauge scale (in the tank), a correction given below should be added to the pressure value obtained from (1).

$$\Delta P = \frac{\gamma_g H_0 P}{B} = 12 \cdot 10^{-7} H_0 P, \qquad (3)$$

where γ_g is the specific gravity of air at normal atmospheric pressure B; H_0 is the distance between the above-mentioned levels, cm; P is the measured pressure, kg-wt/cm^2.

If the above level falls above the level gauge, correction ΔP determined from (3) is used with a reversed sign.

State testing of Grade 1 type MP-2.5 manometer is carried out in the institutes of the Committee of Standards, Measures and Measuring Instruments according to the method developed by the VNIIK.

LITERATURE CITED

1. V. N. Gramenitskii, Author's Certificate No. 99180 dated October 3, 1954.
2. V. N. Gramenitskii, Reference Manometric Instruments with a Balanced Piston [in Russian] (Works of the VNIIK, 4, Standartgiz, 1960).

INSTRUMENT FOR REGISTERING AUTOMATICALLY THE OPERATING CONDITIONS OF LOCOMOTIVE DIESEL ENGINES

M. K. Gavrilenko

Translated from Izmeritel'naya Tekhnika, No. 11, pp. 21-22, November, 1961

For automatic recording of the controller-handle position, registering the loaded operating condition of locomotive diesels and indicating the time, the author of this article together with V. F. Poroshin has developed an instrument* which has now been fitted to a diesel locomotive.

The instrument consists of a mechanism for propelling a chart at a given speed and of an electric portion which provides automatic recording of the controller-handle position, of the loaded operating condition and of the time marker.

The mechanism of a recording dc voltmeter type H 375 with a synchronous motor SD2 is used for propelling the chart and provides a constant speed for the driving drum of a perforated chart 100 mm wide.

The recording of the controller-handle position, the loaded operating condition and the time marker is made on the chart by means of three pens, the first being mounted on the axle of the receiving selsyn, and the other two on the armatures of their respective relays. The pens are in permanent contact with the moving chart. The position of the controller handle is recorded by means of selsyns. Motor SD2 and the selsyns operate on 127 v 50 cps obtained from the diesel locomotive radio power-pack PO-300.

The transmitting selsyn DI-404 is mounted on the top lid of the controller and its axle is connected through a coupling to the controller stem. The receiving selsyn SS-404 is mounted on the instrument casing.

The circuit for a remote transmission of the controller's rotation angle by means of selsyns in shown in Fig. 1.

The position of the transmitting selsyn rotor is set by the rotation of the controller handle, whereas the receiving selsyn is free to move and, under the effect of the electromagnetic moment, assumes a synchronous position with the transmitting selsyn, i.e., is rotated through the same angle. The pen fixed by means of a pointer to the axle of the receiving selsyn rotor records on the chart the rotation angle of the controller spindle.

* The personnel of the KhIIT (Khar'kov Institute of Railroad Transportation Engineers) and the Rtishchevo Depot participated in the testing.

The time marker is obtained from a neon tube timer (Fig. 2). When the instrument is switched-in, capacitors C_1 and C_2 are charged through resistors R_1 and R_2. As soon as the voltage across the condenser plates attains a value for firing the neon tube T_1, the latter ignites and the capacitors discharge, whereupon they start charging again, ignite tube T_1 and the process repeats itself.

Variable resistance R_2 makes it possible to control the time between adjacent ignitions over a wide range from 1 sec to 20 min.

The current flowing through the winding of RSM-2 operates it, thus closing the contacts in the time marker relay 1 supply circuit. The current will then flow from the positive to the negative side of the storage battery.

The magnetic flux generated in the time marker relay attracts its armature together with the pen mounted on it, thus producing a mark on the chart.

When the condensers are discharged, the armature under the action of a spring returns to its normal position. This spring is sufficiently stiff to prevent the vibration of the armature during the running of the locomotive.

The stability of time intervals depends on that of the supply voltage, since the latter determines the time of charging the capacitor up to a voltage which will ignite the neon tube. In an operating engine the supply voltage is maintained by the regulator at 75 ± 1 v, which provides, as tests have shown, high stability of the time marker relay operation.

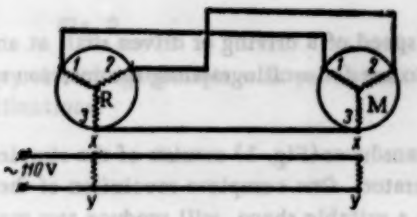

Fig. 1

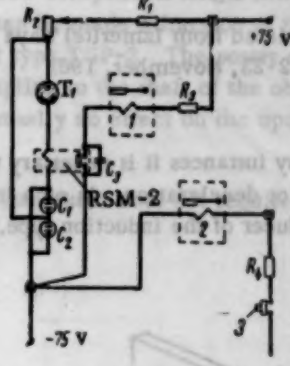

Fig. 2

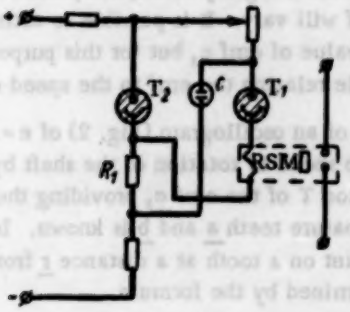

Fig. 3

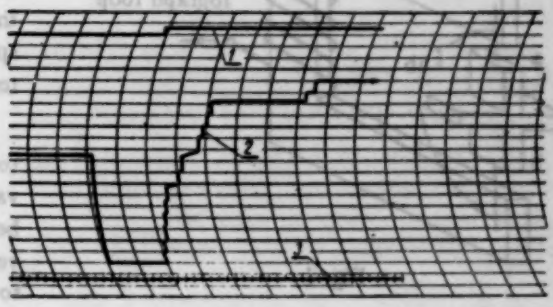

Fig. 4

We have also made a capacitive timer with neon tubes and a balancing circuit which provides high stability in the relay operation with larger variations of the supply voltage. This circuit is shown in Fig. 3.

The supply circuit of the neon tube T_1 and capacitor C is fed by a voltage obtained across a part of a resistance in the stabilivolt T_2 circuit. Supply voltage variations produce corresponding changes in the voltage drop across resistor R_1, and hence in the ignition voltage of neon tube T_1, thus compensating the effect of relatively larger variations of the supply voltage.

The loaded operating conditions are recorded by means of relay 2 (Fig. 2) whose winding is fed from an auxiliary generator when push-button switch 3 of the diesel locomotive control board is operated. The current flows to the

negative pole of the auxiliary generator. The magnetic flux thus produced in the relay winding attracts the armature with its pen which contacts the chart.

When the diesel locomotive runs without a load the relay is de-energized, since push-button switch 3 is disconnected. The relay armature with its pen returns to normal under the effect of a spring.

Fig. 4 shows the chart with a recording of the controller handle position 2), the loaded operation condition 1), and the time marks 3).

This instrument, in conjuction with a speedometer and an instrument recording the temperature of the driving motor windings makes it possible to carry out scientific investigations in determining the optimum weights of trains under actual driving conditions, and study the operation of locomotive diesel engines as well as the handling of trains by the most experienced engine drivers.

TRANSDUCER FOR MEASURING THE ROTATION SPEED OF A SHAFT

P. R. Pugovkin

Translated from Izmeritel'naya Tekhnika, No. 11,
pp. 22-23, November, 1961

In many instances it is necessary to measure the rotation speed of a driving or driven shaft at any instant of its acceleration or deceleration. In such instances it is advisable to use for oscillographing the rotation speed of the shaft a transducer of the induction type.

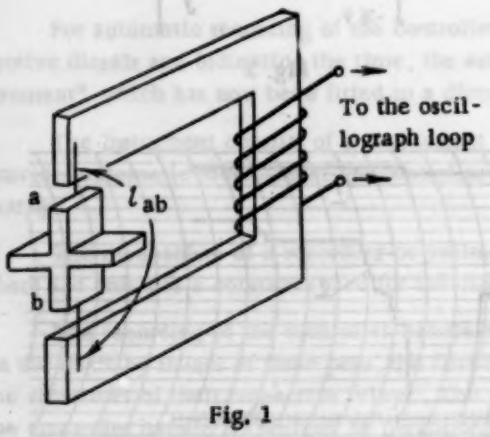

Fig. 1

The transducer (Fig. 1) consists of the simplest induction type ac generator. One complete revolution of the armature, providing it has a suitable shape, will produce two maxima and minima in the magnetic flux Φ of the transducer core.

During the acceleration or braking of the shaft, to which the transducer armature is rigidly fixed, the period and amplitude of the induced emf will vary. It is possible to estimate the rotation speed n by the value of emf e, but for this purpose it is necessary to know the scale relating the emf to the speed of rotation.

By means of an oscillogram (Fig. 2) of $e = f(t)$, it is possible to determine the speed of rotation of the shaft by measuring the variation of period T of the emf e, providing the distance l_{ab} between the armature teeth a and b is known. In fact, the linear velocity of a point on a tooth at a distance r from the center of rotation is determined by the formula

$$v = \frac{l_{ab}}{t}, \qquad (1)$$

where v is the linear velocity of a tooth crest; l_{ab} is the distance between teeth over a circumference of radius r, t is the time in which the crest of a tooth covers distance l_{ab} (recorded by the timer).

Linear velocity v and angular velocity ω of a point are related to each other by the following equality:

$$v = \omega r, \qquad (2)$$

where r is the radius measured from the point to the rotation axis.

By substituting in (2) the linear velocity by its value from (1) and expressing the angular velocity by the rotation speed we obtain

$$\frac{l_{ab}}{t} = \frac{2\pi n}{60} r, \quad \text{whence} \quad n = \frac{30 l_{ab}}{\pi r t}, \text{ rpm} \tag{3}$$

If the transducer armature is made with a radius r = 1 cm the number of armature teeth is z = 4 and the distance between the teeth a and b is equal to l_{ab} = 3.14 cm, the expression for t in seconds obtained from (3) can be simplified to

$$n = \frac{30}{t}, \text{ rpm} \tag{4}$$

In order to raise accuracy in measuring n it is necessary to increase the number of teeth in the transducer armature.

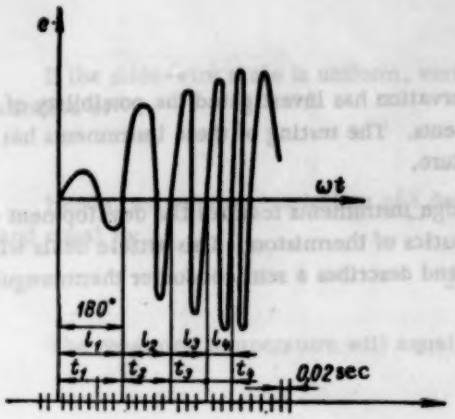

Fig. 2

By means of oscillograms it is possible to estimate the rotation speed for virtually any time interval. The varying amplitudes of the curve seen on the oscillogram provide an estimate of the nonuniformity of the rotation speed of the motor during acceleration. This can also be estimated from the variation in segments ab along the time axis.

Conclusions. The design of the proposed transducer is very simple; it consists of a few components and is simple to manufacture and assemble. It can be made a fraction of the size of the smallest tachogenerator type TGP-3. The power consumed by it is insignificant. Its coupling to the shaft of the object under investigation produces virtually no effect on the operating conditions of the latter.

Contrary to tachogenerators with permanent or electromagnets, this transducer does not require periodic checking of its calibrations.

THERMOTECHNICAL MEASUREMENTS

TRANSISTORIZED INSTRUMENT FOR REMOTE MEASUREMENT AND CONTROL OF TEMPERATURE

S. V. Andreev, B. K. Martens, and A. N. Trushinskii

Translated from Izmeritel'naya Tekhnika, No. 11,
pp. 23-27, November, 1961

The biophysics laboratory of the All-Union Institute of Plant Preservation has investigated the possibility of replacing wire resistors by semiconductors in bridges of electronic instruments. The testing of these instruments has revealed high accuracy (0.2-0.3°C) in measuring and controlling temperature.

The use of thermistors in place of metal resistors in electronic bridge instruments requires the development of new bridge designs to accomodate the large differences in the characteristics of thermistors. This article deals with the principles for designing thermistor bridges in electronic instruments and describes a semiconductor thermoregulator.

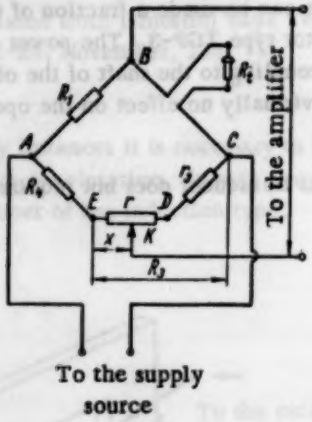

Fig. 1

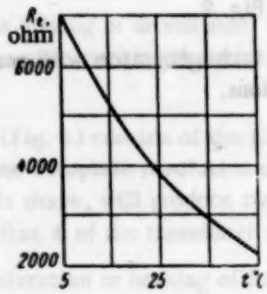

Fig. 2

The instrument with a thermistor R_T is based on a normal bridge circuit (Fig. 1), and in the principle of its operation does not differ from the commercially produced electronic automatically balancing bridges for measuring temperature by means of resistance thermometers.

Let us assume that this bridge is intended for measuring temperatures in the range of t_1 to t_2. At the initial minimum measured temperature t_1 slider K will be in its initial position, i.e., at point E. In this case $x = 0$, and thermistor R_t will be at its maximum value of R_{max}.

Then

$$\frac{R_{max}}{R_1} = \frac{R_3}{R_4}. \quad (1)$$

At the maximum measured temperature t_2 slider K will be in the opposite extreme position at point D.

In this case $x = r$ and the thermistor will have its minimum value R_{min}.

$$\frac{R_{min}}{R_1} = \frac{R_3 - r}{R_4 + r}. \quad (2)$$

In the intermediate positions of the slider

$$X = \frac{R_3R_1 - R_tR_4}{R_1 + R_t} = \frac{R_4(R_{max} - R_t)}{R_1 + R_t}. \quad (3)$$

Let us introduce the notation

$$\frac{R\max}{R_1}=\frac{R_3}{R_4}=n, \tag{4}$$

$$\frac{R_4}{R_1}=m. \tag{4'}$$

Having inserted these notations in (3) we obtain

$$X=\frac{m(R\max-R_t)}{1+\frac{nR_t}{R_{\max}}}. \tag{5}$$

If the slide-wire scale is uniform, variations of temperature by 1° will correspond to changes in the slide-wire resistance of

$$\frac{r}{t_2-t_1}. \tag{5a}$$

Hence, temperature variations of t degrees will correspond to changes in the slide-wire resistance amounting to x and equal to:

$$x=\frac{rt}{t_2-t_1}, \text{ whence } t=\frac{x(t_2-t_1)}{r}. \tag{5b}$$

The measured temperature will equal $t_m=t_1+t$ or

$$t_m=t_1+\frac{x(t_2-t_1)}{r}. \tag{6}$$

The designing of a bridge includes not only determining the resistances of the bridge on the basis of the temperature measuring limits t_1 and t_2 but also obtaining a sufficiently uniform scale for the instrument.

Let us assume that the measuring limits of an electronic bridge amount to $t_1=5°$ and $t_2=45°$. The slide-wire scale of a resistance r = 140 ohm is uniformly calibrated with respect to temperature.

Bridge resistances have the following values: $R_1=7065$ ohm and $R_3=270$ ohm.

Let us determine the readings of the bridge at different temperatures if it incorporates a thermistor whose characteristic is given in Fig. 2.

According to (4) we have n = 1, m = 0.038. By inserting these values in (5) and (6) it is possible to calculate the instrument readings at different temperatures.

On the basis of these calculations a graph was plotted (Fig. 3).

The curve for an actual thermistor shows that in the middle of the scale it provides slightly higher readings (by 2-3°).

By means of the same formulas a scale calculation was made for an "ideal" thermistor which has a linear temperature characteristic.

It will be seen from Fig. 3 that if an "ideal" thermistor is used the middle part of the scale will have a reading by 3-5° lower than the actual temperature.

From a comparison of the actual and "ideal" thermistors it will be seen that it is possible to select a thermistor with a characteristic which will provide instrument readings with an insignificant deviation from the actual temperature.

Such a characteristic can easily be obtained if the thermistor is shunted by a fixed resistor of a definite value. However, the shunting of a thermistor reduces considerably the sensitivity of the circuit.

A second method of obtaining a uniform scale consists of selecting coefficients m and n [see (4)].

In order to find the effect of these coefficients on the instrument readings let us examine a bridge circuit with a thermistor which has a characteristic shown in Fig. 2. The slide-wire resistance is equal to 140 ohm.

Let us see how the instrument readings will vary for various values of bridge resistances R_1, R_3, and R_4, i.e., for various values of coefficients m and n.

Figure 4 shows the relation between instrument readings and temperature measurements for various values of coefficient n with the other coefficient fixed at m = 0.045.

It will be seen from this graph that for values of n > 2 the instrument gives readings below the measured temperature, and its measuring range decreases with a rising n. With coefficient n < 1.5 the instrument provides readings above the measured temperature.

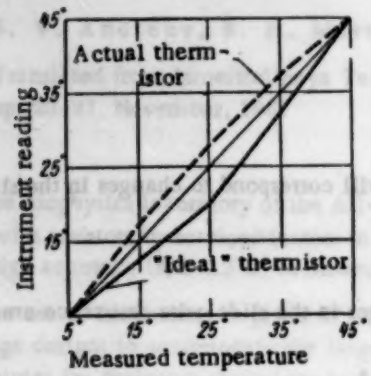

Fig. 3

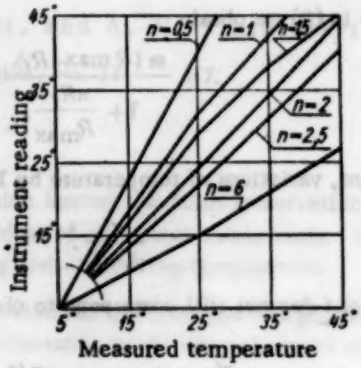

Fig. 4

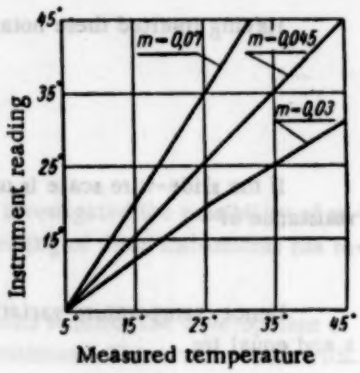

Fig. 5

Let us examine the case when coefficient n is fixed at 1.72 and coefficient m varies.

Let us determine how the variations of coefficient m affect the instrument readings. Fig. 5 shows the relation between the instrument readings and the measured temperature for various values of m.

It will be seen from the graph that the instrument range increases with a rising m.

It will be seen from these graphs (Figs. 4,5) that variations in coefficients m and n also affect the linearity of the instrument scale.

For certain optimum values of coefficients m and n an instrument characteristic is obtained which is linear over a given range of temperatures.

The optimum values for coefficients m and n can be obtained analytically on the basis of the following propositions.

Let us assume that this instrument's temperature range has a lower limit of t_1 and an upper limit of t_2. Let us denote the value of the thermistor at temperature t_1 by R_{max}, and that at temperature t_2 by R_{min}.

After subtracting from (1) equation (2) and performing simple operations we obtain

$$R_{max}-R_{min}=\frac{r\left(1+\frac{R_3}{R_4}\right)}{\frac{R_4}{R_1}+\frac{r}{R_1}}, \tag{6a}$$

and after inserting coefficients m and n from (4) we have

$$R_{max}-R_{min}=\frac{r(1+n)}{m+\frac{rn}{R_{max}}}. \tag{6b}$$

By solving this equation with respect to m we obtain

$$m=\frac{rn\left(\frac{R_{min}}{R_{max}}+\frac{1}{n}\right)}{R_{max}-R_{min}}. \tag{7}$$

We find now the value of n by introducing an additional condition, that the instrument scale should be uniform, i.e., that at a temperature t_m equal to

$$t_m = t_1 + \frac{t_2 - t_1}{2}, \tag{7a}$$

the corresponding resistance x of the slide-wire should be equal to r/2.

Let us assume that the resistance of the thermistor at t_m is equal to R_m. Then we shall have:

$$\frac{R_m}{R_1} = \frac{R_x - \frac{r}{2}}{R_4 + \frac{r}{2}}, \tag{8}$$

or

$$\frac{r}{2}(R_m + R_1) = R_1 R_x - R_m R_4. \tag{9}$$

Let us now, on the basis of equation (4), insert in (9) coefficients m and n

$$\frac{m R_{max}}{n}(R_{max} - R_m) = \frac{r}{2}\left(R_m + \frac{R_{max}}{n}\right). \tag{9a}$$

After substituting m by its value obtained from (7) we have

$$R_{max}\left(\frac{R_{max} - R_m}{R_{max} - R_{min}} - \frac{1}{2}\right) = n\left(\frac{1}{2}R_m - \frac{R_{min}R_{max} - R_{min}R_m}{R_{max} - R_{min}}\right). \tag{9b}$$

By solving this equation with respect to n we finally obtain

$$n = \frac{R_{max}\left(\frac{R_{max} + R_{min}}{2} - R_m\right)}{R_m\left(\frac{R_{max} + R_{min}}{2} - \frac{R_{max}R_{min}}{R_m}\right)}. \tag{10}$$

The evaluation of the optimum bridge supply voltage U_m should be based on the following considerations. The power dissipated by the thermistor for all the bridge operating conditions must not exceed the maximum permissible value W_e which is determined strictly for a given type of thermistor; the output current of the bridge for a given voltage must correspond to the operating current of the instrument connected to the bridge (measuring instrument, amplifying circuit, relay, etc.).

When the bridge is completely balanced the current passing through the thermistor which is at its minimum value amounts to

$$i_t = \frac{U_m}{R_1 + R_{min}}, \tag{11}$$

or

$$i_t = \frac{U_m}{\frac{R_{max}}{n} + R_{min}}. \tag{12}$$

When the bridge is unbalanced a current i_k will flow from its output to the thermoregulator and will amount to

$$i_k = U_m R_4 \frac{R_t}{a + b\Delta R_t}, \tag{13}$$

where ΔR_t is the variation in the thermistor resistance due to the bridge unbalance;

$$\begin{aligned} a &= R_s(R_1 + R_t)(R_3 + R_4) + R_1 R_t (R_3 + R_4) + \\ &\quad + R_3 R_4 (R_1 + R_t); \\ b &= (R_s + R_1)(R_3 + R_4) + R_3 R_4; \end{aligned} \tag{14}$$

R_t is the resistance of the thermistor for a balanced bridge; R_s is the load resistance connected to the bridge output.

The power dissipated in the thermistor is:

$$W = (i_t + i_k)^2 R_t. \tag{15}$$

This power must not exceed the maximum permissible power W_e for the given thermistor, i.e.

$$(i_k + i_t)^2 R_t < W_e. \tag{16}$$

Knowing the value of signal i_k transmitted from the bridge output to the regulator, as well as the value of R_t which ensures a given accuracy of temperature control, it is possible to determine from (12) and (16) the voltage U_m which should be supplied to the bridge.

By means of the above method a transistorized thermoregulator was computed, designed and produced for automatic remote control of temperature.

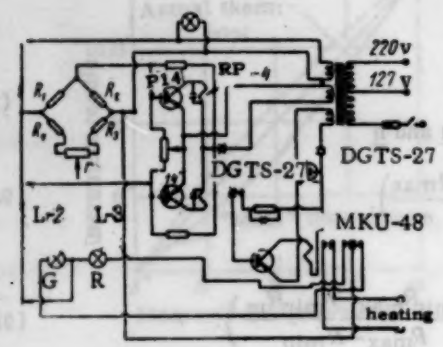

Fig. 6

N.B. L-2 is cooling; L-3 is heating.

Fig. 6 shows the schematic of the thermoregulator, which consists of the following basic units: a supply circuit which includes a step-down transformer; a bridge circuit; an amplifier consisting of two transistors for amplifying the signals fed from the bridge output to the control relay RP-4; and a circuit for amplifying the signals derived from relay RP-4 to the control winding of the actuating relay MKU-48.

One of the secondary windings of the power transformer serves to feed the bridge circuit; another winding connected to a crystal diode supplies two transistors which are fed by an alternating current in the negative halfperiod. The third winding serves to feed transistor P-3A, whose circuit contains a relay, diode DGTs-27 and a reservoir capacitor.

The thermoregulator differs from the bridge described above by the fact that it is not automatically balanced by the displacement of a slider along a slide-wire, but a preliminary setting of this slider adjusts the regulator to the required temperature.

The high resistance of a thermistor provides the bridge with a high output resistance, so that the resistance of the connecting leads does not affect appreciably the operation of the circuit, which is an essential advantage of the transistorized circuit.

For a given position of the slide-wire slider the bridge will become balanced when the temperature of the thermistor becomes equal to the set value.

When the temperature deviates from the set value the bridge becomes unbalanced. The output current of the bridge amplified by transistors P14 is fed to the control windings RP-4 circuit.

Relay RP-4 operates when the phase of the collector current of one of the P-14 transistors coincides with the phase of the bridge output current.

Should the negative phases on the base and collector of one of the transistors coincide, the transistor will become conducting, whereas the other transistor will remain blocked and a current will flow depending on its direction through one of the relay windings.

The operation of relay RP-4 feeds a signal to transistor P-3A. Amplified by the transistor this signal is fed to the control winding of relay MKU-48. This relay can switch electrical heaters with a power up to 5 kva. In this circuit the transistors are connected in such a manner that the current flowing through them, depending on its direction, can switch this relay either to the on or off position.

By mean: of this regulator it is possible to set the temperature to any value within its operating range. In order to reset the operating temperature it is sufficient to move the slider along the slide-wire r.

Each temperature value corresponds to a definite position of the slide on the slide-wire r. The slide-wire is calibrated in degrees Celsius. By means of this scale the position of the slide-wire slide is determined and thus the required temperature is set.

The biophysics laboratory of the All-Union Institute of Plant Preservation has produced several transistorized models of thermoregulators which operate in the range of -10 to $+60°C$. These thermoregulators control temperature with an error not exceeding 0.3°C.

The maximum current flowing through the thermistors of the thermoregulator does not exceed 100-200 μa, and the power dissipated by the thermistor is of the order of 10^{-4} to 10^{-5} w. This power is considerably smaller than the maximum permissible power for thermistors working in measuring circuits (10^{-3} w). For a signal of 20 μa received from the bridge output the thermoregulator has a breaking capacity of 5 kw.

Conclusions. The preceding thermoregulator uses transistors and crystal diodes in addition to thermistors, thus eliminating completely electron tubes from the circuit, and ensuring reliable operation of the relay even for weak signals received from the bridge output.

The transistorized thermoregulator is not inferior to electron tube regulators with respect to control accuracy, but it is considerably smaller and lighter than the latter.

The response of the thermoregulator to weak bridge signals makes it possible to use not only thermistors type MMT-4 in the bridge circuit, but also type MMT-6, which are microthermistors whose small dimensions provide the measurement and control of temperature at a given point.

AUTOMATIC MEASUREMENT OF SMALL TEMPERATURE DIFFERENCES

V. Ya. Kozhukh

Translated from Izmeritel'naya Tekhnika, No. 11,
pp. 27-29, November, 1961

In order to control the operation of many industrial assemblies the possibility of measuring small temperature differences is of considerable interest. Thus, for the correct operation of compressors the permissible heating of the cooling water in the intermediate air cooler amounts to 4°C, in the cooling jackets of the low- and high-pressure cylinders to 6°C, and in the cylinder cover jackets to 4°C. In the area of the well and hearth of a blast furnace water temperature is measured up to 200 times a day by means of mercury thermometers at the input and output of condensers and the temperature difference calculated. In the above and several other instances a measurement error in the range of ±(3-5)% is permissible, since the object of these measurements is not accuracy but the recording of parameter variations with time and the signalling of its deviation from set values. However, the use of standard instruments for automatic measurements of small differences of temperature is impossible without altering their measuring circuits.

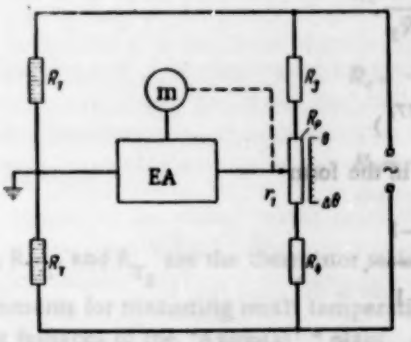

Fig. 1. Schematic of an automatic instrument for measuring temperature differences.

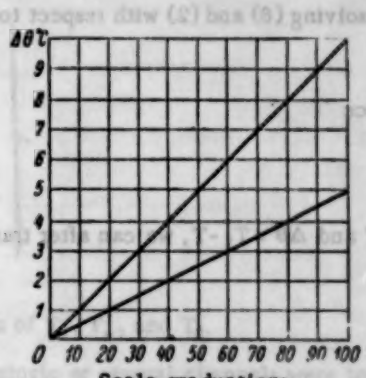

Fig. 2. Graph of the relationship of instrument readings to temperature differences.

Reports on the use of thermistors for measuring temperature are appearing at an increasing rate. However, circuits with automatic compensators and thermistors have not received sufficient attention in literature.

We have investigated one of the many possible varieties of thermistor circuits for measuring temperature differences. This circuit is hown in a simplified manner in Fig. 1. The circuit is made up of standard electronic instruments of the MS (PS) type or other types from whose measuring circuits only slide-wires are used. The possibility of grounding the transducer's casing simplifies its design with the use of thermistors type MMT-4 and KMT-4. For connecting transducers to the instrument a minimum number of leads is required.

The design of the bridge circuit (Fig. 1) by means of the known characteristics (R_T, the initial measurement temperature T (θ), the measured temperature difference $\Delta\theta$ and the slide-wire resistance R_s) can be achieved by deriving and solving bridge balance equations. At the beginning of the scale the bridge is balanced for equal resistances R_T of the transducers and $\Delta\theta = 0$ when:

$$R_T \cdot (R_4 + R_p) = R_T \cdot R_s, \tag{1}$$

or

$$R_s = R_4 + R_p. \tag{2}$$

If the temperature of one of the thermistors is changed by $\Delta\theta$ the balance will be attained when

$$R_T \cdot R_4 = (R_T - \Delta R_T) \cdot (R_s + R_p), \tag{3}$$

where R_T is the resistance of the thermistor for a temperature of T(θ); ΔR_T is the variation in the resistance of one of the transducers for a temperature change of $\Delta\theta$.

By solving (2) and (3) we obtain

$$R_s = 2R_p \cdot \left(\frac{R_T}{\Delta R_T} - 0{,}5 \right), \tag{4}$$

$$R_4 = 2R_p \cdot \left(\frac{R_T}{\Delta R_T} - 1 \right). \tag{5}$$

From (4) and (5) we can calculate the values of resistors R_s and R_4 for instruments with different slide-wire resistances, different thermistors and measuring ranges.

It is known that if transducers are not connected to adjacent arms of a balanced bridge the scale of an automatic instrument becomes nonuniform. The instrument scale equation can be obtained from the balance conditions of the bridge for intermediate values of $\Delta\theta$.

$$R_T \cdot (R_4 + R_p - r_1) = (R_T - \Delta R_T) \cdot (R_s + r_1), \tag{6}$$

where

$$0 < \Delta R_T < \Delta R_{T\,max} \quad \text{for} \quad 0 < \Delta\theta < \Delta\theta_{max}$$

By solving (6) and (2) with respect to r_1 we obtain the instrument scale equation

$$r_1 = R_s \frac{\Delta R_T}{2R_T - \Delta R_T}. \tag{7}$$

Since

$$R_T = Ae^{B/T}$$

$$\Delta R_T = A\left(e^{B/T} - e^{B/T_1}\right) \tag{7a}$$

for $T_1 > T$ and $\Delta\theta = T_1 - T$, we can after transformations write (7) in the form

$$r_1 = R_s \frac{\exp\left(\frac{B \cdot \Delta\theta}{T \cdot T_1}\right) - 1}{\exp\left(\frac{B \cdot \Delta\theta}{T \cdot T_1}\right) + 1}. \tag{8}$$

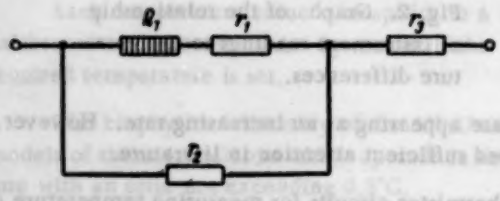

Fig. 3. Schematic for correcting thermistor temperature characteristics.

The bridge supply voltage can be found from the conditions of the maximum permissible dissipation in a thermistor.

$$U = \sqrt{P_{TP}(2R_T - \Delta R_T)}. \tag{9}$$

Calculations made by means of (7) and (8) and investigations of the circuit (Fig. 1) have shown that the instrument scale is virtually linear for the measured temperature differences up to 10°C. Fig. 2 shows the relation between the readings measured temperature differences for instruments with ranges of

$$\Delta\theta = 0{-}5 \quad \text{and} \quad \Delta\theta = 0{-}10°C. \tag{9a}$$

It will be seen from (8) that the instrument calibration changes with variations of the absolute temperature T and the other parameters remaining constant. Calculations and measurements made in a circuit shown in Fig. 1 have revealed that variations in the absolute temperature in the range of 0-50°C introduce an additional error in the measurement results of about ± 6%. This error is due to the nonlinearity of the thermistors' temperature characteristics. In order to provide interchangeability of transducers in multichannel instruments and in circuits with relatively large temperature variations it is, therefore, necessary to correct for the nonlinearity of thermistor characteristics.

The essence of these corrections consists in changing the thermistor characteristics by additional linear resistors connected in series and in parallel with the thermistors.

In [1] and [2] computation formulas are given for matching characteristics in two points, and in [3] for matching them in three points of a given temperature range.

The temperature characteristics of circuits with thermistors are virtually linear if they pass through three chosen points within the temperature range and satisfy the condition

$$R_1+R_3=2R_c, \tag{10}$$

where R_1 and R_2 are circuit resistances which correspond to temperatures T_1 and T_2; R_C is a resistor which corresponds to temperature T_C in the center of the temperature range.

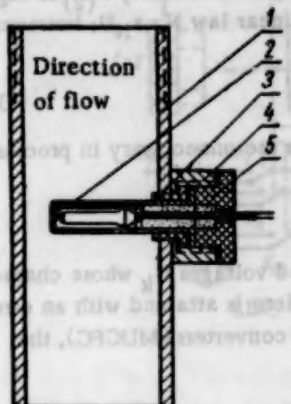

Fig. 4. Construction of a transducer with a thermistor.

Calculations carried out with the assistance of V. A. Rostun by means of formulas [3] for the circuit shown in Fig. 3 have shown that condition (10) is met with an accuracy of 0.2-0.3% in the range of 0 to 50°C and with an accuracy of 0.6-0.8% in the range of 0 to 100°C. Condition (10) for Fig. 3 is met with greater accuracy if in formulas [3] the value of resistors r_1 and r_2 is determined by means of the equation

$$r_1+r_2=\frac{R_{T_1}\cdot R_{T_3}-2R_{T_1}\cdot R_{T_3}+R_{T_c}\cdot R_{T_3}}{R_{T_1}-2R_{T_c}+R_{T_3}}=R. \tag{11}$$

Expression (11) is derived from (10) by inserting into it the values of R_1, R_2, and R_C for the circuit shown in Fig. 3.

$$\left.\begin{aligned} R_1&=\frac{(R_{T_1}+r_1)\cdot r_2}{R_{T_1}+r_1+r_2}+r_3\\ R_c&=\frac{(R_{T_c}+r_1)\cdot r_2}{R_{T_1}+r_1+r_2}+r_3\\ R_3&=\frac{(R_{T_3}+r_1)\cdot r_2}{R_{T_3}+r_1+r_2}+r_3 \end{aligned}\right\}. \tag{12}$$

where R_{T_1}, R_{Tc}, and R_{T_2} are the thermistor resistances at temperatures of T_1, T_C, and T_2.

Instruments for measuring small temperature differences with a single or several channels were tested at one of the blast furnaces of the "Azovstal'" plant. A schematic of the construction of one of the experimental transducers is shown in Fig. 4. The transducer is mounted in a pouring pipe 1 to which steel sleeve 4 is welded. The transducer casing 2 is made of stainless steel. In order to reduce the heat conduction from the surrounding medium and the walls of pipe 1 to the thermistor a textolite bush 3 and nut 5 are used. After securing the thermistor in its casing the latter is filled with a lagging material.

Both calculations and tests have shown that thermistors can be used over long time intervals for measuring small temperature differences when the required accuracy of measurements is not high, ±(3-5%). With a periodic correction of the instrument's calibration, which varies due to the instability of the thermistor characteristic, the accuracy of measurements can be raised considerably.

LITERATURE CITED

1. M. A. Kaganov, Avtomatika i telemekhanika, No. 1, 1952.
2. G. K. Nechaev, Elektrichestvo, No. 4, 1956.
3. G. K. Nechaev, Elektrichestvo, No. 10, 1960.

ELECTRICAL MEASUREMENTS

UNIVERSAL CODERS FOR AUTOMATIC MEASURING SYSTEMS

V. B. Smolov

Translated from Izmeritel'naya Tekhnika, No. 11, pp. 30-35, November, 1961

In developing modern automatic measuring, transmitting and monitoring systems in which subsequent data processing is effected by means of digital computers the problem of converting dc voltages U into a binary $N_{(2)}$ or digital-pulsed $N_{(1)}$ (unit) codes with U→N is topical. Normally, this conversion follows a linear law $N = a_N U$; however in a number of instances functional conversion

$$N = a_N F(U), \tag{1}$$

is required which either simplifies the programming of the digital computer or makes its use unnecessary in processing the measuring results.

In (1) a_N = const is the conversion scale.

If conversion (1) has to be made almost simultaneously for a large number of coded voltages U_k whose characteristics (1) differ considerably from each other, the optimum solution of the above problem is attained with an error not exceeding 0.1-0.5% by means of so-called multichannel universal coding functional converters (MUCFC), the design principles of whose circuits are discussed in this work.

Open-type MUCFC. If the voltage U_k (k = 1, 2 . . . n) received from various transducers of continuous information is coded in the same functional relationship $N_k = a_n F(U_k)$ common to all the channels, the block schematic of an open MUCFC is of the type shown in Fig. 1. This converter operates in the following manner.

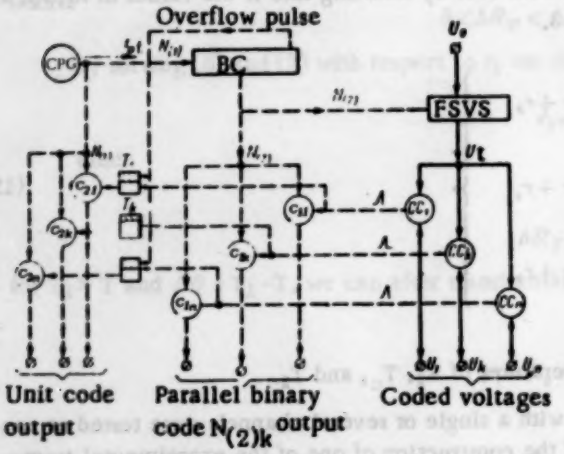

Fig. 1. Block schematic of an open-type MUSFC. CPG is the counting-pulse generator; BC is the binary counter of pulses; FSVS is the universal functional step voltage shaper; T_k are the trigger circuits; P_{1k} and P_{2k} are the pulse potential coincidence elements; CC_k are the pulse circuits for comparing FSVS output voltage U_t with the corresponding coded voltage U_k.

Generator CPG continuously transmits pulses at a frequency of f_p which are counted by the m-th order binary counter BC. After each overflow of the counter the counting cycle is repeated; moreover, the duration of the cycle is equal to $t_c = 2^m / f_p$.

The parallel binary code $N_{(2)}$ of the number of pulses $N_{(1)}$ is supplied from the BC to control the operation of the FSVS whose output voltage U_t is proportional, irrespective of the CPG frequency stability, to a calculated function Φ of the number of pulses $N_{(1)}$.

$$U_t = a_U \Phi(N_{(1)}), \tag{1a}$$

where a_U = const is the decoding scale.

The periodic functional step voltage U_t is fed from the output of the FSVS to the CC_k circuits which produce short pulses when $U_k = U_t$ (k = 1, 2 . . . n). These pulses operate the groups of gates P_{1k}, which transmit to the appropriate converter output the code $N_{(2)k}$.

If during the conversion cycle duration t_c any of the coded voltages U_k changes by less than ΔU_k in which the code increment $\Delta N_{(2)k}$ does not exceed a given error of functional decoding $(\Delta N)_{max}$, the following relation will hold for this device:

$$U_k = \frac{U_{k\,max}}{[\Phi(N_k)]_{max}} \cdot \Phi(N_k) = a_U \Phi(N_k) \tag{2}$$

or

$$N_k = \frac{(N_k)_{max}}{[F(U_k)]_{max}} \cdot F(U_k) = a_N F(U_k), \tag{3}$$

where $F[\Phi(N_k)] = N_k$, and a_U and a_N are the respective decoding and coding scales.

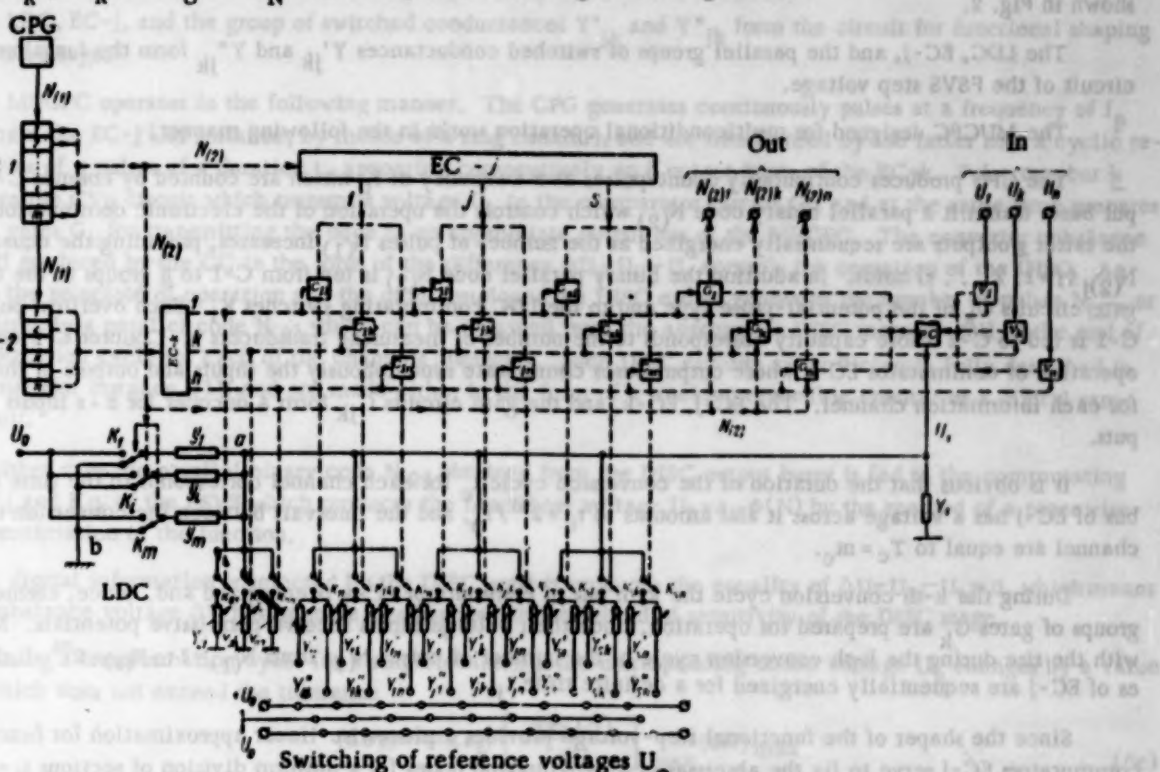

Fig. 2. Block schematic of an open-type MUCFC for multiconditional operation. CPG is the counting-pulse generator; C-1 and C-2 are the binary counters for m and n orders respectively; EC-j and EC-k are electronic commutators for $j_{max} = S$ and $k_{max} = n$ separate outputs respectively; CV_k are electronic circuits for transmitting the values of voltages U_k to the PC input; PC is the pulse comparator; G_k are the groups of gate coincidence circuits; C_{jk} are the individual gate coincidence circuits; LDC is the linear decoding converter to whose output are connected by means of electronic switches K_{jk} rehostats Y'_{jk} and Y''_{jk} which serve as controlled building-out admittances; y_i is the LDC discharging admittance proportional to the appropriate binary powers 2^i; K_i are the two-position electronic switches which serve to switch y_i when code $N_{(2)}$ changes; U_o is the LDC supply of voltage.

The shaping of the digital output in the form of a digital pulse (unit) code $N_{(1)k}$ is obtained in the circuit by means of triggers T_k and the coincidence circuits P_{2k} which they control. At the instant when counter BC is restored, trigger T_k is "tripped" and when the short pulse is received from the appropriate CC_k circuit, the trigger is "blocked." Therefore, element P_k transmits to the appropriate converter output per conversion cycle t_c a number of pulses $N_{(1)k}$ proportional to a given function

$$N_{(1)k} = \frac{[(N_{(1)})]_{max}}{[F(U_k)]_{max}} \cdot F(U_k) = a_N F\ U_k), \tag{4}$$

since $t_k = F(U_k)$.

The use of an open-type MUCFC is of great practical interest for coding each of the n voltages U_k according to an individual relationship

$$\left.\begin{array}{l} N_k = a_N F_k(U_k) \\ (k = 1,2, \ldots n) \end{array}\right\}. \tag{5}$$

It is obvious that in order to put into practice relationship (5) it is necessary to make the circuit of the MUCFC

a little more complicated in order to separate in time the individual transformation cycles t_c for each of which the FSVS must be reset automatically so as to reproduce the required individual relationship (5).

The blockschematic of the MUCFC which meets the requirements of a multiconditional coding operation is shown in Fig. 2.

The LDC, EC-j, and the parallel groups of switched conductances Y'_{jk} and Y''_{jk} form the functional shaping circuit of the FSVS step voltage.

The MUCFC designed for multiconditional operation works in the following manner.

The CPG produces continuously count-pulses at a frequency of f_p which are counted by counter C-1 whose output buses transmit a parallel binary code $N_{(2)}$ which controls the operation of the electronic commutator EC-j. In the latter s outputs are sequentially energized as the number of pulses $N_{(1)}$ increases, providing the equation $N_{(2)} = N_{(2)j}$ (j=1, 2 . . . s) holds. In addition the binary parallel code $N_{(2)}$ is fed from C-1 to n groups of the coincidence gate circuits G_k of the potential-pulse type and to the LDC commutating switches K_i. Each overflow pulse of counter C-1 is fed to C-2 whose capacity corresponds to the number of measuring transducers n. Counter C-2 controls the operation of commutator EC-k whose output buses commutate synchronously the inputs and outputs of the converter for each information channel. The EC-j, EC-k, and the gate circuits C_{jk} form a decoder for n+s inputs and ns outputs.

It is obvious that the duration of the conversion cycle t_c for each channel corresponds to the time the output bus of EC-j has a voltage across it and amounts to $t_c = 2^m/f_p$, and the intervals between the conversion cycles for each channel are equal to $T_c = nt_c$.

During the k-th conversion cycle the k-th bus of commutator EC-k is energized and, hence, elements C_{jk} and groups of gates G_k are prepared for operation, since their voltage inputs receive permissive potentials. Moreover, with the rise during the k-th conversion cycle of the number of pulses $N_{(1)}$ from $N_{(1)}=1$ to $N_{(1)}=2^m-1$, the output buses of EC-j are sequentially energized for a definite time t_j.

Since the shaper of the functional step-voltage provides a piecewise-linear approximation for function $\Phi(N)$, commutators EC-j serve to fix the abscissas of approximation nodes for a uniform division of sections $t_j = t_c/s$ as well. Thus, for each channel number k and approximation section number j the corresponding output potential of element C_{jk} connects an appropriate electronic switch K_{jk} which connects to the output of the LDC a group of parallel admittances Y'_{jk} and Y''_{jk}.

Depending on the type of FSVS circuit used, switch K_{jk} can be either disconnected when bus number j of commutator EC-j is switched off, or remain connected to the end of the cycle. In the first instance the angular coefficient of the LDC output voltage U_t linear variation is provided by connecting to the LDC output admittance the sum of admittances $Y'_{jk}+Y''_{jk}$ and in the second instance by connecting total admittance $\sum_{1=1}^{1=i} (Y'_1+Y''_1)$.

The building-out admittances Y_{jk} are connected to the zero potential bus or the reference voltage $\pm U_o$. Hence, they produce a definite bias voltage U_{ojk}, thus providing a change in the LDC output voltage at the j-th approximation section with respect to the value of the ordinate at the beginning of the section. This provides a functional decoding of $N_{(2)}$ according to the law $U_t = a_U \Phi(N)$ by means of a piecewise-linear approximation.

At the instant of the equality of voltages $U_t = U_k$ the pulse comparator PC operates and its short pulse trips the appropriate group of gates G_k, which transmits to the converter output along channel number k a parallel binary code $N_{(2)k}$ proportional to the voltage function U_k:

$$N_{(2)k} = a_N F_k(U_k). \qquad (5a)$$

This provides functional coding of voltage U_k according to the law $N_k = a_N F_k(U_k)$.

Obviously, if admittances Y'_{jk} and Y''_{jk} are calculated for each information channel according to a given function $F_k(U_k)$ a multiconditional coding operation can be provided.

Closed-type MUCFC. Contrary to the previously-described MUCFC schematics in which the FSVS operates independently by variations in the coded voltage U_k, in a closed-type MUCFC the coded voltage U_k controls directly

the operation of the FSVS. Fig. 3 shows an MUCFC schematic suitable for multiconditional coding operation according to the laws

$$N_{(2)k} = a_N F_k(U_k): \quad k = 1, 2, \ldots n. \tag{5b}$$

The LDC, EC-j, and the group of switched conductances Y'_{jk} and Y''_{jk} form the circuit for functional shaping of the FSVS voltage.

The MUCFC operates in the following manner. The CPG generates continuously pulses at a frequency of f_p which operate the EC-j (for instance, by means of a ring counter), and are transformed by the latter into a cyclic repeating series of $\underline{n}$ pulses of a duration t_c appearing consecutively on $\underline{n}$ output buses of the EC-k. Pulse number $\underline{k}$ commutates the CV_k circuit which transmits voltage U_k to the comparator circuit CC and at the same time prepares a group of gates G_k for transmitting the code to an appropriate output bus of the MUCFC. The converter unbalance voltage ΔU produced by the CC in the form of the difference $\Delta U = U_k - U_t$ controls the operation of the DISC. According to the principle of operation and the units employed the DISC either generates the number of pulses $N_{(1)}$, or produces directly a parallel code $N_{(2)}$ which can be obtained from the appropriate DISC memory cell at the end of the transformation cycle for each of the channels number $\underline{k}$. Such DISC circuits are sufficiently fully described in the literature (for instance, [1]) and are made either in the form of a tracking reversible counter or a digital sampling circuit.

In either case the parallel binary code $N_{(2)}$ obtained from the DISC output buses is fed to the commutating switches K_i and K_{jk} of the FSVS which produces the functional voltage $U_t = a_U \Phi(N)$ by the method of a piecewise-linear approximation of the function.

The digital information is selected by the DISC until it produces the equality of $\Delta U = U_k - U_t \approx 0$, which means that the unbalance voltage ΔU has become smaller than the threshold of sensitivity of the DISC stage.

If during a transformation cycle for a single channel $\underline{k}$ the corresponding coded voltage U_k changes by a value of ΔU_k, which does not exceed the tolerance

$$(\Delta U_k)_{\max} < a_U \left[\frac{d\Phi_k(N)}{dN}\right]_{\max} \cdot (\Delta N)_{\max} \tag{5c}$$

we shall obtain for a balanced device $U_k = U_n = a_U \Phi_k(N_k)$,

whence

$$N_{(2)k} = a_N F_k(U_k). \tag{5d}$$

A readout of the binary code $N_{(2)}$ can only be obtained after the completion of the transformation cycle in a given channel, and the determination of the end of the cycle is attained by various methods depending on the type of the DISC or the EC-k design.

If a closed-type MUCFC is intended for coding all the U_k voltages according to one and the same relationship $F(U_k)$, the schematic shown in Fig. 3 can be simplified considerably by reducing by a factor of $\underline{n}$ the number of building-out conductances Y'_{jk} and Y''_{jk} and the corresponding switches K_{jk}.

Functional step-voltage shaper FSVS is a decoding device and serves to produce voltage U_t which has a relationship to the binary code expressed by

$$U_t = a_U \Phi(N) \tag{5e}$$

Moreover, function $\Phi(N)$ is substituted by linear segments (broken line 012345 in Fig. 4a), whose number and dimensions depend on the chosen accuracy for a piecewise-linear approximation of the function. It will be seen from Fig. 4a that the value of voltage U_t within the j-th segment of the approximating broken line 012345 . . . is formed from the original ordinate $U_{(j-1)t}$ of this segment and the corresponding voltage increment $\Delta jU_t(N - N_j)/\Delta jN$:

$$[U_t] = U_{(j-1)t} + \frac{\Delta j\, U_t}{\Delta j\, N}(N - Nj), \quad N_{j-1} < N < N_j, \tag{6}$$

where N is the current value of the digital argument.

It is obvious that a device for producing function (6) can consist of a digital voltage divider whose transfer constant $A_j = \Delta jU_t / \Delta jN$ varies in steps according to the input digital information N. Moreover, this device must also be able to produce sums of the type of (6).

The value of $U_{(j-1)t}$ is fixed in advance in the form of reference (biasing) voltages and is connected to the summing circuit when argument N attains the corresponding value of the abscissa N_{j-1} at the beginning of the j-th approximation segment.

The FSVS whose circuit for operation with one channel is shown in Fig. 5 possesses the above properties. Multichannel FSVS circuits are shown in Figs. 2 and 3. The basic shaper unit consists of the LDS with the switched admittances $y_i = y_0^{2^i}$ whose switching in and out is made by means of the two-positional switches K_i. The switches are controlled from the digital units of the counting register which fixes the binary code $N_{(2)}$.

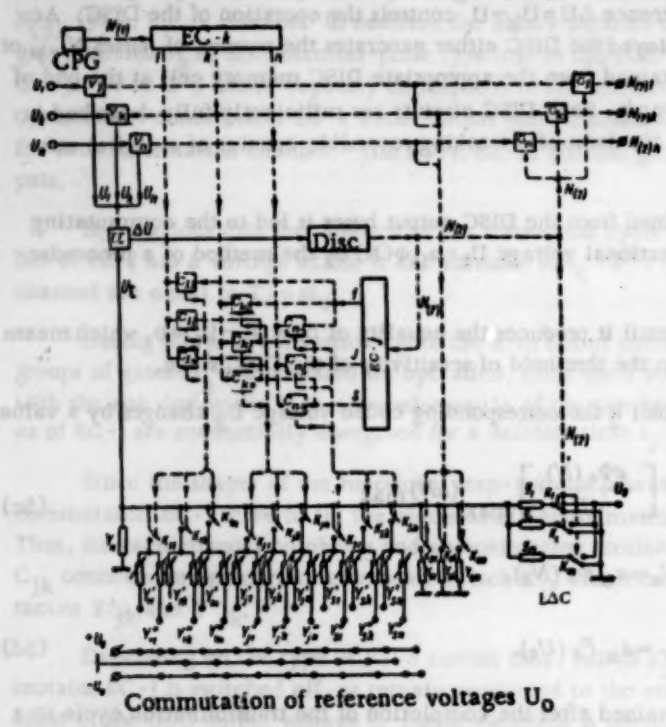

Fig. 3. Block schematic of a closed type MUCFC for multiconditional operation. CPG is the counting pulse generator; EC-k is the electronic commutator which provides cyclic repeating series of n pulses of t_c duration distributed among n buses; CV_k are electronic switches which transmit coded voltage U_k to the potential comparator circuit CC for comparing voltages U_t and U_k; DISC is the digital information selection circuit; EC-j is the electronic commutator which selects the number of the linear approximation segment for function $\Phi(N)$ and excites for a definite precalculated value of code $N_{(2)j}$ the appropriate output bus j; C_{kj} are the coincident circuits which commutate electronic switches K_{jk}; G_k are the groups of coincidence circuits for transmitting to the converter output buses appropriate codes $N_{(2)k}$; LDC is the linear decoding converter which has a constant output resistance and contains digital admittances $y_i = 2^i$ and two-position electronic switches K_i; Y'_{jk} and Y''_{jk} are building-out admittances consisting of precision rheostats designed for setting linear segment parameters of the approximating broken line $U_t = a_U \Phi(N)$.

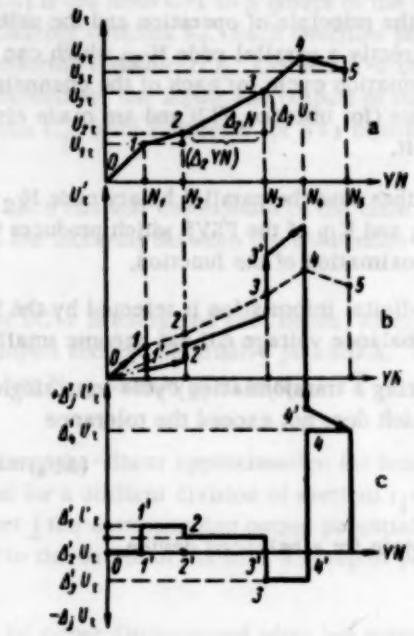

Fig. 4. Graph of the piecewise-linear approximation of function $U_t = \Phi(N)$.

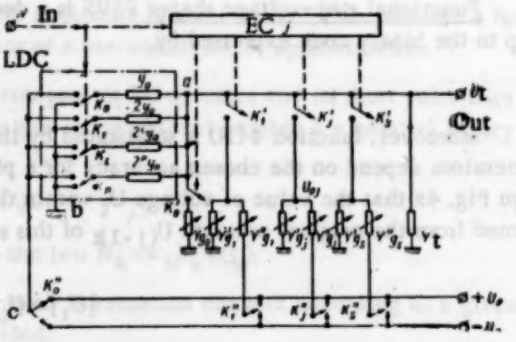

Fig. 5. Block schematic of an FSVS with adjustable admittances for single-channel operation.

If the order digit i (i = 0, 1, 2, . . . p) of code N is equal to 1, switch K_i connects admittance y_i to point c, and if the above figure is equal to 0 then it connects it to point b of the LDS. When K'_j is disconnected to LDS output voltage is proportional to a number whose N code is attained by commutating switches K_i since

$$U_n = U_0 \frac{(\sum y_i)_I}{(\sum y_i)_I + (\sum y_i)_{II}}, \tag{7}$$

where $(\Sigma y_i)_I = y_0 N = Y_N$ is the admittance of arm ac of the LDC; $(\Sigma y_i)_{II} = y_0(N_{max} - N) = Y_{max} - Y_N$ is the admittance of arm ab of the LDC.

It is obvious that for any value of N the following expression holds:

$$(\sum y_i)_I + (\sum y_i)_{II} = Y_{max} = y_0(2^{p+1} - 1) = \text{const.} \tag{8}$$

Hence, with switches K'_j disconnected the output voltage of the LDC is

$$U_t = U_0 \frac{Y_t}{Y_{max}} = U_0 \frac{N}{N_{max}} = A_1 U_0. \tag{8a}$$

Since the LDC output admittance is constant for any value of

$$y_{out} = Y_{max} \tag{9}$$

the LDC retains its linear characteristic when fixed admittances Y'_{gj} and Y''_{gj} are connected to its output; however, the ratio factor A of voltage U_0 is then changed in steps.

Switches K'_j are commutated by means of the electronic commutator of the corresponding approximation section. It consists of a decoding matrix with s outputs which are excited when the equality $N = N_j$ is attained and connect to the LDC the source of the biasing voltage through a rheostat circuit $Y'_{gj} - Y''_{gj}$. Let, for instance, switch K'_1 be operated having connected to the LDC output a group of parallel admittances Y'_{g1} and Y''_{g1}. If there were no biasing voltage $\pm U_0$ at the instant the switch was connected, a sudden jump would have occurred in the output voltage U_t (section 1 - 1', Fig. 4b), which would have built up for further variations of N, in the range of N_1 to N_2, again according to a linear law but with a different angular factor

$$U'_t = U_0 \frac{Y_N}{Y'_{g1} + Y''_{g1} + Y_{max}}. \tag{10}$$

In order to preserve the ordinate at the beginning of the second approximation sector at the instant switch K'_1 is connected through the dividing network Y'_{g1}, Y''_{g1}, and Y_{max}, a compensating voltage $\Delta'_1 U_t$ must be fed to the output of the LDC from the biasing source $U_0 = \text{const}$ (section 1' - 1', Fig. 4c).

Moreover, the linear variation of the output voltage U_t on the second approximation section will start at the level of ordinate U_{1t} at the beginning of that section (section 1-2, Fig. 4a).

Similar reasoning can be used in order to explain the operation of the FSVS at any approximation section when any of the switches K'_j are connected. Thus, at the instant of connecting the switch a jump in voltage $\Delta'_j U_t$ at the output of the LDC is compensated by voltage $\Delta'_j U_t$, and the required angular coefficient of the j-th section is provided by changing the ratio factor

$$A_j = \frac{Y_N}{Y'_{gj} + Y''_{gj} + Y_{max}}. \tag{11}$$

Fig. 4b shows a graph of the variations of U_t without a biasing voltage $\pm U_0$, Fig. 4c shows a graph of the compensating voltage $\Delta'_j U_t$ which is used for fixing the ordinates $U_{(j-1)n}$ at the beginning of the linear approximation sections.

With a convenient choice of the values of U_0, Y'_{gj} and Y''_{gj} it is possible to make the sum of voltages U_t broken line 011'2'3'4' . . ., Fig. 4b) and $\Delta'_j U_t$ (broken line 01'23'34'4 . . ., Fig. 4c) equal to voltage U_t (broken line 01234 . . ., Fig. 4a). Thus, the product of voltage $U_t = a_U \Phi(N)$ is obtained by means of the piecewise-linear approximation method.

If the FSVS is intended for the production of a constant relationship $\Phi(N)$, the building-out admittances Y_{gj}

are made in the form of fixed wire resistors soldered to the reference voltage source. If the application of the FSVS must cover all types of reproduced functions, it is more convenient to make admittances Y_{gj} in the form of precision multiturn rheostats by means of which it is possible to set any computed value for Y'_{gj} and Y''_{gj}. In the latter case the possibility of commutating the reference voltage $\pm U_0$ should be provided by mean of u-links shown in Fig. 5 as manually operated switches.

Bipolar voltage $\pm U_0$ supplied to the FSVS is necessary in order to provide negative incremental steps of the output voltage if $\Phi(N)$ is not monotonic. In calculating the FSVS for a given function it is necessary to choose according to a set accuracy $(\Delta N)_{max}$ and speed $(dU/dt)_{max}$ the required building-out admittances Y'_{gj}, and Y''_{gj} and voltage U_0 of the supply source. Calculations are made for each channel k=1, 2 . . . n of received information [2].

The coding cycle time t_c is determined on the basis of an obvious inequality

$$t_c\left[\frac{dF_k(U_k)}{dt}\right]_{max} < \delta\,[F_k(U_k)]_{max} \qquad (12)$$

where δ is the given relative error of coding in %.

Conclusions. The above block schematics of universal multichannel coding functional converters can be used for making up automatic digital measuring systems.

By means of these converters the measuring systems acquire computing characteristics which provide an evaluation and correction of errors due, for instance, to the nonlinearity of continuous information transducers. Moreover, the functional coding operation considerably widens the application of measuring equipment with a digital output by extending it to indirect measurements.

It should be noted that the solution of a similar problem of functional coding by combining linear coding converters with electronic functional converters of a continuous type (for instance, diode functional converters) leads to more cumbersome, less reliable devices whose coding accuracy is inferior to that of the functional devices described in this article. Moreover, in using functional converters of a continuous type it is difficult to provide multiconditional coding operations.

LITERATURE CITED

1. M. Klein, G. Morgan, and M. Aronson, Digital Techniques for Computation and Control [Russian translation] (Foreign Literature Press, 1960).
2. V. B. Smolov, Computing Converters with Digital Control Resistances [in Russian] (Gosenergoizdat, Moscow, Leningrad, 1961).
3. V. B. Smolov, Avtomatika i telemekhanika, No. 2, 1961.

FUNCTIONAL ANALOG-TO-DIGITAL CONVERTERS FOR AC TRANSDUCERS OF SCANNING CONTROL SYSTEMS

Yu. I. Semko, Yu. S. Solodov, and M. I. Levin

Translated from Izmeritel'naya Tekhnika, No. 11,
pp. 35-39, November, 1961

In designing centralized scanning control systems it is necessary to convert the output signals of primary instruments from an analog to a digital form.

The majority of primary instruments (converters) used for controlling production processes at their output provide a direct current or voltage. Analog-to-digital conversion of a direct voltage (current) has at present been solved successfully both in our own and foreign scanning control systems and digital instruments.

The conversion conditions are much more complicated for a large group of primary instruments whose output

variable consists of an alternating voltage. For these instruments the analog-to-digital (code) conversion can be attained by two methods, namely, by a preliminary rectification of the alternating voltage into a digital form.

The first method has several advantages. It requires, however, a relatively complicated equipment which must provide accurate rectification (0.2-0.4 %) of the small alternating voltages received from the transducers (of the order of tenths of a volt), and a negligible alternating component in the rectified voltage, and must provide a close coupling between the alternating current which feeds the transducers and the direct voltage which feeds the analog-to-digital converter at any possible variations of the supply voltage. The solution of these questions involves considerable difficulties which have not, as yet, been solved.

Hence, the second method which provides the possibility of converting alternating voltages into a digital form (code) is of considerable interest. These converters have certain disadvantages, but can be used in many cases for feeding information from ac transducers to controlling machines.

It is normally required that the code at the output of an analog-to-digital converter intended for feeding to a recording (digit-printing) device or a controlling machine should have a linear relation to the value of the controlled parameter. For primary instruments with a linear characteristic (manometers, vacuum gauges, etc. with differential transformer or ferrodynamic [1] transducers) the analog-to-digital converters must also have a linear characteristic. In the case of instruments with a nonlinear characteristic the analog-to-digital converters must perform functional conversion. Thus, flowmeters used with variable pressure differences in conjunction with differential manometers and equipped with alternating voltage transducers have a square law ($U_x = kQ^2$) or approximately square law relation between the output voltage U_x and the controlled parameters (rate of flow Q). For such instruments the converter output discrete variable (code) must be proportional to the square root of the input analog variable (voltage U_x). Moreover, the code at the converter output should be directly proportional to the controlled parameter (rate of flow Q).

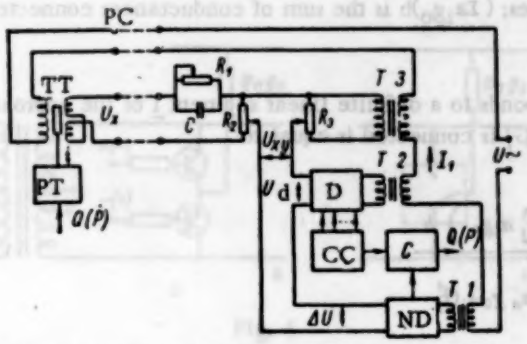

Fig. 1

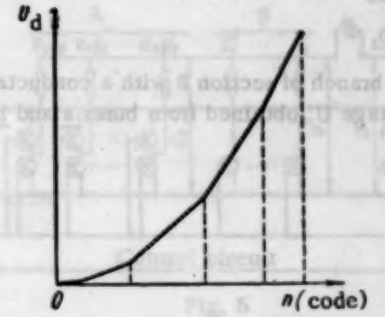

Fig. 2

The designing of a functional converter can be solved in several ways. One method consists of the linear conversion of the analog variable into a code with its subsequent functional conversion. However, this method for a small number of digits and considerable nonlinearity of the primary instrument characteristic can produce considerable errors. The errors can be reduced greatly by functional conversion by means of decoders in the process of analog-to-digital conversion.

Below we describe linear and function analog-to-digital converters designed for commercial frequency voltages by the MÉI (Moscow Power Institute) in 1960 for centralized scanning control systems.

A converter block-schematic is shown in Fig. 1. The secondary voltage of a differential transformer transducer TT is reduced by means of a voltage divider, which consists of resistances R_1, R_2, and capacitance C, to a single nominal value adopted for this system. Capacitance C serves to correct the phase in such a manner that the voltage across resistance R_2 is proportional to the transducer's output voltage and coincides in phase with the voltage across resistance R_3. The converted voltage U_{xy} is compared by means of a phase-sensitive null-detector ND to the decoder D output voltage U_d which is also in phase with the voltage across resistance R_3. The decoder is operated by the control circuit CC. At the instant when the two voltages U_{xy} and U_d are equal the null-detector operates and stops counter C.

In the above system a scanning conversion method is used. However, in principle this converter can also use the method of digital balancing.

As has been shown, the analog-to-digital converter can be, according to the type of primary instrument used, either linear or functional. For instruments with linear characteristics the converter circuit must use a linear decoder LD. In this instance the analog output variable, the alternating voltage U_d, is proportional to the decoder input discrete variable (code). For an instrument with a nonlinear characteristic it is necessary to use a functional decoder FD which performs a definite functional conversion of the input discrete variable (code) into an output analog variable U_d.

It should be noted that differential-transformer and ferrodynamic transducers are of the parametric type whose operation is based on the variation of the coupling (mutual inductance) between the primary and secondary windings. The decoder in such an analog-to-digital converter should also be parametric. The transducer and the decoder are supplied by the same current I_1, thus eliminating the error due to variations in the value and frequency of the supply voltage U~, and to changes in the resistance of the transmission line or transducer primary windings.

The decoder, whether linear or functional, is the basic part of an analog-to-digital converter. The linear decoder consists of a linear discrete voltage divider [2] whose conductances (resistances) are assembled according to a binary law ($a_1=1, a_2=2, \ldots a_N=2^{N-1}$).

A functional decoder is designed on the basis of approximating a given functional relationship by a piecewise-linear curve* (Fig. 2). A functional decoder which can express virtually any single-valued output voltage U_d as a linear function of a code is shown in Fig. 3.

$$U_1=U_1\frac{\left(\sum a_i g_0\right)b}{\sum_1^N a_n g_0}, \tag{1}$$

where $\sum_1^N a_n g_0$ is the sum of all the linear decoder conductances; $(\Sigma a_i g_0)b$ is the sum of conductances connected to the supply bus b.

Each branch of section B with a conductance G_i' corresponds to a definite linear segment i of the approximating curve. Voltage U' obtained from buses a and b when branch G_i' is connected is equal to

$$U'=U_1\frac{\left(\sum a_i g_0\right)b}{\sum_1^N a_n g_0+G_i'}. \tag{2}$$

It will be seen from this expression that by changing the value of G_i' it is possible to change the conversion factor of the decoder. However, the changing of conductances G' for a definite condition of the linear decoder produces jumps in voltage U'. These jumps can be eliminated by means of the C section conductances $G_I^* - G_F^*$ which are connected at the same time as the corresponding branches of section B. Voltage U* obtained from section C is equal to

$$U''=U_1\frac{G_1}{G_1+G_2+G_i^*}. \tag{3}$$

The decoder output voltage is equal to

$$U_d = U'-U''=U_1\left[\frac{\left(\sum a_i g_0\right)b}{\sum_1^N a_n g_0+G_i'}-\frac{G_1}{G_1+G_2+G_i^*}\right], \tag{4}$$

and is a nonlinear function of the code.

By means of these formulas and the decoder approximating characteristic (Fig. 2) it is possible, by setting a discrete conversion error (the number of digits in the linear portion of the decoder) and the error caused by keys and

* A similar method was used in [3] for designing a functional decoder.

switches, to calculate the conductances (resistances) for all the three sections of the functional decoder g_0, $G_1' - G_F'$, $G_1'' - G_F''$, G_1, G_2 as well as for the supply voltage U_1.

The actual circuit of the functional decoder developed by us uses switching transistors. Theoretical problems of applying switching transistors as gates and switches (Fig. 4) are thoroughly discussed in [4] and [5].

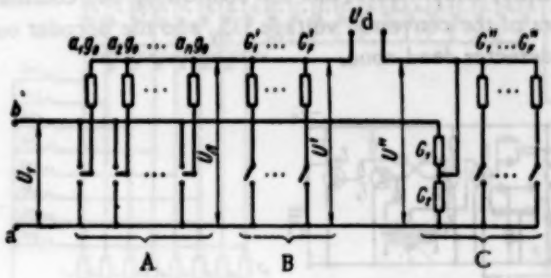

Fig. 3

Depending on the polarity of the control signals applied between point O and the base of transistors, one of them is conducting and the other blocked. The resistance of the decoder branches $a_n g_0$ are connected through the conducting transistor to the supply bus a or b. The controlling voltage is taken off the collectors of two transistors which for a trigger circuit not shown on the diagram. The transistors in the switch can be connected in a common collector or common emitter circuit. Transistors with similar or different conductances can be used.

A wide experimental investigation of Soviet-made switching transistors has shown that transistors types P8 - P11, P13 - P16 can be used in switching circuits and transistors P101 - P106 in keying circuits.

A functional decoder circuit which uses switching transitors is shown in Fig. 5. The decoder control circuit is also transistorized and consists of a system of trigger elements and coincidence circuits. The phase-sensitive null-detector uses P15 transistors and operates when the phase of the unbalance voltage at its input is reversed ($\Delta U = U_{xy} - U_d$).

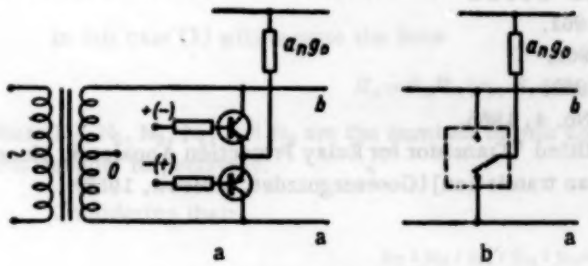

Fig. 4

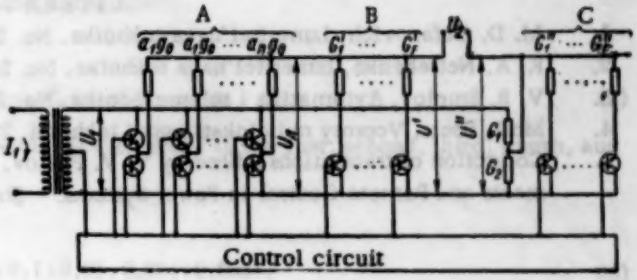

Fig. 5

Fig. 6 shows the operating principle schematic of the zero detector. The zero detector consists of a selective amplifier limiter $T_1 - T_6$, a phase-sensitive device $T_7 - T_9$, Tr1* and the output stage T_{10}. The input signal of the null-detector, having passed through an amplifying and limiting stage is fed to the base of transistor T_7 in the shape of rectangular pulses which are periodic at a frequency of 50 cps and serve to trip and block the keying transistor T_7. Thus, the midpoint of transformer Tr1 secondary winding is also periodically connected to the ground bus of the null-detector. The primary winding of the differentiating transformer Tr1 has a ferrite core and is fed with current I_1. Pulses arise in the secondary winding of the transformer at the instant current I_1 passes through its zero values. Since the phases of voltages U_{xy} and U_d with respect to current I_1 are equal to each other and approach 90°, the phase of the null-detector input voltage $\Delta U = U_{xy} - U_d$ has also an angle of approximately 90° with respect to current I_1. This provides a ninety-degree phase difference between the rectangular pulses which control the keying transistor T_7 and the pulses in the secondary winding of transformer Tr1. The latter are fed to the base of one of the transistor triggers, for instance, T_8. When the phase of the null-detector input voltage is reversed, the pulses from the secondary winding of transformer Tr1 are fed to the base of another transistor, for instance, T_9, thus throwing over the trigger. The operation is 0.5-1 mv, and its input resistance is 150 kilohm.

The speed of operation of an analog-to-digital converter as a whole is determined by the operation time of the null-detector. When the scanning conversion method is used the maximum conversion time amounts to $T \cdot 2^N$, where N is the number of figures provided by the decoder. In the digital balancing method the maximum conversion time of an analog variable (alternating voltage) into a code is equal to TN.

* The phase-sensitive device is based on Lisichanskii's circuit.

The accuracy of operation of an alternating voltage analog-to-digital converter is determined by a number of errors, the most important of which are: the error of approximating a given functional relation by a piecewise-linear curve; the error of discrete operation determined by the number of significant figures provided by the decoder; the error due to the instability of the parameters of transistor keys and switches, which is determined by the dispersion of the transistor switch parameters and by their variation with time, temperature, and the controlling and commutating currents; the error due to inaccurate matching of the phases of the converted voltage U_{xy} and the decoder output voltage U_d; the error provided by the existence of a null-detector dead zone.

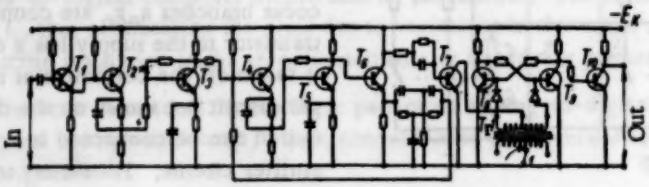

Fig. 6

Calculations and tests of an analog-to-digital converter model have shown that by a correct choice of the decoder null-detector parameters and by providing a sufficiently large number of linear sections for the approximation curve and significant figures in the decoder, the total conversion error of an alternating voltage into a code can be reduced to the order of 0.5-1% for a nominal value of the converted voltage of the order of 300 mv.

Conclusions. As the result of the work in designing an analog-to-digital converter it has been found that it is possible to construct relatively simple and reliable noncontact converter units for supplying information from primary instruments with alternating current transducers to recording (digit-printing) devices and computers.

LITERATURE CITED

1. M. D. Gafanovich, Izmeritel'naya tekhnika, No. 2, 1961.
2. K. A. Netrebenko, Izmeritel'naya tekhnika, No. 2, 1960.
3. V. B. Smolov, Avtomatika i telemekhanika, No. 2, 1961.
4. Moll, Ebers, Voprosy radiolokatsionnoi tekhniki, 28, No. 4, 1955.
5. Collection of translations edited by V. V. Pavlov, entitled "Transistor for Relay Protection Apparatus, Measurements and Remote Control in Power Systems." [Russian translation] (Gosénergoizdat, Moscow, 1958).

MEASURING CIRCUIT OF AN AUTOMATIC DIGITAL BRIDGE

V. P. Kotel'nikov

Translated from Izmeritel'naya Tekhnika, No. 11,
pp. 39-42, November, 1961

The measuring circuits of automatic digital bridges with noncontact switching devices [1] can at present only be used in instruments of a relatively low grade of accuracy (0.5-0.2%).

In instruments with a higher degree of accuracy (0.1-0.01%) switching devices still consist of relays, therefore, in designing the measuring circuit it is necessary to take into account the presence of relay contacts, low stimulation of relays, and the high contact resistance of their contacts.

The digital bridge measuring circuit shown in Fig. 1 is intended for a bridge with a wide range (10^{-2} - 10^{7} ohm) and is designed to reduce to a great extent the effect of the low insulation of relays and their large contact resistance, and to provide other advantages.

The bridge comparison arm R_c consists of 20 parallel resistances r_1 - r_{20} chosen according to a binary-decimal

system and divided into 5 groups (decades): $r_1 - r_4$ (first): 2 - 1 - 2 - 4 kilohm; $r_5 - r_8$ (second): 20 - 10 - 20 - 40 kilohm; $r_9 - r_{12}$ (third): 200 - 100 - 200 - 400 kilohm; $r_{13} - r_{16}$ (fourth): 2 - 2 - 4 meg; $r_{17} - r_{20}$ (fifth): 20 - 10 - 20 - 40 meg.

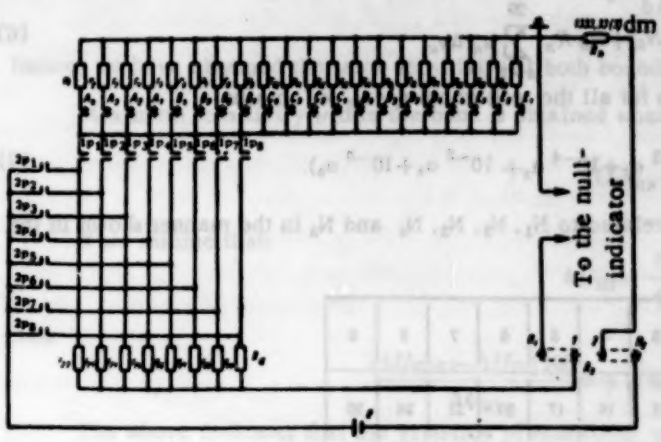

Fig. 1

The bridge circuit is balanced by means of a set of conductances in arm R_c. The balanced condition of the bridge is determined by the equation

$$R_x = R_d R_n y_c. \tag{1}$$

where

$$y_c = \sum_{k=1}^{20} a_k y_k; \quad y_k = \frac{1}{r_k};$$

a_k is a coefficient which assumes the value of 1 or 0 depending on whether the appropriate conductance y_k in the bridge arm R_c is connected or disconnected.

All the relay contacts have a common point which simplifies the design of the control circuit.

The balance conditions of the bridge circuit can easily be expressed in the form usual for multidecade manually operated circuits providing the conductances

$$y_{01} = \frac{1}{r_4}; \; y_{02} = \frac{1}{r_8}; \; y_{03} = \frac{1}{r_{12}}; \; y_{04} = \frac{1}{r_{16}}; \; y_{05} = \frac{1}{r_{20}} \tag{1a}$$

are taken as unit conductances for the first to the fifth decades respectively.

In this case (1) will assume the form

$$R_x = R_d R_n (y_{01} N_1 + y_{02} N_2 + y_{03} N_3 + y_{04} N_4 + y_{05} N_5), \tag{2}$$

where N_1, N_2, N_3, N_4, and N_5 are the numbers of unit conductances connected in the first, second, third, fourth, and fifth decades respectively.

Considering that:

$$y_{01} : y_{02} : y_{03} : y_{04} : y_{05} = 1 : 0,1 : 0,01 : 0,001 : 0,0001, \tag{3}$$

we finally obtain:

$$R_x = R_d R_n y_{01} (N_1 + 10^{-1} N_2 + 10^{-2} N_3 + 10^{-3} N_4 + 10^{-4} N_5). \tag{4}$$

The weighting factors 2:4:2:1 for the conductances in each decade are chosen so as to obtain this minimum number of "false" counts, i.e., to obtain one and the same number of connected conductance units by means of two or more combinations of connected and disconnected conductances.

In the above case one "false" count is possible. Number 7 can be obtained as 0+4+2+1 or as 2+4+0+1.

If the conductance weighting factors for each decade were chosen as 4:2:2:1, in the above case there would be three "false" counts. Number 7 could then be represented as 4+2+0+1 and as 4+0+2+1. Figure 5 could be represented as 4+0+0+1 and as 0+2+2+1, and Figure 3 as 0+2+0+1 and as 0+0+2+1.

In order to deal with "false" counts as additional complication of the circuit is required, hence the choice of conductances in each decade according to the system 2:4:2:1 simplifies the control circuit.

The values of resistances $r_1 - r_{20}$ in the comparison arm R_c have been chosen so as to account for the relay contact resistances and their variations. According to experimental data variations in the contact resistance of RSM relays do not exceed $16 \cdot 10^{-3}$ ohm after $5 \cdot 10^6$ operations with 0.8 amp flowing through the contacts at 24 volts across them (the initial resistance including that of the contact springs amounts to 0.012 ohm).

Let us denote by Δr_k the deviation of the resistance from its nominal value caused by the effect of the relay contact resistance. In this case

$$\Delta y_k = -\Delta r_k y_k^2. \tag{5}$$

The balance condition of the bridge can be expressed, taking into account the relay contact resistance, in the following form

$$R_x = R_d R_n y_{01} (N_1 + 10^{-1} N_2 + 10^{-2} N_3 + 10^{-3} N_4 + 10^{-4} N_5) + R_d R_n \sum_{\kappa=1}^{20} a_\kappa \Delta y_\kappa. \quad (6)$$

Providing $\Delta r_k = \Delta r$ is equal in magnitude and sign for all the resistances $r_1 - r_{20}$ we obtain:

$$\sum_{\kappa=1}^{20} a_\kappa \Delta y_\kappa = \Delta r y_{01}^2 (\alpha_1 + 10^{-2} \alpha_2 + 10^{-4} \alpha_3 + 10^{-6} \alpha_4 + 10^{-8} \alpha_5). \quad (7)$$

In this formula the values of α_1, α_2, α_3, α_4 and α_5 are related to N_1, N_2, N_3, N_4 and N_5 in the manner shown in the table attached

N_i	0	1	2	3	4	5	6	7	8	9
α_i	0	1	4	5	16	17	20	21	24	25

The relative error of the comparison arm is

$$\delta = \frac{\sum_{\kappa=1}^{20} a_\kappa \Delta y_\kappa}{y_c} - \frac{\Delta r y_{01} (\alpha_1 + 10^{-2} \alpha_2 + 10^{-4} \alpha_3 + 10^{-6} \alpha_4 + 10^{-8} \alpha_5)}{N_1 + 10^{-1} N_2 + 10^{-2} N_3 + 10^{-3} N_4 + 10^{-4} N_5}. \quad (8)$$

It can easily be shown that the relative error will be maximum for $N_1 = 4$ and $N_2 = N_3 = N_4 = N_5 = 0$. For $\Delta r = 16 \cdot 10^{-3}$ ohm, $y_{01} = 1/4000$, $N_1 = 4$, and $\alpha_1 = 16$ we have

$$\delta = \frac{16 \cdot 10^{-3}}{4 \cdot 4000} = 16 \cdot 10^{-6}. \quad (9)$$

Thus, the effect of the variation in the contact resistance (for RSM relay) can be evaluated at 0.002%.

The contacts of relays $P_1 - P_8$ adjust resistances in the following ranges, which expressed in ohms are: relay P_1 in the range of $0 - 999.99 \cdot 10^{-3}$, P_2 in 1 - 9.9999, P_3 in 10 - 99.999, P_4 in $10^2 - 999.99$, P_5 in $10^3 - 9.9999 \cdot 10^3$, P_6 in $10^4 - 99.999 \cdot 10^3$, P_7 in $10^5 - 999.99 \cdot 10^3$, and P_8 in $10^6 - 9.9999 \cdot 10^6$.

The ratio of the bridge arms resistances $m = R_n/R_c$ at the upper boundary of each band of measured resistances is chosen to equal 3.33 (3) instead of ten. This provides an approximately equal sensitivity of the circuit inside each band of measured resistances.

The voltage across the measuring diagonal of the bridge for a supply voltage of U_0 and an infinite input resistance of the amplifier is determined by the equation

$$\Delta U = \frac{U_0 \xi}{m + 2 + \frac{1}{m}}, \quad (10)$$

where

$$\xi = \frac{\Delta R_c}{R_c}$$

If $m = 10$ at the upper boundary of the band of measured resistances (for instance, $R_x = 9.9999$ kilohm), at the lower boundary of the band $m = 1$ ($R_x = 1$ kilohm). For the first and second cases we shall obtain respectively

$$\Delta U_1 = \frac{U_0 \xi}{12} \quad \text{and} \quad \Delta U_2 = \frac{U_0 \xi}{4}. \quad (11)$$

Thus the sensitivity of the circuit within a band of measured resistances varies by a factor of 3. An approximately uniform sensitivity can be obtained if we take $m = 3.33$ (3) at the upper boundary of the band of measured resistances (for instance, $R_x = 9.9999$ kilohm):

$$\Delta U_1 = \frac{U_0 \xi}{5\,63(3)}. \quad (12)$$

At the lower boundary of the band we shall then have m = 0.3 and

$$\Delta U_3 = \frac{U_0 \xi}{5.63(3)}. \tag{13}$$

Hence, we have obtained the same sensitivity at both boundaries of the band.

Maximum sensitivity within the band is obtained when the measured variable attains a value for which m = 1.

$$\Delta U_{max} = \frac{U_0 \xi}{4} \tag{14}$$

If we assume that:

$$\Delta U_m = \frac{U_0 \xi}{4{,}68},$$

then

$$\frac{(\Delta U_{max} - \Delta U_m)\,100}{\Delta U_m} = +17\%, \quad \frac{(\Delta U_1 - \Delta U_m)\,100}{\Delta U_m} = 17. \tag{15}$$

The above indicates that the variation of sensitivity within each band does not exceed ± 17% of the set mean value

A uniform sensitivity of the bridge circuit ensures its reliable operation. The accuracy of resistance measurements by means of a dc bridge is affected by insulation leakages. In manually operated circuits these resistance couplings are relatively easily eliminated by using high-quality insulation.

According to GOST (All-Union State Standard) 7165-54 the insulation resistance in dc bridges between any point of the bridge electrical circuit and the edges of insulating panels on which the conducting components are mounted must not be, in the most vulnerable places with respect to leakage, less than:

$$R_{is} = \frac{1}{1000\,a} R_{max} \tag{16}$$

where R_{is} is the insulation resistance, meg; R_{max} is the maximum measured resistance for single bridges, ohm; a is the number indicating the accuracy grade of the bridge.

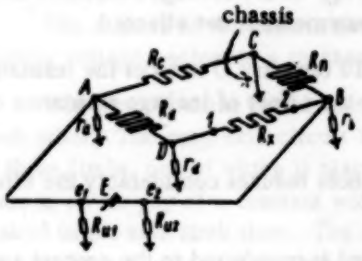

Fig. 2

According to the above formula for a Grade 0.05 bridge and R_{max} = 100 kilohm we shall obtain:

$$R_{is} = \frac{1 \cdot 100000}{1000 \cdot 0.05} = 2000 \text{ meg} \tag{17}$$

If we represent the insulation resistance as connected in parallel with the measured resistance of 100 kilohm (the top measurement limit for single Grade 0.05 bridges according to GOST 7165-54), its effect on the measured resistance will amount to 0.005%.

Such high insulation in automatic digital bridges (with relay switching devices) cannot be obtained in practice. Thus, for instance, relay RSM (whose parameters are most suitable for automatic digital instruments) has a minimum insulation resistance, determined experimentally at t = 20°C and a relative humidity of 80%; between its windings and contacts of $5 \cdot 10^{10}$ ohm, and between the contacts of 10^{11} ohm.

When the ends of relay windings are grounded at one point as shown in Fig. 1 the insulation resistances between the winding and the contacts and between contacts are placed in parallel.

Thus, the insulation resistance of one relay according to the above data will amount to:

$$\frac{5 \cdot 10^{10} \cdot 10^{11}}{5 \cdot 10^{10} + 10^{11}} = 3.33 \cdot 10^{10} \text{ ohm} \tag{18}$$

Since the comparison arm contains 20 relays, it is obvious that the effect of the insulation resistances on arm R_c is equivalent to connecting in parallel with it a resistance of

$$\frac{3{,}33 \cdot 10^{10}}{20} = 1.66 \cdot 10^{9} \text{ ohm} \tag{19}$$

This value should be taken for computations in determining the effect of insulation resistance on arm R_c, and hence on the error of measurements.

It is convenient to trace the effect of the insulation resistance on a simplified bridge circuit (Fig. 2). On this circuit the leakages to ground are represented by resistances r_a, r_b, and r_d connected between the three nodes of the bridge circuit and ground.

The grounding of point C of the bridge measuring diagonal considerably reduces the effect of leakage resistances concentrated at nodal points if the bridge components are mounted on a conducting grounded panel, since in this case the leakage paths do not pass through several nodal points.

If insulated panels are used it can be assumed that not a single circuit component, neither the supply source nor the null-indicator have any definite electrical coupling with ground. In this case the grounding of any point of the circuit will not change it in any way, since none of the existing couplings which shunt various bridge arms will be affected by it.

When a metal panel is used and point C grounded (Fig. 2) the leakage resistance r_d is connected in parallel with the measuring diagonal and does not affect measurement results.

The insulation of points A and B on the metallic panel must be high as compared with the resistance of 4 kilohm and 1333.33 ohm (with an automatic selection of measuring ranges the conductance of the comparison arm is $y_c \geq y_{01}$, and for $y_c = y_{01}$ the effect of the insulation resistance will be at its maximum).

If according to the above reasoning we should assume the leakage resistance to be $r_a = 1.66 \cdot 10^8$ ohm, its effect on the bridge arm R_c will amount to 0.006%.

The leakage resistance r_b which shunts arm R_n can easily be made large, since the arm R_n does not contain any relay contacts and the effect of leakage on arm R_n will be negligible.

The bridge supply circuits (points e_1 and e_2) must also be carefully insulated from the panel, since any leakage to the panel will shunt arms R_c and R_n. In this case the leakage resistance must also be large as compared with 4 kilohm.

The leakage from terminal x_1 of the measured resistance R_x shunts the measuring diagonal and does not affect the measurement results, whereas the leakage from terminal x_2 shunts the arm R_n. If the leakage resistance from terminal x_2 is large as compared with $R_n = 1333.33$ ohm, the accuracy of measurements is not affected.

Let us also note that the choice of m = 3.33 (and m = 0.3) instead of m = 10 (and m = 1) reduces the resistance of R_c (for a constant R_n) by a factor of 3.33 (3), thus making it easier to lower the effect of leakage resistance on the measurement results.

A bridge circuit with a comparison arm in the form of a set of conductances reduces considerably the effect of thermo-electric potentials in relay contacts.

During operation the relay winding becomes warm, the heat thus produced is transferred to the contact system. Differences in the material of the two contacts with a temperature difference across them produce a thermal emf whose value for a RSM relay amounts to 3 μv with 24 volts connected across its winding for more than 40 min.

Let us denote the thermal emf across the contacts which switch-in admittance y_k by Δe_k. Then the voltage drop across the comparison arm due to the thermal emf will be:

$$\Delta U = \frac{\sum_{\kappa=1}^{n} \Delta e_\kappa y_\kappa}{\sum_{\kappa=1}^{n} y_\kappa}. \tag{20}$$

If we consider that the thermal emf is the same for all the contacts $\Delta e_k = \Delta e_{max}$, we shall have:

$$\Delta U = \frac{\Delta e_{max}\left(\sum_{\kappa=1}^{n} y_\kappa\right)}{\sum_{\kappa=1}^{n} y_\kappa} = \Delta e_{max} \tag{21}$$

Thus, the value of the thermal emf does not depend on the number of relay contacts in the circuit. Even when the voltage drop across the comparison arm amounts to 1 v (produced by the operating current), the error due to the thermal emf is negligibly small at 0.003%.

Resistances up to 50 ohm are measured in a four-terminal network. Such a connection in a single-bridge circuit reduces the effect of connecting leads and contact resistances as compared with a two-terminal network.

The switching of the measuring range resistances R_d and the measuring arm resistances R_c is made by means of two relay contacts (a three-terminal network), so that the contact resistance of one of the contacts is included in the battery circuit and the other in that of a high-value resistance R_c (not less than 400 ohm). The effect of the relay contact resistances in this case is obviously small.

Conclusions. Measuring circuits similar to that described above are the most suitable for use in automatic digital bridges with a wide measuring range and in comparator instruments supplied from the mains and fitted with a null-indicator.

LITERATURE CITED

1. V. N. Malinovskii and R. R. Kharchenko, Izmeritel'naya tekhnika, No. 11, 1960.
2. M. A. Bykov, Izmeritel'naya tekhnika, No. 6, 1956.
3. K. A. Netrebenko, Priborostroenie, No. 4, 1960.

FERRODYNAMIC RECTANGULAR-COORDINATE VECTOR METER

M. I. Belyi and N. P. Makarov

Translated from Izmeritel'naya Tekhnika, No. 11,
pp. 43-44, November, 1961

The authors of this article have designed and produced a ferrodynamic vector meter* for measuring and recording voltage vectors in a rectangular system of coordinates.

The ferrodynamic vector meter (Fig. 1) consists of two identical magnetic systems placed at right angles to each other. The magnetic circuit 1 of each system is made of sheet electrical steel, is dismountable, and consists of three limbs, one of which is placed in the middle and two on either side of it. Between the middle and side limbs there is an air gap of a constant width in which frameless coil 2 can be displaced. Two excitation windings 3 are placed in the side limb slots. The instrument has an independent excitation system. The excitation windings of each magnetic system are connected in series opposing.

The magnetic intensity at any cross section of the core can be represented as

$$U_{mx}=F_m-\int_0^x \Phi_x\, dR_m, \qquad (1)$$

where F_m is the magnetomotive force produced by the excitation coil; Φ_x is the magnetic flux in a core cross section at a distance x from the neutral section;** dR_m is the reluctance of an elementary portion of the magnetic flux path equal to

$$dR_m=\frac{dx}{\mu S}; \qquad (2)$$

d_x, S, μ are respectively the length, cross sectional area, and permeability of the elementary portion of the core; $\Phi_x \cdot dR_m$ is the drop in magnetic intensity across the given elementary portion.

* The idea for producing the instrument was suggested by Prof. L. F. Kulikovskii. The instrument was made at the laboratory of the Ul'yanov Automechanical Technical School.

** The term neutral or zero is here given to the middle cross section of the central core limb in which the resulting magnetic flux is equal to zero.

In a magnetic core of such a construction made of a high permeability material it is possible to consider that under conditions of low saturation the reluctance of the core can be neglected as compared with that of the air gap, i.e., it is possible to assume that $dR_m = 0$. Then:

$$U_{mx} = F_m. \tag{3}$$

For a stable excitation current the magnetomotive force will not vary and, therefore, the magnetic intensity will be the same in each cross section of the core.

The magnetic flux linking across the air gap will be equal for each elementary cross section of the core to:

$$d\Phi_a = 2U_{mx}\, g\, dx, \tag{4}$$

where g is the conductivity of air in the gap per unit length. The air gap conductance, with the other conditions remaining constant, is determined by the value of the gap δ (see Fig. 1). For a constant gap width conductivity g will also be constant and:

$$\frac{d\Phi_a}{dx} = \text{const}. \tag{5}$$

For any cross section of the core the following equation holds:

$$\Phi_x = d\Phi a + (\Phi_x + d\Phi_x). \tag{6}$$

Hence,

$$\frac{d\Phi_x}{dx} = \text{const}. \tag{7}$$

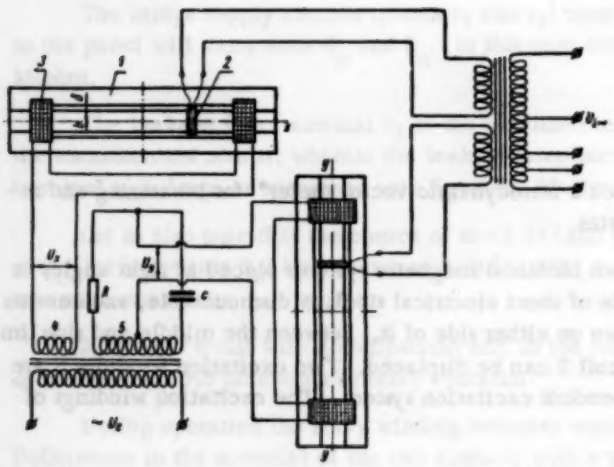

Fig. 1

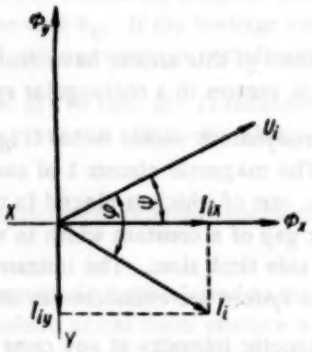

Fig. 2

For a sufficiently constant width of the air gap it can be considered that the magnetic induction in it will be constant along the length of the central limb, and hence the magnetic flux in the middle limb will vary according to a linear law:

$$\Phi_x = k_\varphi \cdot x, \tag{8}$$

where k_φ is the factor of proportionality.

The excitation windings of the vector meter are fed from a phase-shifting bridge. The bridge is formed by transformer secondary windings 4 and 5 with a capacitance C and resistance R. For appropriate values of the bridge paramaters (R and C) the voltages U_X and U_Y, which are fed to the excitation windings of the magnetic systems, have a phase difference of 90° between them. These voltages produce in the middle limb fluxes Φ_X and Φ_Y which also have a phase difference of 90° between them.

The measured voltage U_i is fed to the moving coils of the instrument by means of a voltage instrument trans-

former which has one primary and two secondary windings. The primary winding has several taps for signals of 10, 50, 127, and 220 v.

The measured voltage vector U_i in a general case has a certain angle ψ with respect to the X-axis of the vector diagram shown in Fig. 2 (without taking into account the 180° phase shift provided by the instrument transformer). The current I_i flowing through the measuring circuit will lag on voltage U_i by a certain angle ψ which is determined by the ratio of the resistive and reactive impedances in the measuring circuit.

As a result of the interaction of the signal current components I_{ix} and I_{iy}, which are in phase with the corresponding magnetic fluxes, a force is produced which reacts on the moving coil of each of the magnetic systems, displacing it along the core.

The moving coil of one of the magnetic systems is affected by force:

$$F_{ix}=2B_a I_{ix} l W_k=2B_a l W_k I_i \cos(\psi-\varphi), \tag{9}$$

where B_a is the flux density in the air gap; W_k is the number of turns in the moving coil; l is the length of the active side of a turn.

The moving coil of the second magnetic system is affected by a force:

$$F_{iy}=2B_a I_{iy} l W_k=2B_a l W_k I_i \sin(\psi-\varphi). \tag{10}$$

Under the effect of these forces the moving coils are displaced to one or the other side of the neutral position. The direction of the forces' operation is determined by that of the measured signal phase angle.

The displacement of the coil induces an electromotive force

$$E_x=\Phi_x \omega W_k, \tag{11}$$

where ω is the angular velocity of the current.

Since $\Phi_x = k_\varphi \cdot x$, we have

$$E_x=k_\varphi \omega W_k x. \tag{12}$$

In a certain position of the moving coil balance is obtained which is characterized by the equation:

$$x=\frac{Z_i \cos(\psi-\varphi) I_i}{k_\varphi \omega W_k \sin\varphi}, \tag{13}$$

where Z_i is the impedance of the measured circuit.

This balance position corresponds to a certain displacement x of the moving coil from the neutral position. By means of this displacement it is possible to evaluate the measured current's component (I_{ix}).

The displacement of the moving coil in the second magnetic system can be represented by a similar formula

$$y=\frac{Z_i \sin(\psi-\varphi) I_i}{k_\varphi \omega W_k \sin\varphi}. \tag{14}$$

Thus, the displacement of the moving coils represents the right angle components of the measured voltage vector, and the vector itself can be determined as the geometrical sum of these components. The moving coils of the instrument carry thin steel pointers which indicate the value of the right angle components of the measured voltage vector and their intersection indicates the end of the vector.

The sensitivity of the instrument to current measurements is:

$$S_i=\frac{Z_i}{k_\varphi \omega W_k \sin\varphi}. \tag{15}$$

The instrument measures and records simultaneously three parameters, namely, the time, the size of the vector and its phase. In the instrument produced by us the excitation voltage amounts to 50 v and the maximum signal voltage to 10 v.

Laboratory investigations have revealed relatively small temperature and frequency errors of the instrument. The largest error is that due to friction. The friction force which arises in the displacement of the moving system

can be represented as consisting of two components: that of the friction of centers in the bearings and the friction of rollers over the guides.

The absolute value of the error due to friction is:

$$\Delta = \frac{F_T}{F'_c}, \tag{16}$$

where F_T is the force of friction for a uniform movement of the system; F'_c is the specific restoring force of the instrument.

Calculations show that the error is $\Delta = 0.4$ mm. The referred error amounts to 0.5% in either magnetic system.

HIGH-FREQUENCY MOVING-IRON INSTRUMENTS

P. P. Ornatskii, N. F. Suvid, and Yu. M. Tuz

Translated from Izmeritel'naya Tekhnika, No. 11,
pp. 45-47, November, 1961

Among the various systems of electrical instruments used for measurements at commercial frequencies, moving-iron instruments are widely used owing to the simplicity of their construction, reliability in operation and their capacity for large overloads. The use of new reliable and stable stressed suspensions and luminous display has considerably raised the sensitivity and reduced the power consumption of these instruments. However, the possibilities of extending the frequency range of moving-iron instruments has not been utilized fully.

The work carried out by the department of measuring devices of the Kiev Polytechnical Institute has shown that the frequency range of moving-iron instruments can be extended considerably, not only in ammeters but also in milliammeters and voltmeters, with a relatively small consumption. Moreover, new designs of moving-iron instruments provide them with an improved scale characteristic.

Frequency errors in moving-iron ammeters and voltmeters are caused by [1]: eddy currents in the moving ferromagnetic core, in the copper of the winding and other metallic components of the stationary part of the instrument which are within the effective alternating field of the coil and the effect of the interturn and interwinding capacitance.

In voltmeters frequency errors are also due to changes in the reactance of the instrument coil. The effect of eddy currents predominates in ammeters owing to their small number of turns and small interturn capacitance. Eddy currents produce fluxes which have a demagnetizing effect on the main magnetic flux of the stationary coil, they reduce this flux and produce a negative error in the instrument readings.

It can be shown that the error in moving-iron instruments due to eddy currents is equal to:

$$\gamma_{ec} = -\frac{k M_e L_e \omega^2}{R_e^2 + \omega^2 L_e^2}, \tag{1}$$

where M_e is the equivalent mutual inductance coefficient between the coil and eddy-current circuits; L_e is the equivalent self-inductance coefficient of the eddy-current circuits; R_e is the equivalent resistance of the eddy-current circuits.

It is obvious that at low frequencies, i.e., when $\omega^2 L^2 \ll R^2_e$ the error γ_{ec} is proportional to the square of the frequency, but with a further rise in frequency when $\omega^2 L_e^2 > R^2_e$ the error γ_{ec} stops rising and approaches asymptotically its maximum value.

It is difficult to determine the values of R_e, M_e, and L_e either by calculation or experimentally. Therefore, in order to determine the relative importance of these error components, which are due to the effect of eddy cur-

rents in the core, in the copper of the winding and in the metal of the instrument's stationary part, a special experiment was performed. In this experiment the operation of the mentioned factors was excluded one by one, by certain design alterations, such as using a blended metal core made of permalloy strips 30-50 μ thick, using litz wire in coil windings, and replacing the instrument's stationary frame by a textolite one. It was shown experimentally that ammeter type AST, previously made by the "Toch-elektropribor" plant with a range of 5 amp had at 10,000 cps a total eddy-current error of 2% uniformly distributed among the three above-mentioned components. The above design alterations reduced the total error γ_{ec} to 0.2% at 10,000 cps.

Frequency error γ_{ec} can also be reduced in ammeters by making their cores of magnetically-soft powdered materials with a small coercive force H_c. It will be seen from [1] that for relatively low frequencies

$$\gamma_{ec} = -k_1 f^2 100\%, \tag{2}$$

where k_1 is the factor of proportionality; f is the frequency.

This error can be compensated by the shunting effect of a capacitance which can be calculated from (2) taking into account stray capacitances

$$\delta_c \approx \omega^2 LC 100\%, \tag{3}$$

where δ_c is the variation in the instrument reading due to the presence of a shunting capacitance; C is the value of the shunting capacitor; L is the inductance of the instrument coil.

Compensation is attained when $\delta_c + \gamma_{ec} = 0$, and hence from (2) and (3) we obtain

$$C = \frac{k_1}{4\pi^2 L}. \tag{4}$$

It will be seen from (4) that the compensation condition does not depend on frequency. However, it should be borne in mind that error γ_{ec} can be compensated by a shunting capacitance only for instruments with a current measuring range not exceeding 10 amp, since the inductance of the coil decreases as the square of the increasing range and the required capacitance becomes excessively large.

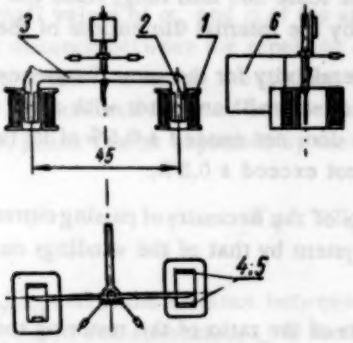

Fig. 1. 1) Coil; 2) moving core; 3) moving core holder; 4) additional core; 5) fixed core; 6) damper vane.

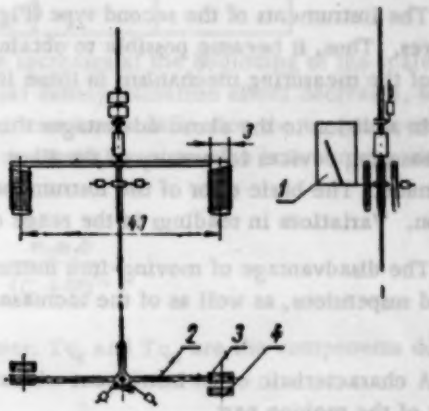

Fig. 2. 1) Damping vane; 2) moving coil holder; 3) moving core with winding; 4) stationary core with winding.

The rising number of turns in moving-iron milliammeters increases their interturn capacitance and, hence, the error due to its shunting effect exceeds the demagnetizing error of the eddy-currents and the total error becomes positive. A method developed in [2] consists in compensating this error by the demagnetizing effect of a special compensating winding W_k terminated by a resistance R_k. However, the application of the compensation methods described in [2] is restricted. With a rising frequency the absolute value of the mutually compensated errors (γ_{ec} δ_c) increases, and the inevitable difference in the laws of their variation with frequency leads to a considerable resultant error.

A more reliable method of extending the frequency range of these instruments consists in reducing the error due to eddy-currents by applying the above-mentioned design alternations, and also by reducing the interturn capac-

itance and inductance of the coil, reducing the number of ampere turns in the coil, and decreasing the size of its core to the absolute minimum.

All these conditions are best met by a new design of an astatic moving-iron instrument developed and tested in the measuring devices laboratory of the Kiev Polytechnical Institute. This instrument has two pairs of repelling cores, stressed suspensions and a luminous display. The instrument's measuring mechanism is placed for additional protection from external magnetic fields in a permalloy screen, the components of the instrument's moving system are made of textolite and pertinax, and it employs air damping. The instrument uses the optical system and the casing of voltmeter S50 made by the "Tochélektropribor" plant.

Two types of new moving-iron instruments have been developed.

In the first type (Fig. 1) the adjustment is carried out by positioning additional cores which provides a ± 10% variation in the full-scale readings. In order to avoid parallax the scale is drawn directly on a plexiglas base which has been previously painted white. Thus, the projection of the luminous spot and the scale markings are virtually in the same plane. The instrument range is changed by connecting the measuring coils either in parallel or in series.

Electrostatic interaction between the winding and the moving cores is eliminated by connecting the suspensions to one of the instrument's terminals.

Dc and ac ammeters, milliammeters and voltmeters were made according to the above design with ranges of 5-10 amp, 5-10 ma, and 7.5 v, respectively.

The operating part of the scale from 10 to 100% of the full deflection has a nonuniformity factor not exceeding 1.3.

The instrument's basic error at 50 cps does not exceed ± 0.5% of the full-scale deflection. Variations in readings in a range of 20 to 20,000 cps do not exceed ± 0.5%.

In dc measurements the maximum deviation of readings amounts to ± 0.25% of the full-scale deflection.

Instruments of this design have been developed by agreement with the "Tochélektropribor" plant.

The instruments of the second type (Fig. 2) have their operating coils wound directly on the moving and stationary cores. Thus, it became possible to obtain instruments with a double scale 300 mm long, since the deflection angle of the measuring mechanism in these instruments is not limited by the internal dimensions of the coil.

In addition to the above advantages this design provides higher sensitivity for the same frequency range. In the measuring devices laboratory of the Kiev Polytechnical Institute a dc-ac milliammeter with a 2.5 ma range has been made. The basic error of the instrument at a frequency of 50 cps does not exceed ± 0.5% of its full-scale deflection. Variations in readings in the range of 20 to 20,000 cps does not exceed ± 0.3%.

The disadvantage of moving-iron instruments of this type consists of the necessity of passing current through the stressed suspensions, as well as of the increased weight of the moving system by that of the windings on the moving cores.

A characteristic of an instrument with stressed suspensions consists of the ratio of the restoring torque to the weight of the moving part

$$A = \frac{W}{G} 2 \frac{100}{l_0}, \qquad (5)$$

where W is the specific restoring torque at 90° for a stressed suspension 100 mm long; G is the weight of the moving part, g-wt; l_0 is the length of the stressed suspension, mm.

According to the data in [3], an instrument becomes workable for $A \geq 4$, which is met in the above design.

The most characteristic data for instruments of both types are shown in the table.

It is known that the scale of moving-iron instruments is normally uneven and approaches a square law distribution for small deflection angles, thus reducing the accuracy at the beginning of the scale. In the new moving-iron instruments, as already stated, an almost uniform scale has been obtained. The scale was straightened out by a relative increasing of the torque at the beginning of the scale and by utilizing the repelling effect of the cores at very small distances between them, and decreasing the torque T_q at deflection angles approaching the full-scale deflection of the instrument.

The relation between the torque and the deflection angle of the instrument is

$$T_v = \frac{km_1m_2}{r_0^2(\alpha_0+\alpha)^2}, \quad (6)$$

where m_1 and m_2 are magnetic masses of the core; r_0 is the distance between the axis and the center of the core; α_0 and α are the initial and the variable deflection angles of the instrument's moving parts.

Designation of parameters	Dimensions	Types			
		first			second
		ammeter	milliammeter	voltmeter	milliammeter
Measuring range		5-10 amp	5-10 ma	7.5 v	2.5 ma
Amper-turns	av	20	9	8.7	10
Winding data					
Number of turns		2×2	2×900	2×250	4×1000
Resistance	ohm	$2\times4\times10^{-3}$	2×50	4	4×50
Inductance	mh	$2\times6\times10^{-5}$	2×14	0.7	70
Full-scale current	ma	—	—	35	—
Core dimensions	mm	5×10×0.1			3×15×0.1
Wt. of moving part	g-wt	0.5			1
Specific restoring moment of a stressed suspension made of Br-SnZn 4-3	$\frac{\text{mg-wt·cm}}{90^\circ}$	2	0.5	0.5	0.7
Ratio of the restoring moment to the weight of the moving part	$\frac{\text{mg-wt·cm}}{\text{g-wt·90}^\circ}$	24	6	6	4

For small values of α_0 and α of the same magnitude the torque increases at the beginning of the scale. Moreover, as the distance between the repelling cores increases, their mutual demagnetization effect decreases, which is equivalent to a relative rise in the torque. For angles approaching the maximum deflection the torque decreases not only due to an increased distance between the repelling cores, but also due to the attraction between opposite poles of the cores, which can be expressed by the following relation:

$$T_q = T_{qr} - T_{qa} = kr_0\left[\frac{m_1m_2}{\delta^2} - \frac{m_1m_2\delta}{(l_c^2+\delta^2)^{3/2}}\right], \quad (7)$$

where $\delta = r_0(\alpha_0+\alpha)$ is the distance between the moving and fixed cores; Tq_r and Tq_a are the components due to the forces of repulsion and attraction; l_c is the length of the core.

It was established experimentally that the straightening-out of the scale at its beginning and in its second half is improved by reducing the length of the core.

Conclusions. The instruments developed by us have an almost uniform scale starting at 10% of the full-scale reading. The first design is simpler and more reliable.

As far as we know such instruments are not being produced anywhere.

LITERATURE CITED

1. V. O. Arutyunov, Electrical Measuring Instruments and Measurements [in Russian] (Gosenergoizdat, Moscow, 1958).
2. P. P. Ornatskii, I. K. Khodeev, and V. A. Dem'yanenko, Bulletin of Higher Educational Institutions. Priborostroenie, No. 4, 1958.
3. S. M. Pigin, Izmeritel'naya tekhnika, No. 3, 1958.

HIGH-FREQUENCY COAXIAL CYLINDRICAL CAPACITOR WITH A CONTACTLESS PLUNGER

A. L. Grokhol'skii

Translated from Izmeritel'naya Tekhnika, No. 11, pp. 48-49, November, 1961

In [1] we have examined the theory and design of reference coaxial cylindrical capacitors. These capacitors provide effective values of capacitance at frequencies up to 200-300 Mc with an error of 0.1% ± 0.1 μμf. They are single-valued standards and when connected into sets provide discrete values of capacitance, but they are not suitable for obtaining any required value of capacitance in a given range, which is normally obtained by variable capacitors. However, the majority of variable capacitors owing to their variation with frequency cannot always be used, especially at frequencies above 100 Mc.

Recently a new type of a variable high-frequency capacitor has been produced. It consists of a coaxial cylindrical capacitor with a contactless plunger, and is known as a plunger capacitor.

The plunger capacitor scores over other types by its small variation with frequency, which at 200 Mc does not exceed 5-10% and can be calculated with considerable accuracy.

The schematic of a plunger capacitor is shown in Fig. 1.

The value of the capacitor depends on the depth to which the contactless plunger is inserted into the gap between the coaxial cylindrical electrodes. At low frequencies it can be calculated by means of the formula which, owing to its simplicity, is given without proof:

$$C_n = C_1(l-k) + C_2 k, \qquad (a)$$

where $C_1 = \frac{1}{18\ln(D_4/D_1)}$ is the unit capacitance of section I of the capacitor without the plunger, μμf/mm;

$C_2 = \frac{1}{18\ln(D_4/D_3) + 18\ln(D_2/D_1)}$ is the unit capacitance of section II of the capacitor with the plunger, μμf/mm;

l is the length of the capacitor, mm; k is the depth to which the plunger is inserted, mm.

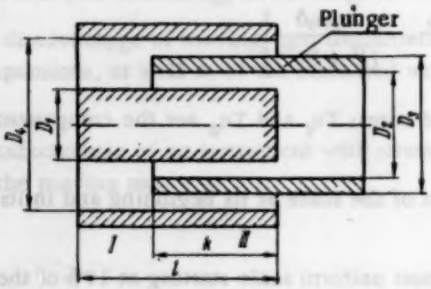

Fig. 1

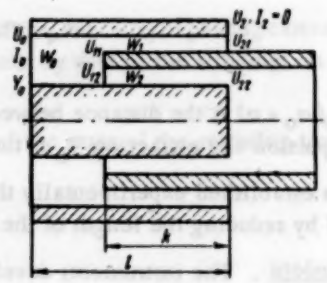

Fig. 2

The value of the plunger capacitor at high frequencies can be calculated from its input admittance by considering the capacitor as a line with distributed constants.

The admittance in turn is calculated from the distribution of currents and voltages in the capacitor.

If we denote them as shown in Fig. 2, voltage U_2 at the output of the capacitor will consist of the sum of two voltages, namely of U_{21} in the first gap which forms a line with a wave impedence W_1, and of voltage U_{22} in the second gap with a wave impedance of W_2.

It has been shown in [2] that voltage U_1 at the front end of the plunger also consists of two voltages, namely U_{11} and U_{12}, so that

$$U_1=U_{11}+U_{12}=U_{22}\cos 2\pi\frac{k}{\lambda}+U_{21}\cos 2\pi\frac{k}{\lambda}=U_2\cos 2\pi\frac{k}{\lambda}. \tag{1}$$

This, as well as further calculations, is based on the assumption that the electrodes have an infinitely large conductance. The error due to this assumption is negligible, and has been analyzed in [1].

Current I_1 at the front end of the plunger is equal to

$$I_1=j\frac{U_{22}}{W_2}\sin 2\pi\frac{k}{\lambda}. \tag{1a}$$

but considering that

$$\frac{U_{22}}{U_{21}}=\frac{W_2}{W_1};\quad U_2=U_{22}+U_{21}, \tag{1b}$$

we obtain

$$I_1=j\frac{U_2}{W_1+W_2}\sin 2\pi\frac{k}{\lambda}. \tag{2}$$

From (1) and (2) voltage U_0 and current I_0 at the input of the capacitor have values of

$$U_0=U_2\left[\cos 2\pi\frac{k}{\lambda}\cos 2\pi\frac{l-k}{\lambda}-\frac{W_0}{W_1+W_2}\sin 2\pi\frac{k}{\lambda}\sin 2\pi\frac{l-k}{\lambda}\right],$$

$$I_0=jU_2\left[\frac{1}{W_1+W_2}\sin 2\pi\frac{k}{\lambda}\cos 2\pi\frac{l-k}{\lambda}+\frac{1}{W_0}\cos 2\pi\frac{k}{\lambda}\sin 2\pi\frac{l-k}{\lambda}\right]. \tag{2a}$$

From the above we derive the input admittance

$$Y_0=j\frac{1}{W_0}\frac{\frac{W_0}{W_1+W_2}\operatorname{tg}2\pi\frac{k}{\lambda}+\operatorname{tg}2\pi\frac{l-k}{\lambda}}{1-\frac{W_0}{W_1+W_2}\operatorname{tg}2\pi\frac{k}{\lambda}\cdot\operatorname{tg}2\pi\frac{l-k}{\lambda}}. \tag{3}$$

It is capacitative if $1<\lambda/4$, thus it becomes possible to substitute the input admittance by a capacitor so that $Y_0=j\omega C_b$; hence

$$C_b=\left[\frac{\operatorname{tg}2\pi\frac{k}{\lambda}}{\omega(W_1+W_2)}+\frac{\operatorname{tg}2\pi\frac{l-k}{\lambda}}{\omega W_0}\right]\frac{1}{1-\frac{W_0}{W_1+W_2}\cdot\operatorname{tg}2\pi\frac{k}{\lambda}\cdot\operatorname{tg}2\pi\frac{l-k}{\lambda}}. \tag{4}$$

The first term in the square brackets represents the high-frequency value of the part of the capacitor with the plunger

$$C_{2b}=\frac{\operatorname{tg}2\pi\frac{k}{\lambda}}{\omega(W_1+W_2)}; \tag{4a}$$

the second term represents the capacitance of the part without the plunger

$$C_{1b}=\frac{\operatorname{tg}2\pi\frac{l-k}{\lambda}}{\omega W_0}. \tag{4b}$$

Each of these capacitances can be represented, in a manner similar to that adopted for (1), as consisting of two parts, namely the static capacitance equal to the unit capacitance multiplied by the length of the section, and of frequency correction p represented by the series

$$p_2=\frac{1}{3}\left(2\pi\frac{k}{\lambda}\right)^3+\frac{2}{15}\left(2\pi\frac{k}{\lambda}\right)^4+\frac{17}{315}\left(2\pi\frac{k}{\lambda}\right)^6+\ldots. \tag{5}$$

or

$$p_1 = \frac{1}{3}\left(2\pi\,\frac{l-k}{\lambda}\right)^2 + \frac{2}{15}\left(2\pi\,\frac{l-k}{\lambda}\right)^4 + \frac{17}{315}\left(2\pi\,\frac{l-k}{\lambda}\right)^6 + \ldots$$

Taking the above assumption into account we have

$$C_{2b} = C_2 k\,(1+p_2); \quad C_{1b} = C_1\,(l-k)(1+p_1). \tag{6}$$

and (4) assumes the form

$$C_b = \frac{C_n + C_1 p_1 (l-k) + C_2 p_2 k}{1 - \dfrac{W_0}{W_1+W_2}\,\mathrm{tg}\,2\pi\,\dfrac{k}{\lambda}\,\mathrm{tg}\,2\pi\,\dfrac{l-k}{\lambda}} \tag{7}$$

The factor $W_0/(W_1+W_2)$ in the denominator can be substituted by the ratio of unit capacitances C_2/C_1 which is equal to it. The final expression for the value of a plunger capacitor will then become

$$C_b = \frac{C_n + C_1 p_1 (l-k) + C_2 p_2 k}{1 - \dfrac{C_2}{C_1}\,\mathrm{tg}\,2\pi\,\dfrac{k}{\lambda}\,\mathrm{tg}\,2\pi\,\dfrac{l-k}{\lambda}}. \tag{8}$$

The first term of the numerator in (8) is best obtained by a measurement with low-frequency reference standards, since in this manner the edge effects are taken into account. The remaining terms are considerably smaller than the first, and it is simpler to calculate them, since the possible inaccuracies in calculating even with approximate formulas will not produce any excessively large errors in the final result.

Experimental checking of (8) has shown that it provides effective capacitances up to 100-200 $\mu\mu$f at 200 Mc with an error not exceeding 0.2-0.3%. At lower frequencies the error decreases rapidly.

It should be noted that a minimum error will be obtained in (8) if all the diameters throughout the capacitor are kept as closely as possible to their nominal values.

In the experimental capacitor the diameters at any cross section did not deviate from their mean value by more than ± 2 μ. It is possible to use this capacitor for substitution measurements at any of its settings up to 200 Mc with an error of 0.1-0.2% $\pm$ 0.05 $\mu\mu$f.

LITERATURE CITED

1. A. L. Grokhol'skii, Izmeritel'naya tekhnika, No. 6, 1960.
2. B. V. Plodukhin, Coaxial Wide-Band Resonators [in Russian] ("Sovetskoe Radio" press, 1956).

NEW METHOD OF DETERMINING THE Q-FACTOR OF QUARTZ-CRYSTAL RESONATORS

E. D. Novgorodov

Translated from Izmeritel'naya Tekhnika, No. 11, pp. 50-51, November, 1961

Below we suggest a new method of measuring the Q-factor of quartz resonators based on determining the phase difference between the current and the voltage across the quartz resonator when the generator frequency is changed.

If in a three-tube quartz generator (Fig. 1) a phase difference between the current and voltage is produced owing to the existence of reactances, it is necessary for a correct operation of the generator that this phase difference be compensated by a phase difference between the current and voltage across the quartz resonator which should

be equal in magnitude and opposite in phase to the former phase difference. Such a phase difference can only be obtained at a definite frequency distinct from the natural frequency of the quartz resonator. This new frequency is produced by the generator.

It can be easily shown that the required phase difference φ is related to a variation Δf in the generator frequency by the expression:

$$\frac{\Delta f}{f} = \frac{1}{2Q_1} \operatorname{tg} \varphi, \qquad (1)$$

where Q_1 is the quality factor of the quartz resonator taken together with the leakage resistance R_2 in the grid of the third tube.

Since the quality is inversely proportional to the power losses we have:

$$\frac{Q}{Q_1} = \frac{R_q + R_2}{R_q}, \qquad (2)$$

where Q is the quality factor of the quartz resonator alone; R_q is its equivalent resistance.

It follows from (1) and (2) that a rising Q-factor and decreasing resistance R_2 will provide decreasing generator frequency variations due to constant changes in the circuit parameters, i.e., they will provide an increased stability of the quartz generator. From (1) and (2) we also obtain:

$$Q = \frac{\operatorname{tg} \varphi}{2 \frac{\Delta f}{f}} \left(1 + \frac{R_2}{R_q}\right). \qquad (3)$$

The above circuit provides an experimental determination of the values of Δf, φ, and R_q from which the Q-factor can be found. The above values are measured in the following manner. The voltages across resistors R_1 and R_2 are brought into phase by means of the variable capacitor in the anode circuit of the first tube (the Lissajous figure on the oscilloscope screen assumes the shape of a straight line). The quartz resonator will then represent a pure resistance, and hence, Δf and φ will be equal to zero. The quartz resonator is then replaced by a variable resistor R_e which is adjusted for the amplitude of oscillations to attain the same value as it had when the quartz resonator was in circuit. In this case $R_q = R_e$.

Having thus obtained the value of R_q, the quartz resonator is again connected to the circuit and the variable capacitor adjusted for the minor axis b of the ellipse, to become equal to $\sqrt{8} \cdot a$ where a is the value of the major axis which must be tilted at an angle of 45°. This setting is checked by bringing the ellipse obtained on the oscilloscope screen to coincide with a previously-drawn ellipse. We shall now have

$$\operatorname{tg} \varphi = \frac{b}{\sqrt{a^2 - b^2}} = 2 \text{ and } Q = \frac{f}{\Delta f} \left(1 + \frac{R_2}{R_q}\right). \qquad (4)$$

The variation Δf in the generator frequency is determined by comparing it with the frequency of a reference quartz generator by any of the known methods.

An analysis of the error in the above method has shown that it is mainly determined by the phase measurement error, i.e., by the error in making the two ellipses coincide on the oscilloscope screen. This error can easily be reduced to less than 3-5%. If the ellipse is obtained at a harmonic frequency n times greater than the fundamental, the error is reduced by a factor of n.

When the vertical and horizontal signals are set up on the screen of the oscilloscope by means of its amplifiers, it is necessary to check whether the latter introduce a phase-shift. For this purpose both inputs are fed with the same signal, which should produce a straight line on the screen. If an ellipse is obtained, it is necessary to place a phase-shifting element in front of one of the amplifiers and by adjusting it obtain a straight line on the screen.

It is more convenient and accurate to determine the phase difference by means of a differential phase meter (Fig. 2). If in Q-factor measurements the value of the calibrated variable resistance R_2 (Fig. 1) is set to the value of the equivalent resistance R_q, which has been found, and the frequency of the generator is always changed by the

same amount of $\Delta f/f$, the voltmeter at the output of the differential phase meter, whose pointer deflections are proportional to the phase difference of the voltages fed to it, can be calibrated, as will be seen from (3), directly in values of the Q-factor.

When a differential phase-meter is used the error in Q-factor measurements can easily be reduced to less than 1% for fundamental frequency measurements.

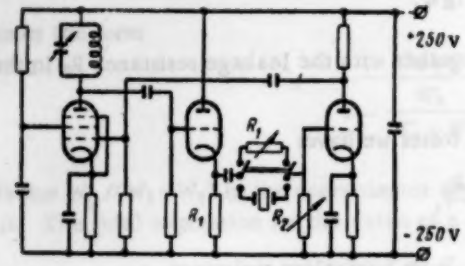

Fig. 1

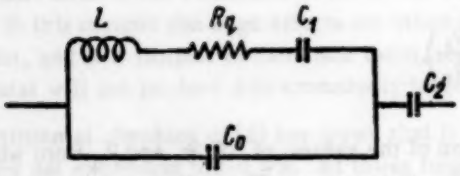

Fig. 3

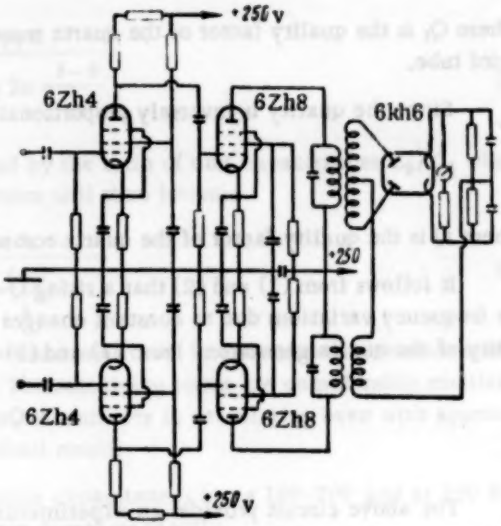

Fig. 2

The above methods assume a symmetrical characteristic of the quartz resonator tuned circuit, whereas, strictly speaking, the existence of a parallel capacitance C_0 (see the equivalent circuit of a quartz resonator in Fig. 3) makes the resonant curve asymmetrical. However, this asymmetry virtually has no effect on measurement results in the range of frequency detuning by $\Delta f/f$ used in this calibration. In fact the full impedance of a quartz resonator can be represented as:

$$Z = \frac{r + j\omega L \frac{2\Delta f}{f}}{1 + j\omega C_0 \left(r + j\omega L \frac{2\Delta f}{f} \right)}. \qquad (5)$$

In existing types of quartz resonators resistance r is about three orders smaller than the reactance of C_0 at the tuned frequency of the resonator. Since in the detuned frequencies used in these measurements the modulus of the impedance $r + j\omega L \cdot 2\Delta f/f$ does not exceed 2.5 r, we shall have $\omega C_0 (r + j\omega L \cdot 2\Delta f/f) \ll 1$, and this product can, therefore, be neglected with an error of tenths of one per cent. We can then consider that

$$Z = r + j\omega L \frac{2\Delta f}{f}, \qquad (6)$$

which provides a symmetrical resonance curve.

Conclusions. The measurement error of the above method does not depend on the Q-factor of the quartz resonator nor on its frequency, which makes it applicable in any frequency or Q-factor range, whereas other methods are restricted in their application either by their minimum decay time or by their minimum bandwidth.

Knowing the Q-factor, the equivalent resistance and the frequency of the quartz resonator, it is possible to calculate its equivalent inductance and dynamic capacitance. Thus, the above circuit makes it possible to determine all the parameters of a quartz resonator equivalent circuit.

AUTOMATIC INSTRUMENT FOR MEASURING ULTRASONIC ATTENUATION

V. A. Markelov

Translated from Izmeritel'naya Tekhnika, No. 11,
pp. 52-53, November, 1961

Ultrasonic methods are widely used in various industries for measuring viscosity, density and other physicochemical parameters of various substances. The application of these methods to continuous automatic measurements under production conditions is, in certain cases, difficult owing to the lack of measuring circuits which can work for a long time with the required accuracy and reliability.

Among the various methods of measuring ultrasonic absorption, the pulse method is the one most commonly used owing to its relative simplicity and universal applicability. However, the available pulse instruments intended for measuring ultrasonic absorption have substantial defects which reduce their accuracy and reliability and impede their application.

The differential pulse circuit developed by I. G. Mikhailov and G. N. Feofanov [1] is the best of its kind whose description has appeared in print, but it is not devoid of defects. In this circuit the signals are not amplified in a single, but in two parallel channels (the master oscillator contains two output amplifiers, the receiver uses two coincidence stages, two peak detectors and two delay circuits); this arrangement not only makes the equipment more complicated, but also limits its accuracy, since any variations in the parameters of components and tubes will affect measurement results. An additional source of instability in this equipment is provided by a dc amplifier with its inherent zero drift. Instruments based on a direct amplification of signals suffer from even greater defficiencies, since the instability of their circuit parameters and of the supply voltage affect them to an even greater extent.

The Scientific Research Institute of Basic Chemistry has developed a continuously operating automatic instrument for measuring ultrasonic absorption by a pulse method which is devoid of the aforementioned defects [2].

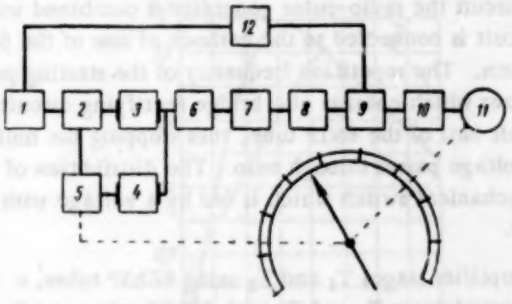

Fig. 1. 1) Oscillator; 2) switch; 3) comparison cell; 4) measurement cell; 5) attenuator; 6) amplifier; 7) detector; 8) video-amplifier; 9) demodulator; 10) low-frequency amplifier; 11) reversible motor; 12) delay unit.

The instrument (Fig. 1) uses a differential method of comparison with an automatic compensation of the signal unbalance. The equipment contains two cells, a measurement and a comparison cell associated with two channels and a common amplifying and converting channel. The instrument's principle of operation consists of the following: the master oscillator 1 provides radio-pulses of a rectangular waveform with a repetition frequency of 100 pps synchronized with the supply frequency. The pulses are distributed by means of switch 2 between two channels so that the even pulses are fed to the radiator of comparison cell 3 and the odd pulses to the radiator of measurement cell 4. The measurement cell circuit contains attenuator 5 which varies the amplitude of the pulses fed to the converter. Having passed through the cells the pulses are fed to a common amplifier 6. The amplified pulses are detected and fed to demodulator 9. The difference in the amplitude of the even and odd pulses is proportional at the input of the demodulator to the difference of the ultrasonic absorption coefficients in the comparison and measurement cells.

Simultaneously with each pulse the demodulator is fed with a rectangular selecting pulse, which is obtained from delay unit 12. The trailing edge of the selecting pulse coincides in time with the middle of each of the main pulses. The pulse sequence is converted in the demodulator into a commercial frequency unbalance voltage whose

amplitude is proportional to the difference between the amplitudes of the even and odd pulses, and whose phase depends on the direction of unbalance. When the direction of unbalance changes the phase is reversed.

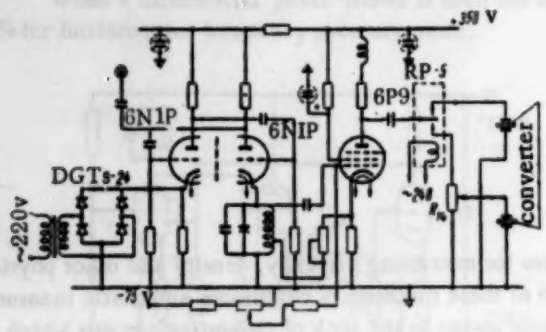

Fig. 2

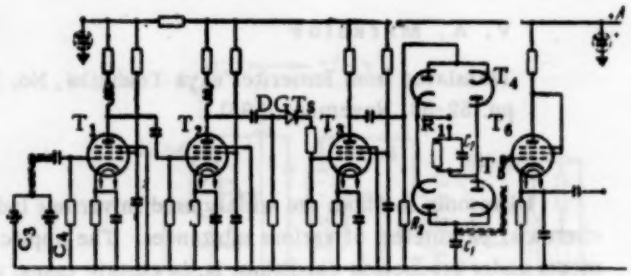

Fig. 3

The unbalance voltage is amplified by a low-frequency amplifier 10 and is fed to reversible motor 11 which displaces an attenuator slider, thus varying the voltage of the radiator in the measurement cell. The motor is operated by the unbalance voltage until the amplitudes of the even and odd pulses become equal and the alternating component at the output of the modulator disappears. A pointer which is fixed to the demodulator slider is displaced together with it along a scale calibrated in absorption units. In order to provide reliable measurements it is necessary to have reserve amplification and oscillator power.

The threshold of sensitivity of the instrument is determined by that of the low-frequency amplifier, which in the case of a standard automatic electronic bridge (EMD or MS) is of the order of 50-100 μv. Hence, the sensitivity of the above instrument can be made considerably higher than that of the best modern laboratory installations intended for measuring absorption. Thus, the instrument can also be used in laboratories for evaluating absorption in low-absorbing media in whose measurements instrument sensitivity becomes a decisive factor.

The instrument's circuit is changed but little if each cell uses one converter and reflected pulses are measured.

The schematic of the pulse-generator used in the instrument is shown in Fig. 2. The multivibrator uses 6N1P tubes and produces rectangular pulses whose duration corresponds to that of the radio-pulses. The rectangular pulses serve to start the radio-pulse generator. In order to simplify the circuit the radio-pulse generator is combined with one of the multivibrator tubes. For this purpose an oscillatory circuit is connected to the cathode of one of the 6N1P tubes and tuned to the natural oscillation frequency of the converters. The repetition frequency of the starting pulses is synchronized with the mains frequency by means of a synchronizer which consists of a bridge rectifying circuit. The rectified voltage obtained from the synchronizer blocks the left half of the 6N1P tube, thus stopping the multivibrator. The multivibrator is restarted at the instant the mains voltage passes through zero. The distribution of radio-pulses along the channels is made by means of an electromechanical switch which is fed by a voltage with a phase difference approaching 90° with respect to the mains voltage.

The receiver circuit (Fig. 3) contains two high-frequency amplifier stages T_1 and T_2 using 6Zh5P tubes, a DGTs-7 detector, a pulse amplifier T_3 with a 6Zh5P tube, and a demodulator T_4 and T_5 with 6Kh2P tubes and T_6 with a 6Zh5P tube which represent a series diode gate controlled by pulses from the delay unit. At the instant of the selector pulse operation the diode switch becomes conducting and transmits the measurement pulse which charges capacitor C_1 up to the voltage equal to the pulse amplitude. When the operation of the selecting pulse is completed, the gate is blocked by the voltage across the R_1C_2 circuit, and the capacitor C_1 retains the voltage equal to the pulse amplitude until the second selective pulse is received, which provides a discharging path for capacitor C_1 through resistor R_2 and then recharges the capacitor to an amplitude of the succeeding measurement pulse. Capacitor C_1 controls a cathode follower at whose output a commercial frequency unbalance voltage is produced.

The delay unit circuit consists of a generator of varying duration pulses which shape the multivibrator and synchronize the symmetrical output amplifier.

The above instrument is suitable for continuous automatic measurements with the required accuracy and reliability under production conditions.

LITERATURE CITED

1. I. G. Mikhailov and G. N. Feofanov, Akusticheskii zhurnal, Vol. 2, No. 2, 1956.
2. V. A. Markelov, Circuit for Measuring Ultrasonic Absorption. Author's Certificate No. 126281.

ULTRASONIC INDICATOR OF THE CLARIFIED ZONE OF PULP

V. A. Nosov and G. D. Mamuta

Translated from Izmeritel'naya Tekhnika, No. 11, pp. 54-55, November, 1961

The development plan of the USSR National economy envisages total automation of production processes in mineral concentration and aluminum industries. One of the most important tasks in this sphere consists in obtaining automatic signalling of the level of the clarified zone of the pulp in processing tanks. Under production conditions this presents considerable difficulties owing to the corrosive medium and relatively high temperatures of the pulp. Thus, the photoelectric method of determining the boundary of the clarified zone cannot be used, since the glass windows of the photoelectric cell become stained by the pulp and the overflow pipes and floats are not suitable for automatic processes. The low accuracy and safety considerations limit the application of the radioactive method, based on measuring attenuation of the radioactive radiation in the settled pulp.

The use of the ultrasonic method considerably simplifies the solution of this problem. In his investigation of the relation between the ultrasonic absorption factor α and concentration by volume β of suspended particles (of 1-10 μ in diameter) in water, Urick [1] obtained the relationship shown in Fig. 1. It will be seen from the graph that for minor variations of small concentrations the absorption factor changes considerably. Small variations of concentration provide considerable changes in the ultrasonic signal owing to the exponential relation between the amplitude attenuation of the ultrasonic wave and the absorption factor [2].

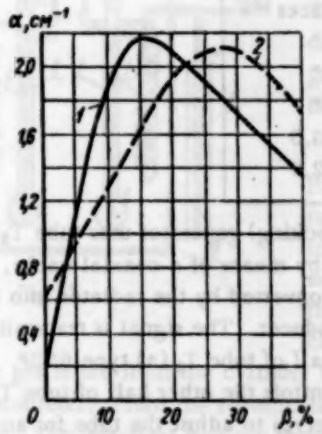

Fig. 1. 1) For a frequency of 1 Mc; 2) for a frequency of 3 Mc.

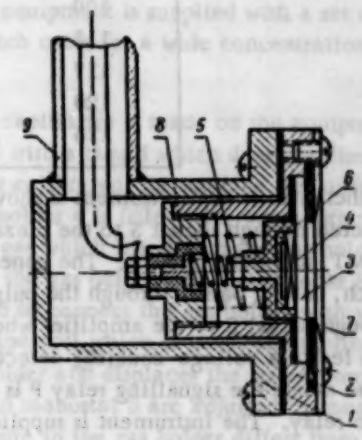

Fig. 2

The Institute of Automation of the Ukr. SSR State Planning Committee, on the basis of these relations, has developed an ultrasonic device for signalling the clarified zone level. This device is constructed on the principle of rapid attenuation of an ultrasonic beam due to the presence of solid suspended particles. It consists of measuring transducers designed for transmitting and receiving ultrasonic oscillations in liquids with suspended solid particles,

of an electronic measuring unit and a coaxial cable. The receiving and transmitting transducers are mounted at a distance of 150 mm from each other on a special tubular stainless steel frame, which is placed inside the processing tank at a depth of the clarified pulp zone to be tested. The transducers are connected to the electronic measuring instrument by means of a coaxial cable type RKTF-2 which is protected inside the tank by a metal covering.

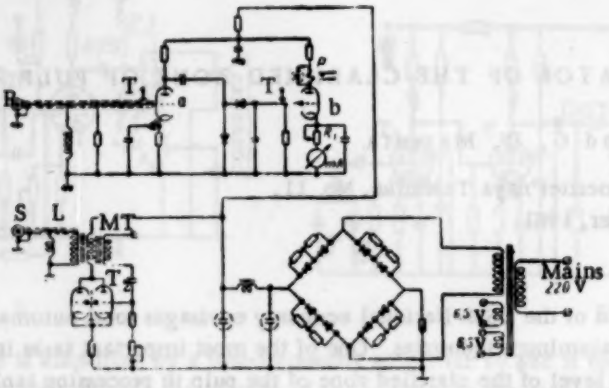

Fig. 3

The design of measuring transducers for corrosive media is shown in Fig. 2. Capsule 2 has a titanate-barium plate 4 with a diameter of 20 mm and a thickness of 2.2 mm, secured by spring 5 between quartz plate 3 and reflector 6. The electrical connection to the titanate-barium plate is made at one end through spring 5 and at the other through a thin foil on transducer casing 1. The coaxial cable is protected from the corrosive medium by metal tube 9. The transducer components 7 and 8 are made of Teflon, the remaining components of stainless steel. The acoustical contact between the piezoelectric plate and the quartz plate is made through a thin layer of oil.

Sampling depth in processing tank, cm	Instrument readings, ma	Pulp content, g/liter
80	0	Traces
100	0	"
115	0.6	"
117	0.9	"
120	7.5	13.5
125	7.5	62.0

The schematic of the instrument is shown in Fig. 3. The pulse (blocking) generator uses tube T_2 type 6N1P and is connected through socket S to the piezoelectric transducer's plate by means of a coaxial cable, a matching transformer MT, and inductance L. The generator's electrical signal is converted by the radiator into ultrasonic vibrations which, having passed through the pulp, excite the receiving transducer. The signal is transmitted from the receiver through socket R to the amplifier where it is amplified by one-half of tube T_1 (a) type 6N3P. The amplified signal is fed to a voltage-doubling detector. The detected signal controls the other half of tube T_1 (b) type 6N3P to whose anode the signalling relay P is connected. Resistance R_1 serves to adjust the tube for an efficient operation of the relay. The instrument is supplied from 220 v ac mains through semiconductor rectifiers DGTs-27. The instrument operates by unblocking one half of tube T_1 when any suspended particles are present between the receiving and transmitting transducers. In such a case the ultrasonic wave is dispersed by the suspended particles of the pulp, the tube is unblocked and the signal relay P operates. The sensitivity of the instrument to pulp suspensions at various immersion depths in the processing tank (condenser) used in alumina production can be judged from the data given in the table for a substance with a density of 3.2.

LITERATURE CITED

1. R. Urick, Journ. Acoust. Soc. Amer. 20, 225, 285 (1948).
2. L. Bergman, Ultrasonics [Russian translation] (Foreign Literature Press, 1956).

DYNAMIC GAS-MIXING INSTALLATION FOR CALIBRATING AND CHECKING AUTOMATIC GAS ANALYZERS

E. M. Malkova and Z. T. Kezina

Translated from Izmeritel'naya Tekhnika, No. 11,
pp. 55-57, November, 1961

The Sverdlovsk branch of the VNIIM (All-Union Scientific Research Institute of Metrology) has made and tested a dynamic gas-mixing equipment for batching sulfur dioxide, oxygen, nitrogen oxide, and other gases. Gas mixtures of a precise composition are obtained in this equipment by mixing the flows of two or several gases, or by means of rheometers with previously graduated capillary tubes. The equipment (Fig. 1) can be used for batching both small and medium concentrations of the aforementioned gases.

Two symmetrically placed rheometers 1 and 2 are fitted with capillary tubes 3 and 4, and interconnected by gas-mixer 5. All these components are placed in a water thermostat 10. In order to make the gas fed from the cylinder acquire the temperature of the thermostat it is passed through glass tube coils 6 and 7 which have 12-14 turns each and are placed in the thermostat.

The water thermostat consists of a brass container with a removable lid and double walls with the space between them filled with asbestos. The front wall is made of plexiglas to provide a convenient reading of the rheometer scale. The thermostat is fitted with an electrical heater, which provides the heating of water up to 8-10°C. Brass pipe coils are used for cooling purposes. The water is stirred by means of an electrical mixer. The temperature is controlled by means of a contact thermometer and an electronic heat regulator. The thermostat provides a constant temperature with an error of ± 0.1°C. Manometers 8 and 9 are connected to the pipe coils, placed outside the thermostat and filled with the same liquid as the rheometers. All the components of the equipment are butt-connected to each other by means of short lengths of rubber tubing The scale (0 to 450 mm) is fixed directly on the rheometer in order to reduce the reading error. The equipment is supplied with a set of previously graduated capillary tubes which cater for a wide concentration range of the batched component.

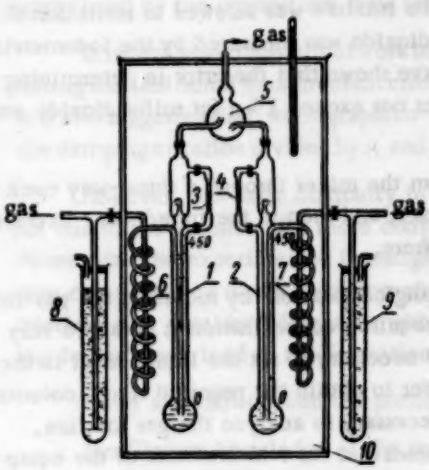

Fig. 1

The calibration of the capillaries is made on the equipment shown in Fig. 2. Rheometer 1 is filled with a liquid which does not dissolve the gas for which capillary 2 is being calibrated, for instance, for sulfur dioxide transformer oil is used. Gas holder 4 is filled with water through the funnel with cock 10 open. The gas which filled with the gas holder is ejected through tap 8. Having filled the gas holder with water cocks 8 and 10 are closed, and cock 11 is opened to connect the gas holder with water manometer 6. The gas is fed from the cylinder through a manostat to the pipe coil which is inside the thermostat, and then to the rheometer. From the rheometer the gas is fed to the gas holder and displaces the water from it through the open tap 9. The gas-flow into the rheometer and the water level in manostat 3 are adjusted by means of pinch-cock 12 until the water level in manometer 6 is set to zero. The pressure in the gas holder differs from that of the atmosphere, since the gas enters the holder through a layer of water. This pressure difference is registered by water manometer 7 and is taken into account in computations.

Measurements are started when the rate of water-flow becomes constant (the liquid levels in manometer 6 and the rheometer must not vary). A stopwatch is started and at the same time the calibrated retort 5 is placed under tap 9. For calibrating capillaries over 0.3 mm in diameter it is recommended that retorts 1000-2000 ml in capacity be used, and for capillaries below 0.3 mm, 100-250 ml retorts should be used. Having measured the volume of the gas (by the amount of ejected water) and the time for which it flowed, its rate of flow in volume per minute is de-

termined. The relation of the rate of gas-flow to the height of the liquid column in the rheometer is determined at 7-8 points and a graph for each capillary is plotted.

The capacity of a dynamic gas-mixing equipment amounts to 5 to 70 liters/hr. The equipment was tested in preparing gas mixtures containing from 0.01 to 20% sulfur dioxide. For small concentrations of sulfur dioxide (from 0.01 to 1%) the relative error of the equipment does not exceed 2%; for concentrations between 1-20% it does not exceed 1%. In order to produce such gas mixtures it is sufficient to have two cylinders, one containing about 5-30% sulfur dioxide, and another compressed air or commercial nitrogen. By changing the capillaries it is possible to obtain a gas mixture containing from 0.01 to 20% sulfur dioxide.

For gas mixtures containing up to 10% sulfur dioxide it is possible to use in calibration either compressed air or nitrogen. For gas mixtures containing over 10% sulfur dioxide, a gas mixture of sulfur dioxide should be used in calibration.

The manostat connected to the rheometer through which sulfur dioxide passes is filled with transformer oil. By changing the liquid level in the manostat it is possible to vary the rate of gas-flow through the rheometer. The manostat has a rubber stopper with an additional hole for letting out the excessive sulfur dioxide into the atmosphere.

By means of this equipment the calibration of industrial automatic gas analyzers GÉM-U_2 and GÉB-U_2 was checked with respect to sulfur dioxide.

The principle of operation of these gas analyzers is based on comparing the thermal conductivity of the analyzed gas mixture and air.

Gas analyzers GÉM-U_2 are produced with two ranges, of 0-1% SO_2 and 0-1.5% SO_2.

Calibration of this gas analyzer was checked by means of a gas mixture containing 3.2% SO_2. Compressed air was used as a ballast gas. The gas mixture with sulfur dioxide was made in a 10-liter steel cylinder first covered with a double layer of bakelite lacquer. The cylinder was first evacuated, then filled with a measured quantity of 100% sulfur dioxide to which the ballast gas was added up to a preset pressure. The mixture was allowed to settle for 48 hours before the content of sulfur dioxide was measured by the iodometric method. Repeated experiments have shown that the error in determining the consistency of this method does not exceed 1% (for sulfur dioxide concentrations above 0.1%).

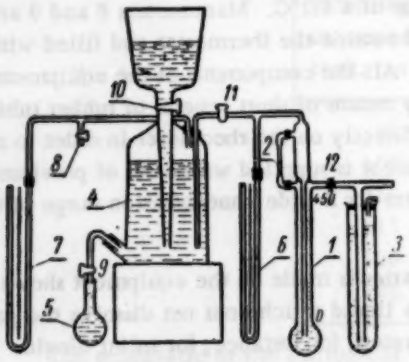

Fig. 2

The gas mixture was fed from the mixer through a three-way cock to the purifying unit of the gas analyzer, and then to the transducer. Excessive gas was tapped off into the atmosphere.

The time required for checking calibrations by means of the gas-mixing equipment is small, since the required concentration is obtained very quickly. For this purpose it is only necessary to set the liquid level in the manostat for the batched gas in order to obtain the required liquid column level in the rheometer. It is not necessary to analyze the gas mixture, since repeated experiments have shown that the relative error of the equipment over the whole concentration range does not exceed 1%, providing the concentration in the supply cylinder has been accurately established and the capillaries correctly calibrated.

The calibration of gas analyzer GÉB-U_2 with a scale of 0 to 10% was also checked. A cylinder with a gas mixture containing 8.8% SO_2 was used for this test with the same capillaries as were used for testing the GÉM-U_2 gas analyzer.

Conclusions. 1. The dynamic gas-mixing equipment based on obtaining gas mixtures by means of rheometers with calibrated capillaries can be recommended for calibrating and checking calibrations of commercial automatic gas analyzers used for determining the content of sulfur dioxide.

2. Commercial gas analyzers which have an error of 3-10% can be calibrated by means of the gas-mixing equipment without a thermostat, since room temperature vibrations in the range of 5-7°C have virtually no effect on measurement results.

LIQUID AND GAS-FLOW MEASUREMENTS

MEASURING PULSATING GAS-FLOWS

S. B. Bulatov, S. S. Kivilis, and A. S. Nemirovskii

Translated from Izmeritel'naya Tekhnika, No. 11,
pp. 57-58, November, 1961

According to the standard specification contained in Regulation 27-54 [1] adopted in the USSR the evaluation of the additional error in measuring a pulsating flow of gas (steam) by means of a differential manometer-flowmeter is accomplished by means of a dimensionless pulsation-damping criterion H_0 (Hodgson's number [2]). In conjunction with the work now being carried out in reviewing Regulation 27-54 it is interesting to analyze the present state of pulsation gas-flow rate measurements.

The analytical relation between the additional measurement error and criterion H_0 is given in [3,4]. This relation only characterizes the error due to the fact that the pulsating pressure difference in the constricting device of the flowmeter is averaged by the measuring system of the differential manometer, which is followed by the extraction of the square root from this mean value, whereas the actual mean rate of flow is equal to the mean root of the instantaneous pressure difference. Thus, computation error always remains positive.

In deriving the relation between the error and criterion H_0 the effect of the properties of the gas (the adiabatic index $\varkappa$) and the shape of pulsations are taken into account among other things. The evaluation of the error by means of criterion H_0 is approximate, it is therefore customary [4-7] to determine the error in all the cases by taking the mean value of $\varkappa = 1.37$, and accounting for the shape of pulsations by the flow time factor (for an interrupted gas supply) and by the nonuniform flow factor (for continuous gas supply).

In recent years theoretical work has appeared [8-10] which confirms the abovementioned computing formulas for evaluating the additional measurement error in pulsating gas-flows in relation to the damping criterion and the adiabatic index. It is also suggested that, when graphico-analytical evaluations of this error are made a family of curves should be used with the damping criterion divided by $\varkappa$ and plotted along the y-axis, instead of a family of curves for the mean value of $\varkappa = 1.37$.

However, the basic difficulty in measuring pulsating flows by means of differential manometers-flowmeters is not due to the absence of a more convenient or accurate method of computation, but to the fact, confirmed both by theoretical and experimental investigations [11-14], that gas pulsations in a pipeline near the constricting device are very complex, and much more complex than had been assumed when the simplified theory was derived. Wave effects interfere to a considerable extent with measurements. Acoustical waves arise which, on reflection from the constricting device, may lead to the formation of standing waves. This effect is particularly characteristic for diaphragms.

Cases are known when the pressure difference in measuring pulsating flows becomes negative [11,12].

Insufficient knowledge of the pulsation process and flow measurements, in this instance, are confirmed in particular by the discrepancies between the calculated and experimental data: a) it has been established by a number of tests [4,11,12,15,16] that the error in measuring a pulsating flow often has a negative sign; b) a rise in the pressure difference obtained for a constant flow by decreasing the constricting device modulus m may lead to a rise in the error [11], whereas according to calculations it should decrease; c) with a decreasing modulus for a constant pressure difference the error increases [11] (according to the damping criterion it should decrease).

Thus, the damping criterion and a certain approximate analytical relation of the additional error to the criterion is an insufficiently reliable characteristic for determining the error of pulsation measurements.

The latest document of Working Group 3 of the International Standardizations Organization Technical Committee 30, ISO/TC 30/WG 3 [17], and the draft of the new British Standard for measuring flows [18] indicate that the present tendency abroad consists in abandoning any further development of the damping criterion technique, and restricting considerably its application with the proviso that even in that restricted sphere it is only approximate. Thus, the damping criterion virtually loses its practical importance.

In view of the fact that available data for measuring the pulsating flow are insufficient for producing, on their

basis, a standard specification, these problems have not been included in the latest draft project of the International Recommendation for Measuring Flows by Means of Orifice Plates and Nozzles [19]. Taking into consideration the importance and problematic nature of these questions the ISO/TC 30 conference held in 1960 decided to establish a special working group to study pulsating flows.

Conclusions. The above considerations show that until reliable data are available there is no point in including in the All-Union standard specification for measuring flows a recommendation for evaluating the error in measuring pulsating flows by means of the damping criterion and to classify the differential manometers combined with constricting devices among instruments with standardized errors.

Differential manometers can be used in pulsating flows only as indicators of the flow (instruments with a nonstandard error). In this connection the instructions embodied in Regulations 27-54 and referring to the measurement of pulsating flows should be revised.

LITERATURE CITED

1. Regulations 27-54 on the application and checking of the flow-meters with normal orifice plates, nozzles and Venturi tubes [in Russian] (Mashgiz, Moscow, 1955).
2. J. L. Hodgson, Jour. Inst. Fuel, Vol. 2, p. 17 (1928); Trans. ASME, Vol. 51, p. 303 (1929).
3. O. Lutz, Ing.-Archiv, No. 2 (1932).
4. F. Herning and C. Schmid, VDI-Z, No. 38 (1938).
5. C. Schmid, VDI-Z, No. 33 (1940).
6. Einfluss pulsierender Strömung, VDI (ISA 30) 4, 1939.
7. DIN 1952. Durchflussmessregein, 6. Auflage, 1948.
8. P. P. Kremlevskii, "Smoothing of pulsating flows of liquids, gases and steam," from the collection entitled Thermal Power Instruments and Regulators [in Russian] (Mashgiz, No. 3, Moscow, 1956).
9. P. P. Kremlevskii, "Measurement of the rate of pulsating flows. Investigations in the sphere of mechanical measurements." Works of the Institutes of the Committee of Standards, Measures and Measuring Instruments, No. 50 (110). [in Russian] (Standartgiz, Moscow, 1961).
10. P. P. Kremlevskii, "Damping criterion for pulsating flows." From a collection entitled Thermal Power and Chemico-Technological Instruments and Regulators [in Russian] (Mashgiz, Moscow, 1961).
11. A. R. Deschere, Trans. ASME, No. 6 (1952).
12. S. I. Sergeev, Measurements of Pulsating Flows [in Russian (Report of the VNIIKIMASh, 1951).
13. N. P. Bailey, Trans. ASME, No. 8 (1939).
14. R. C. Baird and I. C. Bechtold, Trans. ASME, No. 4 (1952).
15. H. S. Bean, Western Gas, No. 10 (1935).
16. E. J. Lindahl, Trans. ASME, No. 8 (1946).
17. The influence of installation conditions on discharge coefficient accuracy and tolerances for orifice plates and nozzles, ISO/TC 30/WG 3 (Secretariat 15) 61 (1959).
18. Draft revision of B. S. 1042: 1943 "Flow measurement," A (INE) 3300 (1960).
19. Fourth draft proprosal for an ISO Recommendation for measurement of fluid flow by means of orifice plates and nozzles, ISO/TC 30 (Secretariat 75) 176 (1960).

REVIEWS AND REPORTS

ANALOG-TO-DIGITAL AND DIGITAL-TO-ANALOG CONVERTERS*

Translated from Izmeritel'naya Tekhnika, No. 11,
pp. 59-61, November, 1961

Digital computers are used on an increasing scale in production automation. They facilitate processing large quantities of data which are required for an efficient controlling of complex systems according to a given program.

Variable quantities, such as temperature, pressure, acceleration, position, etc. can acquire any value in a given limited range. A digital computer processes information in the form of numbers (figures). The transmission channel between the system and the computer is equipped with an intermediate device which converts analog information into a digital form and vice-versa. Such devices are known as analog-to-digital and digital-to-analog converters.

In remote measurements and control the conversion of analog quantities into a digital form provides a very accurate transmission of data over long distances, eliminates line noise and makes it possible to transmit several different types of information over a single line.

In order to convert any analog quantity into a digital form a certain time is required, known as the conversion time. The analog quantity is divided with respect to time into a number of intervals. The value of the analog quantity is determined for each interval. In order to represent accurately the development of a continuously changing quantity it is necessary to have a high frequency both for the "sampling" input signal and for the conversion. The speed of conversion depends in the first place on the conversion principle used. For instance, parallel working devices (with simultaneous determination of all the figures in a digital count) have a higher speed than consecutively operating devices in which the digits of various orders are obtained consecutively.

The accuracy with which the value of an analog signal is expressed at a given moment depends not only on the width of the frequency interval (wider intervals result in rougher approximations), but also on the accuracy of expressing the value of each "sample," i.e., on the number of discrete conditions which it is possible to express. This number determines the smallest calibration of the "scale." For an accuracy of 1% (with respect to the maximum value) it is necessary to divide the range into 100 divisions. In a decimal code it means that the number must be expressed by two decimal figures. In a binary code this corresponds to seven binary figures (orders), since $2^7 = 128$. For an accuracy of 0.1% three decimal figures are required, or 10 binary figures ($2^{10} = 1024$).

The converters can be divided according to their method of conversion into three groups, namely, those with intermediate conversion into time intervals; comparators; and those with a spatial representation of the code. Devices of the first two groups are, as a rule, used when the measured physical quantity has already been converted into a proportional voltage or current. The devices of the last group are used for coding angular displacements of a shaft or a forward movement of a component.

Devices with an intermediate conversion into a time interval transform the output voltage into a time interval. This width-modulated rectangular signal is converted into a digital form by counting the number of pulses transmitted by a generator during the operation of the rectangular voltage. A width-modulated signal can be formed, for instance, by comparing the input voltage with a linearly varying saw-tooth voltage (Fig. 1). The time interval between point A, where the saw-tooth voltage is equal to the reference voltage, and point B where it is equal to the input voltage, is proportional to the value of the input voltage at point B. During interval AB the counter receives constant frequency pulses. The condition of the counter at the end of the interval indicates the numerical value of the input voltage. The block-schematic of this converter is shown in Fig. 2. The converter works periodically. At the beginning of the cycle the counter, which is made up, for instance, of a trigger chain is returned to zero; the distributor sends a pulse and starts the rising saw-tooth voltage; simultaneously the blocking device is tripped and the counter begins to register the constant frequency pulses supplied by the clock-pulse generator. At the instant when the saw-tooth voltage becomes equal to the input voltage the blocking device operates and the counter can be read out either by the parallel or consecutive methods. The cycle ends with the counter returning to zero.

*Review of the article by J. Janku and Z. Malec. Prevodniky analogovecislicové a cislicové analogové. From the Czechoslovak journal "Automatizace," No. 1 (1961).

The accuracy of conversion depends on the linearity of the saw-tooth voltage with which the measured voltage is compared, and also on the sensitivity of the comparison circuit and the frequency of the clock-pulse generator. The source of the saw-tooth voltage consists of fantastrons, integrating amplifiers and diode circuits which form a step curve. A Schmidt circuit is used for comparison purposes. Such converters can attain a speed of 10,000 conversions per second with an error down to 0.1%.

The main advantage of converters with intermediate conversion into time intervals consists in their relative simplicity, the use of simple circuits and the absence of logical circuits. Their disadvantage consists in the requirement of a large input signal (50-100 v), especially required for accurate converters.

The comparator analog-to-digital converters (Fig. 3) are characterized by a negative feedback from the output to the input. The input voltages which are proportional to a given physical value are compared (subtracted) from the voltage formed at the output of the converter. According to the sign of this difference comparison of voltages the distributor controls the value of the output voltage in such a manner at to decrease the difference.

The basic component of the circuit in Fig. 3 is a reversible counter which can add or subtract pulses received from the clock-pulse generator. The state of the counter elements represents the digital output of the converter. The drawback of this type of converter consists of its low speed of conversions due to the reversible counter.

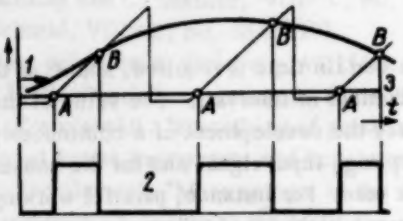

Fig. 1. Formation of width-modulated rectangular signals by means of a saw-tooth voltage. 1) Input (analog) signal; 2) width-modulated signal; 3) zero level.

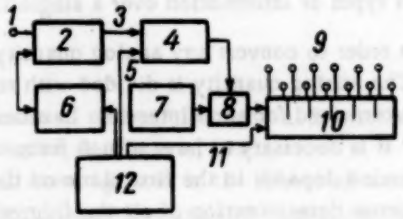

Fig. 2. Block schematic of an analog-to-digital converter using a width-modulated rectangular signal shown in Fig. 1. 1) Input (analog) voltage; 2) comparison circuit; 3) stop; 4) starting circuit; 5) start; 6) saw-tooth voltage generator 7) clock-pulse generator; 8) blocking device; 9) counter output; 10) counter; 11) restoring; 12) distributor.

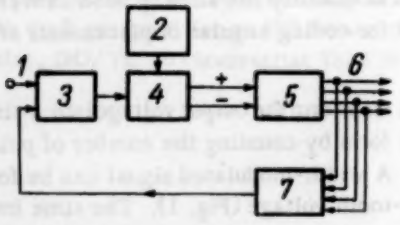

Fig. 3. Comparison analog-to-digital converter with a feedback. 1) Input (analog) voltage; 2) clock-pulse generator; 3) comparison circuit; 4) distributor; 5) reversible counter; 6) digital output; 7) digital-to-analog converter.

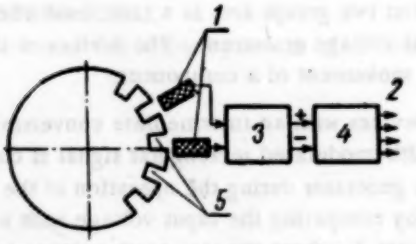

Fig. 4. Operating principle of a differential converter. 1)Transducers (photoelectric cells); 2) digital output; 3) unit for determining direction of movement; 4) reversible counter; 5) illuminated slogs.

A circuit in which the input analog signal is compared with a voltage formed by the sum of switched reference voltages from a single accurate source has a higher speed of operation. In this circuit each voltage corresponds to a definite digit order. For instance, for a binary system the value of this voltage is determined by powers of two. Ac-

cording to the sign of the difference between the input and output voltages the distributor forms various combinations of these voltages until the difference attains a minimum. The combination of reference voltages thus obtained represents the output digital reading.

The accuracy of such converters is determined in the first place by the sensitivity of the comparison circuit and the accuracy of the reference voltages. An accuracy of 0.1% can be attained with an operating speed of 100,000 conversions per second. Their disadvantage consists in their complexity and the use of logical circuits.

Converters with a spatial representation of the code are based on the use of certain geometrical configurations which represent a definite digital code. They are suitable for the numerical expression of the position or rotation angle of a shaft, etc. These converters can be divided into three groups. The first group consists of so-called differential converters and they produce one output pulse for each increment in the difference of their position. These converters must possess an element which distinguishes the direction of motion, and a reversible counter which either adds or subtracts the input pulses according to the direction of the movement. The existing state of this converter indicates the position of the observed object.

The simplest example of such a converter is shown in Fig. 4. The shaft, whose angle of rotation has to be expressed in a digital form, carries a circle with slots. The light which passes through these slots falls on two photocells. The photocells are separated from each other along the circumference by a distance of $k+\frac{1}{2}$ of a slot spacing. The number of pulses from one of them indicates the rotation angle, and the sequence of their operation indicates the direction of the movement. If, however, three photocells are placed along the circumference at a distance of $k+\frac{1}{3}$ of a slot spacing between them, the sensitivity of the device is trebled since the photocell signals can be processed in the manner of a Vernier scale. The whole device can be made extremely accurately. It is possible to obtain a slot spacing of a 10 μ by photographic means. Other similar devices use electro-mechanical collectors with several brushes or discs with periodic magnetic recording in place of the illuminated slots. Forward movements can be converted in a similar manner by using strips with illuminated slots or laminations with brushes.

The advantage of these converters consists in their simplicity, and their disadvantage in the requirement for distinguishing between the direction of the movement and the probability of keeping and accumulating any errors which are produced.

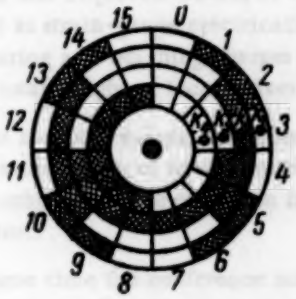

Fig. 5. Code disc for a multifigure positional converter (Gray's code with a change in one binary place).

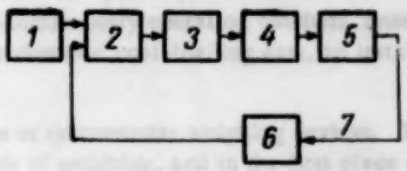

Fig. 6. Connection of a digital-to-analog converter to a controlled system. 1) Program; 2) digital comparison element; 3) digital-to-analog converter; 4) operating (actuating) link; 5) controlled system; 6) analog-to-digital converter; 7) controlled variable.

Another group of positional converters consists of those producing a combination of signals according to a definite code for each position of the object. The collector shown in Fig. 5 can serve as an example of such converters. The shaded portions represent conducting segments from which brushes K_1, K_2, K_3, and K_4 obtain their voltages. By means of four channels 16 positions can be detected. The device can also be made in the form of a strip for coding linear displacement. It is impossible theoretically, however, to place all the transducers quite accurately in a straight line; hence, in passing from one position to another false signals may by obtained which provide errors in the count. In such instances it is advisable to use certain special codes, for instance, Gray's code (Fig. 5).

"Multifigure" converters require higher precision in manufacture than differential converters for the same absolute accuracy. The advantage of these converters consists in the fact that any errors which may arise are not additive as in the case of differential converters, and that the processing of signals received from the transducers in this case is much simpler.

Digital-to-analog converters consist of devices which convert digital data at their input to proportional signals at their output, usually in the form of a voltage or a rotation angle of a shaft. In order to convert a number into a rotation angle of a shaft (or a displacement of two components with respect to each other) it is possible first to form a series of pulses whose number corresponds to the required increment in the rotation of the shaft or the movement of a component. Pulses can be converted into rotations of the shaft by a step-by-step motor or a relay circuit.

Digital-to-analog converters are often used in digital servomechanisms (their block schematic is shown in Fig. 6). The controlled variable follows a program which is set by the digital comparison circuit and simultaneously by a feed back signal which provides the actual condition of the controlled variable. The digital output signal of the comparison circuit is converted by the digital-to-analog converter into an analog signal and is directed to the actuating link which controls the system in the required manner. The feedback signal must be converted into a digital form by an analog-to-digital converter.

Digital data are normally converted into a corresponding dc voltage by means of an analog-to-digital converter circuit. Digital-to-analog converters of this type are simpler than the analog-to-digital converters, since the switching circuits can be controlled directly by the digital information and there is no need to use comparison circuits.

INFORMATION

CONFERENCE ON AUTOMATION OF WEIGHING

S. I. Gauzner

Translated from Izmeritel'naya Tekhnika, No. 11,
p. 62, November, 1961

The regional department of the Scientific and Technical Society of the Instrument-Making Industry and the Council of National Economy organized in Odessa on September 27 to 30, 1961, a scientific and technical conference on the problems of automation of weighing, with the participation of over 150 representatives from metallurgical and chemical industry plants, scientific research institutes and plants and organizations which design, manufacture, and use automatic scales.

Over 20 papers and reports were presented to the conference on the work of the Odessa SKBIM (Special Design Bureau of the Institute of Metals), the NIKIMP (Scientific Research and Design Institute of Test Machines, Instruments and Equipment for Measuring Mass), OPI (Odessa Polytechnical Institute), TsNII MPS (Central Scientific Research Institute of the Ministry of Railroads), the Tsvetmetavtomatika (Nonferrous Metallurgy Automation Institute), the Ukrgipromeza (Ukranian State Institute for the Design and Planning of Metallurgical Plants), the Chelyabinsk Metallurgical Plant, the Dnepropetrovsk Mining Institute, etc. on the subject of designing and using new, mainly strain-gauge, automatic scales and batchers of a continuous and periodic action.

Papers were also read on the development of a number of standardized elastic elements for dynamometers in the range of 0.1 to 50 ton-wt (NIKIMP) and on the effect of precision in manufacturing lever systems on scale measurement errors (OPI-SKBIM of Odessa).

In the reports and contributions made at the conference it was noted that since the 1st conference on weighing instruments (see Izmeritel'naya tekhnika, 1959, No. 4) considerable work has been carried out in the design and construction of new and improved models of weighing instruments. For instance, mass production has been organized of such equipment as strain-gauge electrically-operated crane scales, continuously operating batchers, systems for automatically gathering and weighing charges for large blast furnaces, automatic coal-loading cars, an installation for measuring the total weight of locomotives, etc.

Important recent achievements were also noted in automation of commercial weighing devices. This involves, above all, the assimilation of new advanced and progressive methods of weighing, and in the first place of electrical strain-gauge methods, and the transition from separate weighing devices to combined automatic systems with programming control.

At the same time the conference noted that insufficient attention is being paid to the unification, standardization and development of standard measuring equipment units. There is also insufficient coordination in the development, research and design of automatic weighing and batching equipment.

The conference also adopted a broad resolution in which it noted that the development and design and scientific research organizations and institutions which produce weighing equipment are faced with complex tasks. An over-all automation and mechanization of production processes in metallurgy and other industries requires weighing equipment not only for checking by weight these processes and the finished products, but also for carrying out other production operations, such as the selection of materials, batching, transporting, programmed operation of auxiliary equipment, etc. This leads to the main requirement of weighing equipment, namely, its reliable and synchronous operation with the machinery which it services.

The conference expressed the need to eliminate a situation in which the main planning organizations issue different technical specifications for weighing equipment which is intended for either the same or similar functions. The unification of technical specifications for weighing equipment, and the coordination of the work of chief planners and design offices of heavy engineering plants will reduce the quantity of unnecessary developement work and will concentrate it on the most important subjects.

In order to solve all these problems it is necessary, first of all, to concentrate the efforts of scientific-research and development and design institutes and plants in order to: produce and carefully test out improved weighing devices which operate on the basis of new weighing principles, especially various types of electronic strain-gauge instruments; to produce universal multicomponent batchers both for strain-gauge and lever-type scales with flexible remotely-controlled programming; to make completely automatic various designs and processes, including the programming of qualitative and quantitative selection, and to ensure the sequence of production operations; to raise the reliability, increase the life and applicability of the equipment, and reduce its weight and cost.

The conference considered it necessary to introduce wide normalization of units and components, to develop preferred sizes and standard units, to unify weighing and auxiliary production equipment. It decided to approach the appropriate organizations with a request for instructing specialized agencies to: develop and produce for electronic strain-gauge scales a special automatic indicating instrument which would print and add readings; to develop a universal computing high-speed printing machine with an electronon-magnetic control; to develop standard designs and organize commercial production of strain-gauge transducers.

The conference considered it necessary for the Odessa Sovnarkhoz (Council of national economy) to enlarge considerably its research and experimental-design work in the sphere of electrical strain-gauges and automatic weighing equipment, which is now being conducted in its subordinated organizations, by strengthening and extending their experimental basis.

The conference decided to approach the State Committee for Automation and Engineering with a request that the Institute for Technical Information be entrusted with organizaing a centralized publication of reference and information material on weighing instruments and automation of weight control (catalogs, instructional and technical materials, etc.).

It was also decided to convene in Moscow not later than 1963 an All-Union Scientific and Technical Conference on problems of Automation of Weighing Control.

FROM OTHER JOURNALS

Translated from Izmeritel'naya Tekhnika, No. 11, pp. 63-64, November, 1961

МАШИНОСТРОЕНЕ

1961, No. 1

A. Alexandrov. Determining the optimum consumption of moving-iron voltmeters.

N. Nikolov. Strain-gauge dynamoters.

No. 3

D. Dimitrov. Testing the calibration accuracy of a double-microscope type MIS-11.

No. 4

L. Glushkov and M. Mikhailov. Graphical determination of the main stresses in electrical strain-gauge measurements.

Al Biks. Organization of the work in the Central Test Laboratory of the ZMM (plant of metal-cutting machines) in Sofia.

No. 5

A. Velev and A. Alexandrov. Moving-coil measuring instruments (electrical measuring instruments plant in Sofia).

No. 6

D. Sepetliev and I. Kalpazanov. Checking the quality of engineering products by the dispersion analysis method.

Fourth international exhibition of electronic instruments.

I. Popov. Greater attention should be paid to measurement techniques in engineering plants.

No. 7

V. Konstantinov and N. Nikolov. Errors in measuring deformations by means of strain-gauge converters.

Kh. Artur. Certain problems in the design of moving-iron measuring instruments.

D. Parmakliev. International collocution on semiconductor instruments and devices.

No. 8

S. Slavchev. Possibilities of improving temperature-control circuits in electrical furnaces by means of electronic potentiometer ÉPD-12.

É. Bekyarov. Exhibition of high-precision measuring instruments made in the GDR.

No. 9

Development of instrument-making in Bulgaria.

MÉRÉS ÉS AUTOMATIKA

1961, No. 1

P. Tokodi. Tasks in the development of instrument-making in the second five-year plan.

O. Lechner. Accuracy in industrial measurements of large dimensions.

L. Sándor. Results of unit standardization of electrical measuring instruments in large-scale mass production.

E. Szombati. Pneumatic measurements as a means of automation in engineering measurements.

S. Lakatos. Modern methods of gas analysis in factories.

No. 2

R. Kolos. Tasks of the Measurement Techniques Society in automation.

A. Agoston. Investigating the stability of an automatic compensator.

M. Kenderessi. Measurement of small standing-wave ratios by means of a directive coupling.

E. Bujdoso and I. Aladar. Measuring flow rates by means of radioactive isotopes.

D. Lukaes. Determination of measurement errors.

I. Szabo. Analog summation unit in pneumatic control systems.

No. 3

F. Petik. Control of machines for testing tensile strength and compression.

A. Agoston. Investigating the stability of an automatic compensator.

B. Sebestyen. Computation of a design for a power-pack stabilizer.

K. Payer, I. Safarik, and L. Tari. Measurement of x-ray doses by means of a microcalorimeter.

No. 4

D. Almassy and I. Frigyes. Microwave noise generator with a 2000 Mc frequency band.

S. Kovacs. Instruments for measuring and controlling levels in liquids.

M. Solti. Modern infrared spectrophotometers.

S. Lakatos. Infrared gas analyzer.

No. 5

I. Nagy. Three-phase magnetic amplifier circuits.

P. Bartos. Technical control system and modern calibrating machines.

F. Kovacz. Tester of intermediate frequency parameters in transistors.

T. Kemeny. Uniformly batching loading scales.

No. 6

II IMECO international conference on measurement techniques and instrument-making in 1961.

T. Berczely. Application of an amplifier in wave-measuring techniques.

P. Barta. Technical control systems and modern calibration machines.

P. Bondi. Production process control in engineering workshops (dispatching instruments).

No. 7

J. Sanda. Certain problems of automatic measurements and refractive indices.

A. Ambrozi. Transistorized microammeter with a small voltage drop.

T. Kemeny. Closure of the IMECO 1961 congress.

K. Tarnai. Measurement of negative resistances.

K. Hajduska. Machine-tool exhibition in Hannover, 1960.

Feingerätetechnik

1961, No. 7

S. Melzer. New principles in measuring force and work when testing mechanical properties of materials. An impact dynamometer is described and a device for measuring work. The dynamic and static characteristics of the dynamometer are provided.

Eckerkunst. New FEB (Zull) devices and instruments at the Leipzig Spring Fair, 1961. Brief description of the exhibited multipositional automatic sorting machines.

G. Bemel. New computing-electronic measuring instruments.

No. 8

G. Lenk. Application of Michelson's interferometer with an air-cushioned mobile mirror for registering interference fringes.

A. Wiemer. Measuring instruments at the Leipzig Fair, 1961.

S. Puder. Schematic of a device for continuous checking of lengths.

G. Spred. New pneumatic measuring instrument for measuring profiles of turbine and compressor vanes.

H. G. Laport. Effect of climatic conditions on precision and electrical instruments in Vietnam.

No. 9

E. Gultsch. Basic principles of measurements by means of precision measuring instruments, part 2.

Wile. The problem of measuring the waviness of the surface of teeth in precision gears machined by the running-in method.

Loran. Spectrophotometer with automatic redistering in the visible part of the spectrum.

POMIARY AUTOMATYKA KONTROLA

1961, No. 1

Future development of automation in Poland.

Z. Trybalski. Dynamic properties of a temperature transducer with a convectional heat exchange.

A. Spychalski and K. Referowski. Ratiometer bridge circuit for measuring temperature with resistance thermometers.

Bulleting of the Central Laboratory of Measuring Instruments and Optics (CLIPO).

No. 2

Z. Nagello and R. Chamski. High-speed mechanical recording instrument.

A. Zuchowski. Some remarks on the standard "Electrical Recording Instruments. General technical requirements."

Bulletin of the Principal Measures Administration (GUM).

No. 3

W. Schnabel and F. Soldnar. Recording instrument for measuring thickness (see also Izmeritel'naya tekhnika, 1960, No. 11, p. 57).

W. Gajewski and J. Moddl. Isotope thickness-meter "1MG-1."

Bulletin of the CLIPO.

R. Wisnewski and R. Golembewski. Application of strain gauges for measuring hydrostatic pressure up to 10,000 kg/wt/cm^2.

T. Konopinski. Semiconductor thyratrons.

E. W. Szamotulski. Calibration of hydrostatic manometers.

Report of the Polish Committee of Measurement Techniques and Automation (PKITA).

GUM Bulletin.

No. 5

First Polish conference of optical instrument-making.

Grabecki. Polish measuring and controlling instruments at the 30th international fair in Poznan.

CLIPO Bulletin

No. 6

E. Gibner, S. Mantzacher, and T. Zagaewski. Electrical instrument for measuring pressure of knurling rollers in machines for producing gear journals.

A. Spychalski and L. Referowski. Measurements of grain temperature in storehouses.

C. Markert. Heating of precision instruments and methods of avoiding it.

W. Grabowski. Counting accuracy of counting balances.

GUM Bulletin.

No. 7

The role of measurement techniques in the development of automation.

I. Pankov, J. Klimek, and A. Masljanko. Humidity measurements in the metallurgical industry.

Technical news. Micrometer type ME-2.

CLIPO Bulletin.

No. 8

T. Missaljak. Computation of thermistor circuits for measuring temperature differences.

A. Ambroziak. Germanium photocells.

T. Flurkowski. Progress in the sphere of thickness measurements by means of radioactive isotopes.

A. Sadowski. Limits and accuracy of interference measurements of surface roughness by means of replicas and immersion.

GUM Bulletin.

No. 9

R. Hagel and B. Enca. Tracking selsyn system for measuring the position of the operating roller and manipulator in a blooming mill.

W. Szpany. Symmetrical circuits with additional transitors

M. Chmelewski and A. Stano. Tunnel diodes.

CLIPO Bulletin.

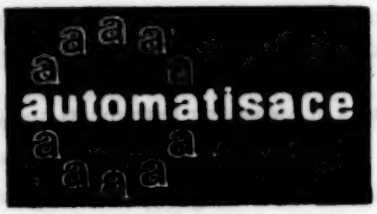

1961, No. 1

J. Janku and Z. Malec. Analog-to-digital and digital-to-analog converters.

P. Gudec and P. Schiller. Continuous measurements of the height of filling with coal by means of radio active isotopes.

Z. Woborski and F. Glawaty. Measuring panels for testing installations.

No. 7

I. Tybor. Balances as an important element in automation.

K. Dabesz. Spiral potentiometer Aripot.

No. 9

Janacz, Zabranski, and Pollak. Infrared analyzer of gases and vapor.

Soviet Journals Available in Cover-to-Cover Translation

ABBREVIATION	RUSSIAN TITLE	TITLE OF TRANSLATION	PUBLISHER	TRANSLATION BEGAN Vol.	Issue	Year
AÉ	Atomnaya énergiya	Soviet Journal of Atomic Energy	Consultants Bureau	1	1	1956
Akust. zh.	Akusticheskii zhurnal	Soviet Physics – Acoustics	American Institute of Physics	1	1	1955
	Antibiotiki	Antibiotics	Consultants Bureau	4	1	1959
Astr(on). zh(urn).	Astronomicheskii zhurnal	Soviet Astronomy–AJ	American Institute of Physics	34	1	1957
Avto(mat). svarka	Avtomaticheskaya svarka	Automatic Welding	British Welding Research Association (London)		1	1959
	Avtomatika i Telemekhanika	Automation and Remote Control	Instrument Society of America	27	1	1956
	Biofizika	Biophysics	National Institutes of Health*		1	1957
	Biokhimiya	Biochemistry	Consultants Bureau	21	1	1956
Byull. éksp(erim). biol. i med.	Byulleten' éksperimental'noi biologii i meditsiny	Bulletin of Experimental Biology and Medicine	Consultants Bureau	41	1	1959
DAN (SSSR) / Dokl(ady) AN SSSR	Doklady Akademii Nauk SSSR	The translation of this journal is published in sections, as follows:				
		Doklady Biochemistry Section	American Institute of Biological Sciences	106	1	1956
		Doklady Biological Sciences Sections (Includes: Anatomy, biophysics, cytology, ecology, embryology, endocrinology, evolutionary morphology, genetics, histology, hydrobiology microbiology, morphology, parasitology, physiology, zoology sections)	American Institute of Biological Sciences	112	1	1957
		Doklady Botanical Sciences Sections (Includes: Botany, phytopathology, plant anatomy, plant ecology, plant embryology, plant physiology, plant morphology sections)	American Institute of Biological Sciences	112	1	1957
		Proceedings of the Academy of Sciences of the USSR, Section: Chemical Technology	Consultants Bureau	106	1	1956
		Proceedings of the Academy of Sciences of the USSR, Section: Chemistry	Consultants Bureau	106	1	1956
		Proceedings of the Academy of Sciences of the USSR, Section: Physical Chemistry	Consultants Bureau	112	1	1957
		Doklady Earth Sciences Sections (Includes: Geochemistry, geology, geophysics, hydrogeology, mineralogy, paleontology, petrography, permafrost sections)	American Geological Institute	124	1	1959
		Proceedings of the Academy of Sciences of the USSR, Section: Geochemistry	Consultants Bureau	106-123	1 6	1957-1958
		Proceedings of the Academy of Sciences of the USSR, Sections: Geology	Consultants Bureau	106-123	1 6	1957-1958
		Doklady Soviet Mathematics	The American Mathematics Society	131	1	1961
		Soviet Physics–Doklady (Includes: Aerodynamics, astronomy, crystallography, cybernetics and control theory, electrical engineering, energetics, fluid mechanics, heat engineering, hydraulics, mathematical physics, mechanics, physics, technical physics, theory of elasticity sections)	American Institute of Physics	106	1	1956
		Proceedings of the Academy of Sciences of the USSR, Applied Physics Sections (does not include mathematical physics or physics sections)	Consultants Bureau	106-117	1	1956-1957
Derevoobrabat. prom-st'.	Derevoobrabatyvayushchaya promyshlennost'	Wood Processing Industry	Timber Development Association (London)		9	1959
	Élecktrosvyaz	Telecommunications	Massachusetts Institute of Technology*		1	1957
Éntom(ol). oboz(renie)	Éntomologicheskoe obozrenie	Entomological Review	American Institute of Biological Sciences	38	1	1959
Farmakol. (i) toksikol(ogiya)	Farmakologiya i toksikologiya	Pharmacology and Toxicology	Consultants Bureau	20	1	1957
FMM	Fizika metallov i metallovedenie	Physics of Metals and Metallography	Acta Metallurgica*	5	1	1957
Fiziol. zhurn. SSSR (im. Sechenova)	Fiziologicheskii zhurnal im. I. M. Sechenova	Sechenov Physiological Journal USSR	National Institutes of Health*		1	1957
Fiziol(ogiya) rast.	Fiziologiya rastenii	Plant Physiology	American Institute of Biological Sciences	4	1	1957
	Geokhimiya	Geochemistry	The Geochemical Society		1	1958
FTT	Fizika tverdogo tela	Soviet Physics–Solid State	American Institute of Physics	1	1	1959
Izmerit. tekh(nika)	Izmeritel'naya tekhnika	Measurement Techniques	Instrument Society of America		1	1959
Izv. AN SSSR, O(td). Kh(im). N(auk)	Izvestiya Akademii Nauk SSSR: Otdelenie khimicheskikh nauk	Bulletin of the Academy of Sciences of the USSR: Division of Chemical Sciences	Consultants Bureau		1	1952

continued

Izv. AN SSSR, O(td). T(ekhn). N(auk): Met(all). i top.	(see Met. i top.)	Bulletin of the Academy of Sciences of the USSR: Physical Series	Columbia Technical Translations		1 1954
Izv. AN SSSR Ser. fiz(ich).	Izvestiya Akademii Nauk SSSR: Seriya fizicheskaya	Bulletin (Izvestiya) of the Academy of Sciences USSR: Geophysics Series	American Geophysical Union		1 1954
Izv. AN SSSR Ser. geofiz.	Izvestiya Akademii Nauk SSSR: Seriya geofizicheskaya	Izvestiya of the Academy of Sciences of the USSR: Geologic Series	American Geological Institute		1 1958
Izv. AN SSSR Ser. geol.	Izvestiya Akademii Nauk SSSR: Seriya geologicheskaya	Soviet Rubber Technology	Research Association of British Rubber Manufacturers	18	1 1959
Kauch. i rez.	Kauchuk i rezina		Consultants Bureau	1	3 1960
		Kinetics and Catalysis	Coal Tar Research Association (Leeds, England)		1 1958
	Kinetika i kataliz	Coke and Chemistry USSR	Consultants Bureau	14	1 1952
	Koks i khimiya		American Institute of Physics	2	1 1957
Kolloidn. zh(urn).	Kolloidnyi zhurnal	Colloid Journal			
	Kristallografiya	Soviet Physics – Crystallography	Acta Metallurgica	6	1 1958
Metalov. i term. obrabot. metal.	Metallovedenie i termicheskaya obrabotka metallov	Metal Science and Heat Treatment of Metals	Acta Metallurgica		1 1957
	Metallurg	Metallurgist	Eagle Technical Publications		1 1960
Met. i top.	Metallurgiya i topliva	Russian Metallurgy and Fuels	American Institute of Biological Sciences	26	1 1957
Mikrobiol.	Mikrobiologiya	Microbiology	American Institute of Physics		6 1959
OS	Optika i spektroskopiya	Optics and Spectroscopy	American Institute of Biological Sciences		1 1958
	Pochvovedenie	Soviet Soil Science	British Scientific Instrument Research Association		1 1959
	Priborostroenie	Instrument Construction	Instrument Society of America		1 1957
Pribory i tekhn. éks(perimenta)	Pribory i tekhnika éksperimenta	Instruments and Experimental Techniques			
Prikl. matem. i mekh.	Prikladnaya matematika i mekhanika	Applied Mathematics and Mechanics	American Society of Mechanical Engineers		1 1958
PTÉ	(see Pribory i tekhn. éks.)				
	Problemy Severa	Problems of the North	National Research Council of Canada		
Radiotekh.	Radiotekhnika	Radio Engineering	Massachusetts Institute of Technology*	12	1 1957
Radiotekh. i élektronika	Radiotekhnika i élektronika	Radio Engineering and Electronics	Massachusetts Institute of Technology*	2	1 1957
	Stanki i instrument	Machines and Tooling	Production Engineering Research Assoc.		1 1959
	Stal'	Stal (In English)	Iron and Steel Institute		1 1959
Stek. i keram.	Steklo i keramika	Glass and Ceramics	Consultants Bureau	13	1 1956
Svaroch. proiz-vo	Svarochnoe proizvodstvo	Welding Production	British Welding Research Association		4 1959
Teor. veroyat. i prim.	Teoriya veroyatnostei i ee primenenie	Theory of Probability and Its Applications	Society for Industrial and Applied Mathematics		1 1956
			Primary Sources		1 1960
Tsvet. Metally	Tsvetnye metally	Nonferrous Metals	American Institute of Physics	66	1 1958
UFN	Uspekhi fizicheskikh Nauk	Soviet Physics – Uspekhi (partial translation)	The Chemical Society (London)		1 1960
UKh	Uspekhi khimii	Russian Chemical Reviews	London Mathematical Society	15	1 1960
UMN	Uspekhi matematicheskikh nauk	Russian Mathematical Surveys			
Usp. fiz. nauk	(see UFN)				
Usp. khim(ii)	(see UKh)				
Usp. matem. nauk	(see UMN)				
Usp. sovr. biol.	Uspekhi sovremennoi biologii	Russian Review of Biology	Oliver and Boyd		48 1959
Vest. mashinostroeniya	Vestnik mashinostroeniya	Russian Engineering Journal	Production Engineering Research Assoc.		4 1959
Vop. gem. i per. krovi	Voprosy gematologii i perelivaniya krovi	Problems of Hematology and Blood Transfusion	National Institutes of Health*		1 1957
		Problems of Oncology	National Institutes of Health*		1 1957
Vop. onk.	Voprosy onkologii	Problems of Virology	National Institutes of Health*		1 1957
Vop. virusol.	Voprosy virusologii	Industrial Laboratory	Instrument Society of America	25	1 1959
Zav(odsk). lab(oratoriya)	Zavodskaya laboratoriya	Journal of Analytical Chemistry USSR	Consultants Bureau	7	1 1952
ZhAKh Zh. anal(it). khimii	Zhurnal analiticheskoi khimii				
ZhETF Zh. éksperim. i teor. fiz.	Zhurnal éksperimental'noi i theoreticheskoi fiziki	Soviet Physics–JETP	American Institute of Physics	28	1 1955
ZhFKh Zh. fiz. khimii	Zhurnal fizicheskoi khimii	Russian Journal of Physical Chemistry	The Chemical Society (London)		7 1959
ZhMÉI Zh(urn). mikrobiol. épidemiol. i immunobiol.	Zhurnal mikrobiologii, épidemiologii i immunobiologii	Journal of Microbiology, Epidemiology and Immunobiology	National Institutes of Health*		1 1957
ZhNKh Zh(urn). neorgan(ich). khim(ii)	Zhurnal neorganicheskoi khimii	The Russian Journal of Inorganic Chemistry	The Chemical Society (London)		1 1959
ZhOKh Zh(urn). obshch(ei) khimii	Zhurnal obshchei khimii	Journal of General Chemistry USSR	Consultants Bureau	19	1 1949
ZhPKh Zh(urn). prikl. khimii	Zhurnal prikladnoi khimii	Journal of Applied Chemistry USSR	Consultants Bureau	23	1 1950
ZhSKh Zh(urn). strukt. khimii	Zhurnal strukturnoi khimii	Journal of Structural Chemistry	Consultants Bureau	1	1 1960
ZhTF Zh(urn). tekhn. fiz.	Zhurnal teknicheskoi fiziki	Soviet Physics–Technical Physics	American Institute of Physics	26	1 1956
Zh(urn). vyssh. nervn. deyat. (im. Pavlova)	Zhurnal vysshei nervnoi deyatel'nosti (im. I. P. Pavlova)	Pavlov Journal of Higher Nervous Activity	National Institutes of Health*		1 1958

*Sponsoring organization. Translation through 1960 issues is a publication of Pergamon Press.

SIGNIFICANCE OF ABBREVIATIONS MOST FREQUENTLY ENCOUNTERED IN SOVIET TECHNICAL PERIODICALS

AN SSSR	*Academy of Sciences, USSR*
FIAN	*Physics Institute, Academy of Sciences USSR*
GITI	*State Scientific and Technical Press*
GITTL	*State Press for Technical and Theoretical Literature*
GOI	*State Optical Institute*
GONTI	*State United Scientific and Technical Press*
Gosénergoizdat	*State Power Press*
Gosfizkhimizdat	*State Physical Chemistry Press*
Goskhimizdat	*State Chemistry Press*
GOST	*All-Union State Standard*
Gostekhizdat	*State Technical Press*
GTTI	*State Technical and Theoretical Press*
IAT	*Institute of Automation and Remote Control*
IF KhI	*Institute of Physical Chemistry Research*
IFP	*Institute of Physical Problems*
IL	*Foreign Literature Press*
IPF	*Institute of Applied Physics*
IPM	*Institute of Applied Mathematics*
IREA	*Institute of Chemical Reagents*
ISN (Izd. Sov. Nauk)	*Soviet Science Press*
IYaP	*Institute of Nuclear Studies*
Izd	*Press (publishing house)*
LÉTI	*Leningrad Electrotechnical Institute*
LFTI	*Leningrad Institute of Physics and Technology*
LIM	*Leningrad Institute of Metals*
LITMiO	*Leningrad Institute of Precision Instruments and Optics*
Mashgiz	*State Scientific-Technical Press for Machine Construction Literature*
MGU	*Moscow State University*
Metallurgizdat	*Metallurgy Press*
MOPI	*Moscow Regional Pedagogical Institute*
NIAFIZ	*Scientific Research Association for Physics*
NIFI	*Scientific Research Institute of Physics*
NIIMM	*Scientific Research Institute of Mathematics and Mechanics*
NIKFI	*Scientific Institute of Motion Picture Photography*
NKTM	*People's Commissariat of the Heavy Machinery Industry*
Oborongiz	*State Press of the Defense Industry*
OIYaI	*Joint Institute of Nuclear Studies*
ONTI	*United Scientific and Technical Press*
OTI	*Division of Technical Information*
OTN	*Division of Technical Science*
RIAN	*Radium Institute, Academy of Sciences of the USSR*
SPB	*All-Union Special Planning Office*
Stroiizdat	*Construction Press*
URALFTI	*Ural Institute of Physics and Technology*
TsNIITMASh	*Central Scientific-Research Institute of Technology and Machinery*
VNIIM	*All-Union Scientific Research Institute of Metrology*

NOTE: Abbreviations not on this list and not explained in the translation have been transliterated, no further information about their significance being available to us — *Publisher.*

Publication of a "Soviet Instrumentation and Control Translation Series" by the Instrument Society of America has been made possible by a grant in aid from the National Science Foundation, with additional assistance from the National Bureau of Standards for the journal *Measurement Techniques.*

Subscription rates have been set at modest levels to permit widest possible distribution of these translated journals.

The Series now includes four important Soviet instrumentation and control journals. The journals included in the Series, and the subscription rates for the translations, are as follows:

MEASUREMENT TECHNIQUES – *Izmeritel'naya Tekhnika*

Russian original published by the Committee of Standards, Measures, and Measuring Instruments of the Council of Ministers, USSR. The articles in this journal are of interest to all who are engaged in the study and application of fundamental measurements. Both 1958 (bimonthly) and 1959-1961 (monthlies) available.

Per year (12 issues) starting with 1961, No. 1

General:	United States and Canada . .	$25.00
	Elsewhere	28.00
Libraries of nonprofit academic institutions:		
	United States and Canada . .	$12.50
	Elsewhere	15.50

INSTRUMENTS AND EXPERIMENTAL TECHNIQUES
Pribory i Tekhnika Éksperimenta

Russian original published by the Academy of Sciences, USSR. The articles in this journal relate to the function, construction, application, and operation of instruments in various fields of experimentation. 1958-1961 issues available.

Per year (6 issues) starting with 1961, No. 1

General:	United States and Canada . .	$25.00
	Elsewhere	28.00
Libraries of nonprofit academic institutions:		
	United States and Canada . .	$12.50
	Elsewhere	15.50

AUTOMATION AND REMOTE CONTROL – *Avtomatika i Telemekhanika*

Russian original published by the Institute of Automation and Remote Control of the Academy of Sciences, USSR. The articles are concerned with analysis of all phases of automatic control theory and techniques. 1957-1961 1959, and 1960

Per year (12 issues) starting with Vol. 22, No. 1

General:	United States and Canada . .	$35.00
	Elsewhere	38.00
Libraries of nonprofit academic institutions:		
	United States and Canada . .	$17.50
	Elsewhere	20.50

INDUSTRIAL LABORATORY – *Zavodskaya Laboratoriya*

Russian original published by the Ministry of Light Metals, USSR. The articles in this journal relate to instrumentation for analytical chemistry and to physical and mechanical methods of materials research and testing. 1958-1961 issues available.

Per year (12 issues) starting with Vol. 27, No. 1

General:	United States and Canada . .	$35.00
	Elsewhere	38.00
Libraries of nonprofit academic institutions:		
	United States and Canada . .	$17.50
	Elsewhere	20.50

Single issues of all four journals, to everyone, each . . . $6.00

Prices on 1957-1960 issues available upon request

SPECIAL SUBSCRIPTION OFFER:

One year's subscription to all four journals of the 1961 Series, as above listed:

General:	United States and Canada . .	$110.00
	Elsewhere	122.00
Libraries of nonprofit academic institutions:		
	United States and Canada . .	$ 55.00
	Elsewhere	67.00

Subscriptions should be addressed to:

Instrument Society of America
530 William Penn Place
Pittsburgh 19, Penna.